Summer 2019

Increased Hydrologic Variability Near the Paleocene-Eocene Boundary (Piceance Creek Basin, Colorado, U.S.A.))

Anna Lesko
Western Washington University, leskoak11@gmail.com

INCREASED HYDROLOGIC VARIABILITY NEAR THE PALEOCENE-EOCENE BOUNDARY (PICEANCE CREEK BASIN, COLORADO, U.S.A.)

By Anna Lesko

Accepted in Partial Completion
of the Requirements for the Degree
Master of Science

ADVISORY COMMITTEE

Chair, Dr. Brady Foreman

Dr. Robyn Dahl

Dr. Kirsten Fristad

Kathleen L. Kitto, Acting Dean

MASTER'S THESIS

In presenting this thesis in partial fulfillment of the requirements for a master's degree at Western Washington University, I grant to Western Washington University the non-exclusive royalty-free right to archive, reproduce, distribute, and display the thesis in any and all forms, including electronic format, via any digital library mechanisms maintained by WWU. I represent and warrant this is my original work, and does not infringe or violate any rights of others. I warrant that I have obtained written permissions from the owner of any third party copyrighted material included in these files.

I acknowledge that I retain ownership rights to the copyright of this work, including but not limited to the right to use all or part of this work in future works, such as articles or books. Library users are granted permission for individual, research and non-commercial reproduction of this work for educational purposes only. Any further digital posting of this document requires specific permission from the author.

Any copying or publication of this thesis for commercial purposes, or for financial gain, is not allowed without my written permission.

Anna Lesko
1 June 2019

INCREASED HYDROLOGIC VARIABILITY NEAR THE PALEOCENE-EOCENE BOUNDARY (PICEANCE CREEK BASIN, COLORADO, U.S.A.)

A Thesis
Presented to
The Faculty of
Western Washington University

In Partial Fulfillment
of the Requirements for the Degree
Master of Science

By Anna Lesko
1 June 2019

ABSTRACT

The Paleocene Eocene Thermal Maximum (PETM) was a rapid global warming event that occurred approximately 56 million years ago and represents the largest and most abrupt warming event of the Cenozoic Era. The PETM caused mean annual temperatures to increase at least 5°C globally above the already warm, greenhouse climate state of the early Paleogene. The warming and associated perturbation of the carbon cycle had numerous consequences for paleoenvironments and paleobiologic systems. This study investigates the hydrologic response to the PETM within the interior of North America and presents a new $\delta^{13}C$ bulk organic record. This study generates reconstructions of floodplain drainage and paleo-precipitation in the Piceance Creek Basin of northwest Colorado (U.S.A.). A semi-quantitative soil morphology index was used to characterize floodplain drainage and whole-rock geochemistry in order to estimate mean annual precipitation from a 124-meter stratigraphic section in the western portion of the Piceance Creek Basin. The section can be roughly litho- and bio-stratigraphically correlated to isotopically, well-constrained PETM stratigraphic intervals. The new bulk organic $\delta^{13}C$ record exhibits a range of values with an average of -22.3‰ ± 0.9 (1σ). Variability in $\delta^{13}C$ values does not appear to be related to the amount of carbon nor lithology sample. Up-section there is a 40-meter thick interval over which $\delta^{13}C$ values shift ~2‰ to lower values and then return to baseline values. This interval corresponds to the lateral equivalent of the lower portion of the Molina Member, which is known to correlate with PETM. This study suggests the new isotopic record documents the PETM, but additional isotopic and biostratigraphic work needs to be performed to confirm. Within the hypothesized PETM interval soil morphology indices double in the upper portion of the structured isotopic shift, which indicates transiently better drainage in the floodplain. Mean annual precipitation (MAP) estimates from soil geochemistry are ~1500 mm/year before and after the

isotopic excursion, and values as low as ~500 mm/year associated with the upper portion of the isotopic shift. This represents a 40% to 60% decrease in MAP in the basin. These results document greater drying in the Piceance Creek Basin as compared to the well-studied Bighorn Basin in northwest Wyoming wherein previous studies documented an increase in the soil morphology by 80% and decrease in MAP by 30-40% using identical methodologies as well as paleofloral records. When combined with other regional proxy datasets the results are consistent with general circulation model outputs that indicate widespread drying within the continental interior of North America as well as increased variability within the hydrologic cycle during the PETM. Moreover, this study supports the hypothesis that an enhanced hydrologic cycle is a robust response by the climate system to elevated atmospheric *p*CO2 levels, whether the carbon is ultimately sourced from anthropogenic sources or otherwise.

ACKNOWLEDGEMENTS

I would like to recognize my advisor, Dr. Brady Foreman, for being a wonderful mentor as well as encouraging and pushing me to succeed. I am incredibly grateful for the opportunities you have provided, and I will carry with me the experiences and knowledge you have given me. I would like to thank my committee members, Dr. Robyn Dahl and Dr. Kirsten Fristad for their generous support and guidance with regards to my research. I would also like to recognize Katie Snell and her lab group for hosting and helping me process my samples. Thank you to Ben Paulson for help within the lab. This manuscript would have not been completed without the lab assistance from WWU undergraduates Lindsey Gibson, Jeffrey Wegener, and graduate student Masoud Miraezi. Funding for this project was provided by National Geographic Society, Research and Exploration Grant (#9867-16).

Table of Contents

LIST OF FIGURES AND TABLES

INTRODUCTION

The early Paleogene (65 Ma through approximately 50 Ma) is a period of time characterized by elevated carbon dioxide levels and warm global temperatures (Zachos et al., 2001). This greenhouse climate is largely a continuation of Mesozoic climatic conditions, but exhibits a long-term warming trend from the Paleocene into Eocene until maximum warming occurs during the Early Eocene Climatic Optimum (Shackleton & Kennett 1975; Kennett & Stott 1991; Zachos et al., 2001; Lourens et al., 2005). In addition to long-term global warming, the early Paleogene experienced transient, "hyper-greenhouse" conditions related to perturbations of the carbon cycle (Zachos et al., 2001; Zachos et al., 2005; Lourens et al., 2005). The Paleocene Eocene Thermal Maximum (PETM) is the largest of these hyperthermal events and occurred at 56 Ma. Global temperatures increased 5-8°C based on marine and nonmarine proxies such as stable oxygen isotopes, Mg/Ca ratios of marine carbonates, organic paleothermometers (e.g., TEX_{86}) clumped isotope thermometry, and paleobotanical records (Kennett & Stott 1991; Zachos et al., 2003; 2006; Wing et al., 2005; Sluijs et al., 2006; McInerney & Wing, 2011; Snell et al., 2013; Gehler et al., 2016;). Coincident with the warming is an abrupt negative carbon isotope excursion (CIE) in organic and inorganic geochemical proxy records that document the input of isotopically-light, exogenic carbon into Earth's oceans and atmosphere (Kennett & Stott, 1991; Koch et al., 1992; Zachos et al., 2003; Slujis et al., 2008; McInerney & Wing, 2011). This input occurred on the timescale of 10,000 years or less, and high atmospheric carbon dioxide levels are thought to have persisted for up to an additional 190,000 years (Murphy et al., 2010). Some researchers estimate the total carbon released was up to 4,000 petagrams, likely from methane clathrates hosted within sea floor sediments (Dickens et al., 1997; Murphy et al., 2010; McInerney & Wing, 2011). In addition to changing global temperatures the PETM caused changes in ocean circulation, ocean

acidification, extinction of benthic foraminifera, and the blooming of thermophilic marine taxa as well as changes in the biogeographic ranges and ecology of plants and animals on land (Crouch et al., 2003; Wing et al, 2005; Zachos et al., 2005; McInerney and Wing, 2011; Slujis et al., 2014; Schmidt et al., 2018). A growing literature also suggests significant perturbation of the hydrologic cycle.

The PETM is an important case study in aiding our understanding of potential long-term and extensive changes CO_2 forcings can have on the hydrological cycle as well as constraining the climate sensitivity of environmental systems. General circulation models that simulate elevated carbon dioxide levels during the PETM produce more seasonal precipitation and higher evapotranspiration in the mid-latitudes with polar areas experiencing greater total rainfall amounts (Carmichael et al., 2017; Carmichael et al., 2018). These changes appear to be a robust output regardless of whether Earth's climate is in a greenhouse or icehouse state (Carmichael et al., 2018; IPCC, 2018). These model results of precipitation are broadly consistent with sedimentologic and proxy records spanning the PETM.

John et al. (2008) inferred enhanced chemical weathering and runoff, from increased sedimentation rates of kaolinite clay on the North American shelf that correlated to the PETM CIE. The North American shelf, however, is not the only marginal marine environment to experience increases in fine-grain sediment deposition. Warming and rainfall resulted in the amplification of clay abundance in the distal portion of the Tremp-Graus Basin as well as the northern region of the Bay of Biscay (Bolle et al., 2000; Bornemann et al., 2014). Nicolo et al. (2007) also found increased sedimentation rates and terrestrial clay export during the PETM along the upper continental slope of New Zealand, further implying climatically influenced shifts in the global hydrologic cycle. Using stable hydrogen and carbon isotope measurements of terrestrial-plant and

aquatic-derived n-alkanes, Pagani et al. (2006) ultimately concluded that during the PETM, precipitation in the Artic had hydrogen isotopic compositions that are similar to modern, mid-latitude precipitation. Thus, arguing that the Artic became wetter and the mid-latitudes experienced less net precipitation (Pagani et al., 2006). Overall, numerous marine and marginal marine records have consistently indicated hyperthermal-related increases in runoff from continents.

Research focused on reconstructing hydrologic changes within nonmarine depositional systems, however, are geographically limited. For example, mean annual precipitation has only been quantitatively reconstructed in one nonmarine sedimentary basin worldwide, the Bighorn Basin of northwest Wyoming, U.S.A. (Wing et al., 2005; Kraus & Riggins, 2007). Moreover, studies of fluvial strata spanning the PETM have been largely restricted to only three basins (Schmitz and Pujalte 2003; Schmitz and Pujalte, 2007; Foreman et al., 2012; Foreman, 2014; Kraus et al., 2015). These basins include the Tremp-Graus Basin in Spain, the Bighorn Basin in Wyoming (U.S.A.), and the Piceance Creek Basin in northwest Colorado (U.S.A.). Results from these areas suggest major changes in rainfall and sediment supply, which have been inferred from fluvial deposits that are consistent with greater variability in the severity and intensity of rainfall events (Schmitz and Pujalte, 2003; Foreman et al., 2012). However, these fluvial responses capture average catchment responses, and can be modified or muted by various sediment transport processes (Romans et al. 2016). With such a limited geographic extent of nonmarine hydrologic constraints spanning the PETM it is difficult to assess and test global circulation models and to determine local modifications of the global climatic signal.

In order to constrain rainfall variability spanning the PETM additional estimates of mean annual rainfall and hydrologic cycle variability need to be developed. Currently, the Bighorn Basin contains the only quantitative reconstruction of mean annual precipitation (MAP) based on soil

geochemistry and paleofloral records, and documents an overall decrease in MAP by 40% and enhanced floodplain drainage during the PETM (Kraus & Riggins, 2007; Kraus et al., 2013; 2015). This is consistent with circulation models, but only represents one geographic location. Therefore, additional data is needed to know if this drying represents a regional trend. In this study, we develop a detailed reconstruction of paleo-precipitation based on a soil morphology index and whole-rock geochemistry of alluvial deposits in the Piceance Creek Basin of Colorado (Figure 1 & 2). This is the same methodology that has been applied to the Bighorn Basin (Kraus and Riggins, 2007; Adams et al., 2011; Kraus et al., 2013; 2015), which serves as an important comparison. The data collected will help determine whether or not the hydrological cycle response during the PETM is representative of climate change throughout the Laramide basins in North America.

The Piceance Creek Basin is located ~500 km to the south of the Bighorn Basin and data from this study indicates that this region also became drier during the PETM with decreases potentially greater than 60% in mean annual precipitation. When integrated with fluvial data sets, we infer greater interannual precipitation variability and, potentially, greater seasonality in rainfall in the region. These proxy-based conclusions compare well with general circulation models outputs of PETM which predict drier, more seasonally variable rainfall within continental interiors (Winguth et al., 2010; Carmichael et al., 2017; Carmichael et al., 2018). Importantly, this pattern appears to be a robust response of the climate system when subjected to an exogenic pulse of carbon regardless of the background climate state, whether greenhouse of the early Paleogene and perturbed by methane clathrates (Carmichael et al., 2018; Winguth et al., 2010) or an icehouse state of the recent and perturbed by fossil fuel release (IPCC, 2007).

GEOLOGIC SETTING

Piceance Creek Basin

This study focuses on well-exposed early Paleogene alluvial strata in the Piceance Creek Basin of northwestern Colorado, U.S.A. (Fig. 1). This basin is one of many formed in the Western Interior of the United States during the Laramide Orogeny, which initiated during the Late Cretaceous and ended approximately 45 Ma during the Eocene (Dickinson, 2004; DeCelles, 2004; Copeland et al., 2016). The Laramide Orogeny divided the pre-existing Sevier foreland basin into a series of intramontane basins bounded by basement-involved reverse faults, and was likely related to low angle subduction of the oceanic Fallon Plate underneath the continental North American Plate (Dickinson et al., 1988; DeCelles, 2004; Dickinson, 2004). This shift in tectonic character displaced the Western Interior Seaway, which is represented by latest Cretaceous fluviodeltaic and marine strata in the Laramide basins. Erosion off the Laramide uplifts within this broken foreland basin system provided the detritus to fill the adjacent flexural basins (Yin and Ingersoll, 1997; DeCelles, 2004; Dickinson, 2004). This transition is represented by unconformities between Latest Cretaceous and early Paleocene strata in several basins (particularly in southern Laramide basins) and fluvial, overbank, and lacustrine strata within the intramontane basins (DeCelles, 2004; Dickinson, 2004; Heller et al., 2013).

The Piceance Creek Basin is bounded by Laramide structures; to the east the White River Uplift, to the southeast and south the Gunnison and Sawatch Ranges, to the southwest the Uncompahgre Uplift, to the west the Douglas Creek Arch, and to the north-northwest the Uinta Uplift (Fig. 1). The main sediment sources of the Piceance Creek Basin during the Paleocene and earliest Eocene were the Sawatch Range and Uncompahgre Uplift based on sandstone compositional and U-Pb detrital zircon geochronologic provenance analyses, isopach thickness,

fault geometries and paleodrainage studies (Tweto, 1975; Johnson and Finn 1986; Bump and Davis 2003; Lawton 2008; Jones et al., 2011; Foreman and Rasmussen, 2016). The White River Uplift likely did not become an influential sediment source until later in the early Eocene (ca. 53 Ma) (Johnson and Finn 1986; Foreman and Rasmussen, 2016), and the Uinta Uplift does not appear to be strongly influential until deposition of the Green River Formation lacustrine strata that post-date 53 Ma (Smith et al., 2008a; Smith et al., 2008b). Based on structural relationships and stratal geometries the Douglas Creek Arch appears never to have been a significantly subaerial feature nor sediment source for the Piceance Creek Basin (Johnson and Finn, 1986). Instead it was more likely a structural sill for most of the early Paleogene until expansion of early Eocene lakes represented by strata of the Green River Formation that can be continuous traced over the Arch (Smith et al., 2008a; Smith et al., 2008b).

Wasatch Formation

This study focuses on extracting a record of hydrologic changes from the Paleocene and earliest Eocene alluvial strata of the Wasatch Formation in the Piceance Creek Basin. This geologic formation conformably overlies the coarse-grained, fluvial sheet sandstone of the Paleocene Ohio Creek Conglomerate, which itself unconformably overlies and latest Cretaceous fluviodeltaic strata of the Williams Fork Formation (Heller et al., 2013). The Wasatch Formation is conformably overlain by the lacustrine Green River Formation. The Wasatch Formation can be divided into three members (from bottom to top), the Atwell Gulch Member, the Molina Member, and the Shire Member (Fig. 2; Fig. 3A&B; Donnell, 1969). Existing data sets suggest that the PETM occurs in the basal portion of the Molina Member (Fig. 2; Burger, 2012; Foreman et al., 2012).

The Atwell Gulch Member contains alluvial strata and is Paleocene in age based on biostratigraphic and radiometric. The member ranges in thickness from 200-350 m and consists of

lithofacies characteristic of both fluvial and lacustrine systems (Donnell, 1969; Johnson and Flores 2003). The fluvial deposits are typically 3.5 m thick, single- and multi-story channel bodies and associated with well-developed levees. Paleosol deposits are ubiquitous within Atwell Gulch Member, often displaying red, orange, and purple mottling (Fig. 3). Fluvial sandbodies represent approximately 10% of the member and overbank strata the remainder of the member. Black organic-rich shales interbedded with fine-grained sandstone containing oscillation ripples are widespread and located in the upper parts of the member (Fig. 3; Donnell, 1969; Foreman et al., 2012; Foreman and Rasmussen, 2016). The lithofacies have been interpreted to be swamp and shallow lake deposits (Donnell, 1969; Johnson et Flores, 2003; Foreman and Rasmussen, 2016). Lying above the swamp and lake deposits are a few meters to tens of meters of fluvial and overbank related units prior to the onset of the Molina Member (Donnell, 1969; Johnson et Flores, 2003; Foreman and Rasmussen, 2016).

The timing of deposition of the Atwell Gulch Member is constrained by several data points. The underlying Ohio Creek Conglomerate contains mammal fossils of the Tiffanian-3 North American land mammal age, specifically *Nannodectes simpsoni*, and pollen indicative of the late Paleocene (Patterson et al., 2003; Burger, 2007). These suggest the lowermost Atwell Gulch Member initiated deposition approximately 60 Ma. This date is further supported by recent maximum depositional age estimates from U-Pb geochronology on detrital zircons recovered from the contact of the Ohio Creek Conglomerate and Atwell Gulch Member of 63.1 Ma ± 1.2 (Foreman et al., in prep). Maximum depositional ages from detrital zircons within the Atwell Gulch Member itself yield dates of 59.3 Ma ± 1.4 (Foreman et al., 2012; Foreman and Rasmussen, 2016). Additionally, the Atwell Gulch Member contains mammal fossils indicative of the Tiffanian and Clarkforkian (*Plesiadapis dubius; Ectocion mediotuber; E. osbornianus*) North American land

mammal ages in the Bighorn Basin that proceeds the Paleocene-Eocene boundary (Fig. 2; Gingerich, 2001; Gingerich, 2003; Burger and Honey, 2008). When combined with radiometric and mammal fossils, pollen records within the Atwell Gulch Member also support a Paleocene age, specifically the presence of *Zlivisporis* which has its last occurrence in the Paleocene (Fig. 2; Johnson and May, 1978) When combined with overlying chronostratigraphic constraints the Atwell Gulch Member was likely deposited between 60 Ma and 56 Ma.

The Molina Member overlies the Atwell Gulch Member and its onset corresponds with the carbon isotope excursion of the PETM (Burger 2012; Foreman et al. 2012). The thickness of the member ranges from 10-150 m and is composed of approximately 60% fluvial sandstones (Donnell, 1969; Johnson and Flores, 2003; Foreman et al., 2012). The Molina Member thins to the north and to the west away from the Sawatch Mountains and Uncompahgre Uplift (Fig. 2). These multi-story sandbodies are composed of abundant upper-flow-regime sedimentary structures, including upper-plane bed laminations (Fig. 3; Lorenz and Nadon 2002; Foreman et al. 2012). The sandbodies are notably thicker and wider, 7 meters and 150 meters on average respectively, than fluvial sandbodies in the rest of the Wasatch Formation (Foreman et al. 2012). Floodplain strata of the Molina Member in the basin center are characterized by abundant crevasse-splay deposits and purple and brown paleosols (Donnell, 1969; Lorenz and Nadon 2002; Foreman et al. 2012, Foreman and Rasmussen, 2016). In the western portions of the Piceance Creek Basin the Molina Member thins towards the Douglas Creek Arch (Fig. 2), and fluvial sandbodies become thinner and less numerous (Fig. 2). The member grades into stratigraphic interval of well-developed paleosols and red-tinted thin sandbodies, informally called the "Rusty Beds" in the Winter Flats study area along South Shale Ridge (Fig. 2&3).

Although no mammal fossils nor pollen records have been recovered from the Molina Member, likely due to a combination of taphonomic causes and modern vegetation cover of the overbank strata, the lower portion of the member most likely correlates to the PETM and the upper portion of the member the earliest Eocene. Foreman et al. (2012) and Burger (2012) both identified an approximately 3‰ negative carbon isotope excursion in bulk organic $\delta^{13}C$ values in two separate stratigraphic sections (Fig. 2), which matches the magnitude observed in several stratigraphic sections in the Bighorn Basin of Wyoming at Polecat Bench (Magioncalda et al., 2004; Baczynski et al., 2013; 2016). Moreover, the PETM is the only major $\delta^{13}C$ excursion between the latest Paleocene and earliest Eocene.

The Shire Member overlies the Molina Member and ranges in thickness from 180-1200 meters. The relative abundance of fluvial sandbodies in the member is lower compared to the Molina Member, approximately 25% (Donnell, 1969; Johnson and Flores, 2003; Foreman et al., 2012). The sandbodies are typically ~5 m thick, lenticular in geometry, ~25 m wide, dominated by lower flow regime sedimentary structures (i.e., trough cross beds), and can be either single- or multi-storied (Foreman et al., 2012). However, the overall abundance of fluvial sandbodies appears to vary across the basin, with a greater density of fluvial sandbodies near the basin margins (Donnell, 1969; Johnson, 2003). Overbank deposition consists predominantly of red, pink, and purple paleosols, with particularly thick accumulations occurring in the center portion of the basin (Donnell, 1969; Johnson and Flores, 2003; Foreman et al. 2012, Foreman and Rasmussen, 2016). The Shire Member is Eocene in age based on biostratigraphic constraints. The lower Shire Member contains the first occurrence of the pollen taxa *Platycarya* an early Eocene index fossil as well as *Syncolporites,* a taxon whose range spans both the Paleocene and Eocene (Johnson and May, 1978). Outside of the Winter Flats study area the Shire Member (north along I-70; Fig. 2) contains

abundant Wasatchian land mammal age fossils indicative of the earliest Eocene (Burger, 2009). Higher stratigraphically, the Shire Member gradually grades into the Green River Formation, and a radiometric date of an ash near this gradational formation contact yielded an age of 53 Ma (Smith et al., 2008).

METHODS

Field and laboratory datasets focus on a 124-meter thick stratigraphic section measured in the Winter Flats area of the Piceance Creek Basin along South Shale Ridge, west of the town of DeBeque, Colorado (N39.30710°, W108.41143°). The Wasatch Formation thins to the west in this area as it abuts the Douglas Creek Arch, but fluvial sandbodies also decrease and the strata dominated by overbank deposition (Mercier and Johnson, 2012). Targeting this area allowed for a more continuous record of floodplain pedogenic development spanning the potential PETM interval in comparison to the stratigraphic section closer to the basin center, which straddled thick fluvial sandbodies (Burger, 2012; Foreman et al., 2012). Our methodologies include detailed field descriptions, bulk organic stable carbon isotope values, and whole-rock geochemistry. Data collection mirrors that of several recent studies in the Bighorn Basin (Kraus and Riggins, 2007; Adams et al., 2011; Kraus et al. 2013; 2015; Baczynski et al., 2016) that aimed to determine mean annual precipitation and floodplain drainage within the continental interior spanning the PETM. All data is available within the Appendices.

Field Techniques

The onset Molina Member of the Wasatch Member correlates with the PETM carbon isotope excursion at multiple locations within the Piceance Creek Basin (Burger, 2012; Foreman et al., 2012). We traced the member to the west of the town of DeBeque, Colorado, where it grades into a series of thinner, rusty-colored tabular sandbodies that overlie a distinct organic-rich black shale unit (Fig. 2; Johnson and Finn, 1986). Our stratigraphic section begins below a thick, dark grey and carbonaceous shale unit, which crops out continuously across most of the basin (Donnell, 1969; Johnson, 1984; Johnson and Finn, 1986). The unit is known to be Paleocene in age based on pollen fossils (Fig. 2; Johnson and May, 1978). At the stratigraphic section fresh rock material was exposed by trenching. We expected the PETM to be recorded above the carbonaceous shale unit and within the 'rusty sandstone beds' that approximately correlates with the Molina Member (Foreman et al., 2012; Burger, 2012). The stratigraphic section was measured using a Jacob's staff and brunton compass. Field descriptions followed standard observations including: bed thickness, grainsize, bed contacts, sedimentary structures, pedogenic structures, general trace fossil descriptions, and mottling patterns were characterized using a Munsell Color Chart. Fist-sized samples were collected every 25 cm on average with higher density sampling occurring within soil horizons (up to 10 cm vertical sampling).

Stable Isotope Geochemistry

This study developed a high-resolution bulk organic stable carbon isotope stratigraphy to constrain the stratigraphic position of the Paleocene-Eocene Thermal Maximum (PETM). While bulk organic $\delta^{13}C$ values tend to be "noisier" than other proxy methods they allow the finest vertical density of samples to be obtained (e.g., Foreman et al., 2013; Baczynski et al., 2013;

Baczynski et al., 2016). The source of this variability and "noise" is examined in more detail below in the Discussion. Carbon isotope values from pedogenic carbonate nodules tend to yield greater signal-to-noise ratios, and distinct, more reliable negative carbon isotope excursions associated with the PETM (Bowen et al., 2001; Baczynski et al., 2013; Baczynski et al., 2016). These proxies have been used extensively in the Bighorn Basin of Wyoming, along with compound specific $\delta^{13}C$ records (Bowen et al., 2001; Smith et al., 2007). However, in contrast to the Willwood Formation in the Bighorn Basin, which contains several soil horizons with pedogenic carbonate nodules and lithofacies appropriate to obtain compound specific $\delta^{13}C$ values, the Wasatch Formation in the Piceance Creek Basin contains only isolated occurrences of pedogenic carbonate nodules. Pilot efforts at compound specific records yielded insufficient concentrations of leaf wax *n*-alkanes to reliably determine $\delta^{13}C$ values (pers. comm. Allison Baczynski).

Preparation techniques for bulk organic carbon isotope records follow the "weak" acid and rinse method utilized by several previous studies (Magioncalda et al., 2004; Wing et al., 2005; Baczynski et al., 2013; Baczynski et al., 2016). This differs from the "strong acid" method (promoted by Larson et al. 2008) applied by Foreman et al. (2012) in the Wasatch Formation and differs from the "soaking" method used by Burger (2012). Both Foreman et al. (2012) and Burger (2012) successfully identified the PETM, and recent work in the Wasatch Formation suggest the "strong" and "weak" acid preparation techniques produce nearly identical $\delta^{13}C$ records even amongst stable isotope laboratories (Denis et al., in prep.). The bulk organic preparation method involves grinding fresh rock with a mortar and pestle into a fine powder (~ 1.5 grams) and dissolving any carbonate (e.g., cements or limestone grains) with 10 mL of 0.5 N HCl. The sample and hydrochloric acid were mixed using vortex mixer and then sat for approximately an hour. The samples were placed into a centrifuge, reacted acid was decanted, and the acidification procedure

repeated 2 times. Subsequent to acidification the samples were rinsed 5 times with deionized water until a neutral pH was achieved. Samples were dried in an oven then weighed and loaded into tin capsules. Carbon isotope ratios and weight percent total organic carbon (%C) were measured using a Thermo Delta V Isotope Ratio Mass Spectrometer with coupled Element Analyzer housed at the University of Colorado at Boulder Earth Systems Stable Isotope Laboratory. In total 260 samples were analyzed, including 38 replicates. The results were reported in ‰ in standard δ notation where,

$$\delta^{13}C = (R_{sample}/R_{standard}-1)*10^3,$$

where R_{sample} and $R_{standard}$ represent the ratio of $^{13}C/^{12}C$ in the sample and reference standard, respectively. All $\delta^{13}C$ values are reported relative to Vienna Pee Dee Belemnite (VPDB) and evaluated against internal standards. Analytical uncertainty for $\delta^{13}C$ values is ±0.1‰. Replicate analyses of unknown samples (n = 38 pairs of replicates) display $\delta^{13}C$ offsets an average of 1.0‰ ± 1.6 (1σ) and %C content offsets on average of 0.48% ± 1.57 (1σ).

Soil Morphology Index

In the field paleosols were identified by a variety of sedimentologic indicators of pedogenic modification and subdivided into horizons. Horizons were identified based on differences between grain size, sedimentary structures, ped structures, matrix and mottle colors, and the presence of pedogenic nodules. Our approach mirrors that of the extensive paleosol studies undertaken in the Willwood Formation of the Bighorn Basin (Bown and Kraus, 1981; Kraus, 1997; Kraus and Riggins; 2007; Adams et al., 2011; Abels et al., 2013). Up-section changes in floodplain drainage were semi-quantitatively assessed by applying the novel soil morphology index developed by

Adams et al. (2011), and applied extensively by Abels et al. (2013) and Kraus et al. (2013) to the Willwood Formation in the Bighorn Basin.

The soil morphology index (SMI) entails a ranking system that assigns points to various morphologic features found in the B-horizon of soils, which are linked to either poorly-drained or well-drained conditions modern soils (Vidic and Lobnik, 1997; Harden, 1982; Calero et al., 2008; Adams et al., 2011). Specifically, it characterizes the soil matrix chroma (using a Munsell Color Chart), the presence/absence/size of pedogenic carbonate nodules, and the presence/absence of Fe-Mn nodules (Adams et al., 2011). Higher indices (those with high chroma, larger carbonate nodules, and no Fe-Mn nodules) indicate drier, well-drained conditions, whereas low indices (those with low chroma, no carbonate nodules, and Fe-Mn nodules) indicate wetter, more poorly drained conditions (Adams et al., 2011). Importantly, the soil morphology index of thick B-horizons (> 1.0 m) appears to track estimates of mean annual precipitation based on paleofloral records and soil geochemistry (Wing et al., 2005; Adams et al., 2011; Kraus et al., 2013; 2015). Adams et al. (2011) proposed this correlation indicated that the thicker B-horizon soils reached equilibrium with prevailing rainfall conditions. Herein we use the soil morphology of both 'thick' (> 1.0 m) and 'thin' B-horizons (<1.0 m). In this study a SMI value is calculated in approximately 10 cm increments through each B-horizon and then averaged in order to account for outliers and variations within the data within the horizon. The soil morphology of the ‘thick’ and ‘thin’ B-horizons are used as both an independent cross-check on mean annual precipitation estimates from soil geochemistry as well as a finer-scale assessment of floodplain drainage.

The justification for using chroma is based on studies that indicate that the duration of soil saturation increases the chroma decreases, and that low values of chroma correspond to seasonal saturation and gleying of soils (Evans and Franzmeier, 1986; Veneman et al., 1998). While

diagenetic overprinting of the original soil colors and chroma can occur (e.g., PiPujol and Buurman, 1994), diagenesis would result in wholesale changes in throughout the stratigraphic interval that would destroy fine-scale variability. This is not observed in the Wasatch Formation. However, it is acknowledged that almost certainly the original colors and chromas have been altered since the time of deposition during burial as well as by incipient modern-day weathering despite our best attempts to expose fresh material (Maxbauer et al., 2016). When interpreting our results we take the conservative approach of previous studies, which concluded that while the true values may be modified during burial diagenesis and lithification the *relative* changes between beds and horizons over relatively short (hundreds of meters) stratigraphic intervals are likely robust indicators of relative paleoenvironmental change (Adams et al., 2011; Kraus et al., 2015; Maxbauer et al., 2016). In total the soil morphology index was calculated for 32 individual B-horizons in the stratigraphic section measured.

Whole-Rock Geochemistry

Twenty-seven paleosol profiles were selected for detailed whole-rock geochemical analyses to determine major oxide and trace element compositions. The profiles were preferentially chosen based on the clear development of the horizons, clear pedogenic features that allowed identification of soil types, and stratigraphic position within the Atwell Gulch, Molina Member equivalent 'Rusty Beds', and Shire Member. Each paleosol profile was sampled at several vertical positions (typically every 10 cm) through C-, B-, and, when present, A-horizons (Fig. 3). This approach matches sampling methodologies of previous studies in other basins during other geologic time periods (Sheldon et al., 2002; Nordt and Driese, 2010; Kraus, 2013; Hyland et al., 2015; Kraus et al., 2015). This approach yields detailed geochemical profiles through the paleosols

that aid in evaluating weathering patterns and identification of specific horizons (Sheldon et al., 2002; Nordt and Driese, 2010; Adams et al., 2011; Kraus et al., 2013; Kraus et al., 2015).

Whole-rock geochemistry was determined by X-ray fluorescence spectrometry using a ThermoARL X-ray Fluorescence Spectrometer (XRF) housed at the Peter Hooper Geoanalystical Laboratory at Washington State University School of the Environment. A total of 172 individual samples were submitted for analysis from 27 distinct paleosol profiles. Details of the single low dilution Li-tetraborate fused bead method and instrument analysis can be found in Johnson et al. (1999) and summarized here. All samples were ground into a fine powder in a tungsten carbide swing mill. Subsequently, 3.5 g of sample powder were mixed with 7.0 g of spec pure dilithium tetraborate, and placed in graphite crucibles. The sample powder is introduced to a muffle furnace set to 1000°C, and fusion takes approximately 5 minutes. After cooling the beads are reground and fused a second time. The refused beads are then polished, washed in an ultrasonic cleaner, rinsed in alcohol, and dried. Beads are introduced to the XRF and unknown sample results include the concentration of 27 elements measured against the X-ray intensity of known external standards, precision is determined by regular analysis of internal standards every 28 unknown samples. The XRF operates at a constant voltage and amperage (50 kV and 50 mA, respectively) using a Rhodium target in a full vacuum. Analytical precision for major oxides is better than 0.05% and better than 2 ppm on average for trace elements with the exception of Ba and Ce, which is better than 11 ppm based on analysis of standards (BCR-P and GSP-1). Replicate analyses of unknown samples display produce major oxide values within 0.2% of one another and trace element concentrations within ~1 ppm of one another on average.

Mean annual precipitation (MAP) estimates were made based on an average of at least three, but typically five independent, sample measurements within the B-horizon of paleosols. Past

studies have shown this to be sufficient to capture typical geochemical variability in a soil horizon (Sheldon et al., 2002; Nordt and Driese, 2010; Adams et al., 2011; Kraus et al., 2013; Kraus et al., 2015). Hydrolysis reactions causes chemical weathering within the soils that cause feldspars to weather into clay minerals, an effect that increases as precipitation and temperature increases in modern soil compilations (Sheldon et al., 2002; Nordt and Driese, 2010). Wetter and warmer climates will accelerate the alteration of Ca-, Mg-, Na-, and K-rich soils into Al-rich soils (Sheldon et al., 2002). This type of weathering process produces a correlation among chemical indices of alteration in soils with mean annual precipitation (MAP) across several soil systems (Sheldon et al., 2002; Nordt and Driese, 2010). A correlation exists with mean annual temperature (MAT), but it is significantly weaker (Sheldon et al., 2002). In clay-rich soils characterized by shrink-swell features (i.e., vertisols), such as those seen in the Bighorn and Piceance Creek basins, researchers have used the CALMAG weathering index, which shows a strong correlation to MAP (Nordt and Driese, 2010). The CALMAG index is defined as $Al_2O_3/(Al_2O_3 + CaO + MgO) \times 100$ (Nordt and Driese, 2010), with oxides converted to mole weight percent. This proxy captures the flux of calcium to magnesium derived from calcium carbonate, detrital clay, and exchangeable Ca^{2+} and Mg^{2+} (Nordt and Driese, 2010). Herein this methodology was applied to obtaining MAP estimates it includes a root mean square error of ±108 mm/year.

RESULTS

Carbon Isotope Record

Bulk organic $\delta^{13}C$ values were determined from throughout the 124-meter stratigraphic section. Over 260 samples were analyzed at an average vertical spacing of approximately 0.5 meters, however, in many cases the vertical sampling density was close to every 10 cm. The $\delta^{13}C$ values exhibit a broad range of values from -29.3‰ (VPDB) to -17.6‰, a mean value of -22.5‰ ± 1.4‰ (1σ), and a median value of -22.4‰. The weight of percent organic carbon (%C) in the section ranges from 0.01% to 7.46%. The mean value is 0.37% ± 0.99% (1σ), and the median value is 0.19%. There is a weak logarithmic correlation (R^2 = 0.32065) amongst %C and $\delta^{13}C$ values (Fig. 4A). Various soil degradation and respiration processes have been documented to generated a strong correlation between these two variables in both modern and ancient soil sequences (Wing et al., 2005; Wynn et al., 2005; 2006; Wynn 2007). Figure 4B shows the relationship between $\delta^{13}C$ values and lithology as box-and-whisker plots. Both parametric (one-way ANOVA) and non-parametric (Kruskal-Wallis) statistical tests yield p-values less than 0.05 (F =3.597; p-value=0.007134 and χ^2 = 25.24; p-value=0.00004495). However, these differences are potentially related to the uneven distribution of lithofacies within the stratigraphic section and the effects of the PETM. Specifically, when sample locations below the 60-meter level (i.e., the hypothesized PETM interval) are removed from the statistical analyses the one-way ANOVA and Kruskal-Wallis tests cannot reject the null hypothesis that the mean and median $\delta^{13}C$ values from the different lithofacies were drawn from the same underlying population (F =1.17; p-value=0.331 and χ^2 = 8.055; p-value=0.08958) at the 0.05 significance level.

Up-section $\delta^{13}C$ values show a large amount of variability (Fig. 5). Samples in relatively close proximity to one another, a few meters, can show difference of up to ~5‰ although the

majority show differences less than 1‰. However, there is larger scale structure to the $\delta^{13}C$ record. A LOESS smoothing procedure (smoothing factor of 0.2) was applied to the dataset to illustrate this structure (Fig. 5). The smoothing procedure is a common, non-parametric regression method that fits a linear function to a subset of the data. The individual $\delta^{13}C$ values are weighted based on their relative vertical distance from one another, and a 95% confidence interval generated on 999 "boot-strapped" random replicates from resampling the residuals of the original data points (Hammer et al., 2001). This procedure emphasizes a gradual negative shift in $\delta^{13}C$ values starting from the base of the stratigraphic section, reaching minimum $\delta^{13}C$ values at approximately the 35-meter level, followed by a gradual return to higher $\delta^{13}C$ values by approximately the 55-meter level. $\delta^{13}C$ values within this stratigraphic interval show decreased range of values as compared to samples above the 55-meter level. Subsequently, $\delta^{13}C$ values progressively become lower, but display a greater range over short stratigraphic distances (Fig. 5).

Floodplain Drainage

We use the soil morphology index (SMI) to broadly characterize floodplain drainage within the measured stratigraphic section. In total 32 paleosols were characterized. Overall SMI values through the entire stratigraphic section range from 3 to 16, on a 20-point scale wherein 20 is the best-drained conditions and 0 the poorest-drained condition (Adams et al., 2011). The average value for the stratigraphic section is 7.3 ± 3.3‰ (1σ), and a median value of 7. Within individual B-horizons, SMI metrics are typically display values within 0-2 points of one another. When plotted against stratigraphic height the SMI results define 3 distinctive stratigraphic zones (Fig. 5). Respectively, these 3 zones correlate with the Atwell Gulch Member, the Molina Member equivalent Rusty Beds, and the Shire Member (Fig. 5)

The first stratigraphic zone occurs within the first ~40 meters within the Atwell Gulch Member. On average, the SMI value within this zone is 6.1 ± 1.6 (1σ) and a range of 3 to 8. The next stratigraphic zone occurs between the 40-meter level and the 55-meter level, and correlates with the Rusty Beds of the Molina Member. The average SMI value in this zone is 13.2 ± 3.0 (1σ), and a median value of 14. The uppermost stratigraphic interval occurs above the 55-meter level and corresponds with the Shire Member of the Wasatch Formation. The average SMI value in this zone is 6.4 ± 2.1 (1σ), and a median value of 6.8. Notably the shift in SMI values corresponds to the upper 5-10 meters of the negative carbon isotope shift identified above.

Mean Annual Precipitation

Estimates of mean annual precipitation (MAP) derived from the CALMAG index (Nordt and Driese, 2010) display an average value of 1396 mm/year ± 332 (1σ), with a median of 1518 mm/year for the entire stratigraphic section studied. However, similar to the floodplain drainage data, MAP estimates define three distinct stratigraphic intervals (Fig. 5). Within the first ~40 meters of the Winter Flats section MAP displays an average of 1572 mm/year ± 48 (1σ), and a median value of 1580 mm/year. Above this stratigraphic zone, between the 40-meter level and 60-meter level heights, MAP averages 883 ± 490 (1σ), with a median of 622 mm/year. However, the lowest three MAP estimates in this interval yield a combined average estimate of 532 mm/year. Above the 55-meter level MAP averages 1490 mm/year ± 128 (1σ), with a median of 1527 mm/year. Importantly, the up-section decrease in MAP corresponds with the Rusty Beds interval of the Molina Member, the higher SMI values, and the upper portion of the shift in bulk organic $\delta^{13}C$ record towards lower values (Fig. 5). This represents between 40% to 65% decrease in MAP.

DISCUSSION

Interpretation of Carbon Isotope Record

Bulk organic $\delta^{13}C$ values tend to be "noisier" than other proxy records of the carbon cycle due to a variety of causes. These include averaging of different plant functional types, plants that use different photosynthetic pathways (i.e., C4, C3, CAM), variability in preservation/degradation of different plant chemical compounds (e.g., lignin, hemicellulose, lipids) or plant anatomy (e.g., leaves, roots, bark), and inclusion of recalcitrant, "fossil" carbon derived from sedimentary rocks in the source area. Some of these factors likely influenced the observed carbon isotope record at the Winter Flats area, however, many can be eliminated as a contributing factor.

Changes in the carbon cycle through time can be tracked using marine and nonmarine geochemical proxies that incorporate stable carbon isotopes into their mineral or organic materials in predictable ways (Koch, 1998). For example, during photosynthesis plants fractionate between ^{13}C and ^{12}C in the atmosphere and preferentially incorporate ^{12}C into their biomass (Farquhar et al., 1980; Arens et al., 2000; Jahren et al., 2008). This fractionation is mostly independent of atmospheric partial pressure of carbon dioxide, weakly dependent on temperature, and partially dependent on the water stress levels of the plant. The strongest control appears to be the photosynthetic pathway utilized by the plant (i.e., C3, C4, CAM) (Farquhar et al., 1989; Ehleringer & Monson. 1993). The majority of paleobotanical evidence suggests C4 plants had not evolved or become widespread until the Neogene (Cerling et al., 1993), and there is no *a priori* reason to suspect that plants that utilize the CAM photosynthetic pathway, mostly succulents that represent a minor plant biomass on modern landscapes, were widespread during the early Paleogene (Wing & Currano, 2013). Finally, the observed range in bulk $\delta^{13}C$ values in this study is wholly within the typical range expected for C3 photosynthesizing plants (Koch, 1998; Arens et al., 2000; Jahren

et al., 2008). Plant functional type (e.g., evergreen gymnosperms, deciduous/evergreen angiosperms) can also influence the average $\delta^{13}C$ value of a plant (Diefendorf et al., 2010), however, at maximum this can account for 2.7‰ of variability in the record and requires the unlikely, wholesale turnover of the entire vegetation structure over incredibly short stratigraphic distances (i.e., 10-50 cm). Thus, we can rule out these factors and posit the observed variability likely represents a combination of changes in the taphonomic/diagenetic, local environmental conditions, and "true" $\delta^{13}C$ values of atmospheric CO_2.

Taphonomic and diagenetic processes result in modified bulk $\delta^{13}C$ values because different plant anatomical parts and chemical compounds are variably susceptible to preservation and break down under burial conditions. Within a plant the $\delta^{13}C$ value of leaves, stems, bark, and roots can vary by at least 2‰ from the bulk average of the plant (Tieszen, 1991; Codron et al., 2005). Thus, differential preservation of these materials within the sediment will produce variability in the bulk organic $\delta^{13}C$ value observed. This variability is difficult to identify directly in the samples because most of the organic matter analyzed for $\delta^{13}C$ values is unobservable due to its small size. However, one might expect differential preservation of plant anatomy related to the energy of the sediment transport process, which roughly corresponds to grain size. However, there does not appear to be a meaningful difference in the $\delta^{13}C$ values of different lithologies (Fig. 4). Relatedly, the introduction of fossil, recalcitrant carbon may, in some cases, affect the bulk organic $\delta^{13}C$ values (Baczynski et al., 2013; 2016). In the Bighorn Basin old carbon, delivered to the basin from eroded Cretaceous-aged sedimentary rock from adjacent Laramide uplifts is sufficient to erase the carbon isotope excursion associated with the PETM as recalcitrant carbon tends to be isotopically heavier than *in situ* vegetation matter (Baczynski et al., 2013; 2016; Lyons et al., 2019). In the Piceance Creek Basin, Foreman and Rasmussen (2016) identified the Cretaceous-aged, deltaic Mesa Verde

Group and open marine Mancos Shale geologic units as the dominant sediment source for the Wasatch Formation, suggesting recalcitrant carbon could be affecting the Winter Flats $\delta^{13}C$ record. Yet this process would also likely produce different $\delta^{13}C$ values amongst lithologies, in particular causing anomalously higher $\delta^{13}C$ values in sandstones. This is not observed at Winter Flats. It is possible, however, that fossil carbon input was not limited to specific lithofacies. Furthermore, several studies have noted the correlation between bulk organic $\delta^{13}C$ values and %C as pedogenic and diagenetic processes proceed during soil formation and lithification of sediment, respectively (Sackett et al., 1970; McKirdy and Powell, 1974; Tissot et al., 1974; Wynn et al., 2006; Wynn, 2007; Blair and Aller, 2012). This is due to the variable stability of different chemical compounds such as lignin, lipids, sugars, and hemicellulose and typically causes a logarithmic relationship to develop between $\delta^{13}C$ and %C values (Deines, 1980; Medina et al., 1986; Benner et al., 1987; Wedin et al., 1995; Boutton, 1993; Dawson et al., 2002; Wynn et al., 2006; Wynn, 2007). This occurs in other early Paleogene strata (Wing et al., 2005), but does not appear to be a significant issue in this study (Fig. 4).

Bulk $\delta^{13}C$ values can also be influenced by local environmental conditions due to a variety of ecophysiological controls and responses in plants to water stress, humidity. moisture, temperature, salinity, and nitrogen availability experienced by the plant during growth (Farquhar et al., 1989; Ehleringer, 1993; Dawson et al., 2002). Water stress tends to be the strongest signal and global compilations suggest a non-linear relationship between mean annual rainfall and the $\delta^{13}C$ value of leaves in an area (Kohn et al. 2010). Roughly, it requires a change in mean annual precipitation of 330 mm/year to 540 mm/year to cause approximately a 1‰ change in leaf $\delta^{13}C$ value (Diefendorf et al., 2010; Kohn et al., 2010). A decrease in mean annual precipitation causes a $\delta^{13}C$ value of leaves as plants close their stomata in response to water stress, leading to greater

incorporation of ^{13}C into the plant tissues (Kohn et al., 2010). This is insufficient to explain the substantial, rapid variability in bulk $\delta^{13}C$ value of several per mille over short stratigraphic distances (Fig. 5). It would require massive change in mean annual rainfall and hydrologic conditions of several magnitudes within a single depositional bed. Thus, we conclude the majority of the bulk organic $\delta^{13}C$ variability observed is related to more stochastic processes, similar to those observed by Foreman et al., (2013) within Paleogene strata of Washington State, U.S.A., and Alberta, Canada.

Although the bulk organic $\delta^{13}C$ record at Winter Flats does not contain as distinct a carbon isotope excursion as Sulfur Gulch section of Burger (2012) and the X section of Foreman et al., (2012) a subtle, but clear shift toward lower $\delta^{13}C$ values in the lower portion of the section and return to previous values does occur (Fig. 2&5). This shift is small 1.5‰ to 2‰, but its structure as well as its lithostratigraphic and biostratigraphic position suggests it may represent the PETM. In global databases the majority of bulk organic $\delta^{13}C$ records document a negative carbon isotope excursion of ~3.5‰ (McInerney & Wing, 2011), and this is the magnitude observed at the Sulfur Guch section of Burger (2012) and X section of Foreman et al. (2012). If the isotopic shift at Winter Flats is the PETM interval, then the reduced magnitude may be due to locally reduced sedimentation rates that time-averages the $\delta^{13}C$ record. Essentially, organic carbon continues to accumulate within the cumulative soil profiles (stacked and overprinted B-horizons) causing mixing of pre-PETM, PETM, and post-PETM organic carbon to be accumulated within the same sedimentary bed. Alternatively, the observed reduction in excursion size and partial offset in hydrologic records and isotopic record may be related to the flux of fossil carbon into the basin. Recent work by Lyons et al. (2019) documented clear a clear "shortening" of the PETM isotopic record in bulk organic $\delta^{13}C$ record relative to carbonate $\delta^{13}C$ records derived from the same core.

This was attributed to the introduction of allochthonous, isotopically-heavier fossil carbon from eroded sedimentary strata in the hinterland (Lyons et al., 2019). Potentially, this could be affecting the records from the Winter Flats area as well. Additional work is necessary to assess this hypothesis specifically targeting pedogenic carbonate nodules for isotopic analysis. For the following section we tentatively proceed under the presumption that this particular isotopic shift represents the PETM.

Hydrologic Changes

Previous work in the Piceance Creek Basin ascribed the major shift in alluvial deposition represented by the Molina Member to either a tectonic origin (Johnson, 2003) or the unroofing of sand-rich eolianite lithologies within the Uncompahgre Uplift (Lorenz & Nadon, 2002). Subsequent research that assessed subsidence histories, paleoclimatic records, and sediment provenance in the basin indicate that most likely the Molina Member is the fluvial response to the PETM (Burger, 2012; Foreman et al., 2012; Heller et al., 2013; Foreman & Rasmussen, 2016). Foreman et al. (2012) documented increases in the flow depths and widths by ~50% within the Molina Member as well as a significant increase in the abundance of upper flow regime sedimentary structures. These observations were interpreted as being driven by increases in fluvial discharge and the peakedness of river hydrographs (Foreman et al., 2012). Greater sandbody thicknesses and widths with no attendant change in subsidence rates and provenance suggest the preferential export of fine-grained sediment out of the basin and deposition of sand within the basin (Foreman et al., 2012). This phenomenon is observed in other alluvial basins such as the Bighorn Basin of northwest Wyoming (Foreman, 2014) and Tremp-Graus Basin of Spain (Schmitz & Pujalte, 2007). In each of these basins an increase in hydrologic variability and "flashiness" of river discharge has been interpreted as these features of the rock record to do not correspond to

mean annual discharge conditions (Fielding, 2006; Plink-Björklund, 2015), but the conditions that do the majority of the "geomorphic work" (i.e., sediment transport). Broadly speaking these would be indicators of seasonal to interannual hydrologic cycle variability, and were interpreted to have increased channel mobility and efficiency of river transport (Schmitz & Pujalte, 2007; Foreman et al., 2012; Foreman, 2014)

Assuming the observed isotopic shift represents the PETM, the proxy records presented by this study suggest a significant increase in hydrologic variability within the basin. Soil morphology indices suggest enhanced floodplain drainage conditions, and soil geochemical records an overall decrease in mean annual rainfall of potentially 60%. Multiple factors are likely at work within this record. A shift in the seasonal distribution of rainfall could feasibly instigate a change in floodplain drainage conditions by two mechanisms. Shifting rainfall from a more uniform annual distribution to a rainy season could result in a longer time interval over which floodplains would dry between rainfall events. This could lead to greater drainage of pore fluids. Moreover, enhanced sediment transport and greater crevasse splay events observed within the Molina Member (Foreman et al., 2012) would have coarsened the grain size distribution of the floodplain allowing more efficient drainage and increased sedimentation rates, which would have led to a relative lowering of the water table. These inferences are consistent with the soil morphology indices (this study) as well as fluvial records (Foreman et al., 2012). Decreases in mean annual precipitation suggests the range of rainfall within the basin increased substantially as well. Using the ~50% increase in flow depths of rivers as a rough estimator of peak annual discharge (likely the rainiest month of the year) and the ~60% decrease in MAP from soil geochemistry, a total increase in rainfall variability of ~100% is inferred.

These observations are consistent with other paleoclimate records spanning the PETM in Laramide basins of the Western Interior. This study was designed to complement detailed paleosols proxy records from the Bighorn Basin of northwest Wyoming (Fig. 1). Soil morphology indices typically range between 2-8 in the Bighorn Basin outside of the PETM interval, within the range of those of the Piceance Creek Basin (Fig. 6; Kraus et al., 2013). Within the PETM interval the soil morphology indices record an increase in floodplain drainage, and indices of 11-17, which again overlaps with the morphology indices within the proposed PETM interval within the Piceance Creek Basin (Fig. 6; Kraus et al., 2013). These observations are consistent with both trace fossil assemblages within the Bighorn Basin that indicate better drained conditions within the floodplains (Smith et al., 2008) and greater fluvial channel mobility and potentially sediment flux during the PETM (Foreman, 2014). Soil geochemistry records document a ~40% decrease in MAP (Kraus & Riggins, 2007; Kraus et al., 2013) as do paleofloral records (Wing et al., 2005). In the Bighorn Basin there was a near 100% overturn in paleofloras from a conifer-dominated to angiosperm-dominated landscape and back again after the PETM (Wing et al., 2005). Some of the taxa (members of the Fabaceae family) present in the PETM are associated with dry tropical and subtropical areas today (Smith et al., 2007; Wing et al., 2005; 2009). When combined with the observations that river flow depths did not change in the Bighorn Basin, a similar pattern of decreased MAP and potentially increased range of rainfall appears to that hypothesized in the Piceance Creek Basin. The new precipitation and floodplain drainage record in the Piceance Creek Basin is also consistent with isotopic evidence for drying found by Bowen & Bowen (2008) in the Axehandle Basin of central Utah (Fig. 1). $\delta^{13}C$ values from pedogenic carbonate nodules record a reduced magnitude PETM carbon isotope excursion relative to the Bighorn Basin and a larger positive $\delta^{18}O$ excursion likely related to greater evaporative conditions in the area (Bowen &

Bowen, 2008). This pattern of greater drying in the southern Laramide-related basins is consistent with larger scale, global predictions that moisture transport bypassed mid-latitudes during the PETM and resulted in greater rainfall in polar regions (Pagani et al., 2006).

This study also supports global simulations of pre-PETM and PETM greenhouse conditions (Carmichael et al., 2017; 2018). During periods of elevated pCO_2 conditions in the atmosphere both paleoclimate models and models of future anthropogenic-induced warming yield an enhanced hydrologic cycle wherein evaporation and precipitation rates increase globally (Allen & Ingram, 2002; Dai & Trenberth, 2004; Trenberth, 2011; Carmichael et al., 2017; 2018). Broadly, during elevated carbon dioxide levels it is hypothesized that wet areas get wetter and dry areas become drier (Held & Soden, 2006; Chou & Neelin, 2004), but this pattern can vary substantially based on local to regional paleogeographic conditions as well as changes in atmospheric transport. The most recent coupled atmospheric-ocean general circulation model (HadCM3L) applied to the PETM suggests widespread drying within the Western Interior of North America. The spatial resolution of the model grid is ~300 km by ~300 km for the Laramide basins (Carmichael et al., 2018), which means basin-scale precipitation patterns are unresolvable. However, the overarching pattern is consistent with proxy-based observations. Specifically, model outputs indicate reductions in mean annual precipitation of 10% or greater, and decreases in the number of precipitation events by a similar percentage (Carmichael et al., 2018). Thus, rainfall was less and more infrequent consistent with soil morphology and geochemistry patterns in both the Bighorn Basin and Piceance Creek Basin. Interestingly, there appears to be an increase in the "tailed-ness" of rainfall during PETM conditions, which is represented in a greater magnitude of the 99th percentile rainfall events (Carmichael et al., 2018). This "tailed-ness" is greater in the southern Laramide region than in the northern (Carmichael et al., 2018). which may explain the prevalence

of upper plane bed, flashy discharge sedimentary structures during the PETM in the Piceance Creek Basin that are not represented in the Bighorn Basin (Foreman et al., 2012; Foreman, 2014).

CONCLUSIONS

This study provides a new record of hydrologic changes in the Piceance Creek Basin of northwest Colorado. It adds to a growing database that seeks to quantitatively constrain paleoenvironmental conditions within the Western Interior of North America during the Laramide Orogeny. New bulk organic carbon isotope records developed in the Winter Flats area of the Piceance Creek Basin, west of the town of De Beque potentially document a subtle isotopic shift related to release of isotopically-light, exogenic carbon during the Paleocene-Eocene Thermal Maximum. However, the carbon isotope record contains a high degree of variability and noise, which necessitates additional future work to more clearly resolve the potential PETM interval. Paleosol proxy records document better-drained conditions and reductions in mean annual rainfall associated with the subtle carbon isotope excursion. These patterns are larger than those observed in the Bighorn Basin of northwest Wyoming (Wing et al., 2005; Kraus & Riggins, 2007; Kraus et al., 2013) and consistent with recent circulation models (Carmichael et al., 2018). When integrated with fluvial sedimentologic datasets in the Piceance Creek Basin the two datasets suggest a greater range of rainfall variability, which is consistent with circulation models that predict an increase in extreme rainfall events during the PETM (Carmichael et al., 2018).

REFERENCES CITED

Abels, H. A., Kraus, M. J. & Gingerich, P. D. Precession-scale cyclicity in the fluvial lower Eocene Willwood Formation of the Bighorn Basin, Wyoming (USA). *Sedimentology* **60**, 1467-1483 (2013). doi: 10.1111/sed.12039

Adams, J. S., Kraus, M. J. & Wing, S. L. Evaluating the use of weathering indices for determining mean annual precipitation in the ancient stratigraphic record. *Palaeogeography, Palaeoclimatology, Palaeoecology* **309**, 358–366 (2011).

Allen, M. R. & Ingram, W. J. Constraints on future changes in climate and the hydrologic cycle. *Nature* **419**, 228–232 (2002).

Arens, N. C., Hope Jahren, A. & Amundson, R. Can C3 plants faithfully record the carbon isotopic composition of atmospheric carbon dioxide? *Paleobiology* **26**, 137–164 (2000).

Baczynski, A. A.., McInerney, F. A., Wing S. L., Kraus, M. J., Jonathan, Bloch I., Boyer, D. M., Secord, R., Morse, P. E. Chemostratigraphic implications of spatial variation in the Paleocene-Eocene Thermal Maximum carbon isotope excursion, SE Bighorn Basin, Wyoming: Bighorn Basin, Wyoming Petm Chemostratigraphy. *Geochemistry, Geophysics, Geosystems* **14**, 4133–4152 (2013).

Baczynski, A. A., McInerney, F.A., Wing, S. L., Kraus, M. J., Morse, P. E., Bloch, J. I., Chung, A. H., Freeman, K. H. Distortion of carbon isotope excursion in bulk soil organic matter during the Paleocene-Eocene thermal maximum. *Geological Society of America Bulletin* **128**, 1352–1366 (2016).

Baczynski, A.A., McInerney, F.A., Wing, S.L., Kraus, M.J., Bloch, J.I., Secord, R. Constraining paleohydrologic change during the Paleocene-Eocene Thermal Maximum in the

continental interior of North America. *Palaeogeography, Palaeoclimatology, Palaeoecology* **465**, 237–246 (2017).

Benner, R., Fogel, M. L., Sprague, E. K. & Hodson, R. E. Depletion of 13C in lignin and its implications for stable carbon isotope studies. *Nature* **329**, 708–710 (1987).

Blair, N. E. & Aller, R. C. The Fate of Terrestrial Organic Carbon in the Marine Environment. *Annual Review of Marine Science* **4**, 401–423 (2012).

Bolle, M.-P., Pardo, A., Adatte, T., Tantawy, A.A., Hinrichs, K.-U., Von Salis, K., Burns, S. Climatic evolution on the southern and northern margins of the Tethys from the Paleocene to the early Eocene. *GFF* **122**, 31–32 (2000).

Bornemann, A. *et al.* Persistent environmental change after the Paleocene–Eocene Thermal Maximum in the eastern North Atlantic. *Earth and Planetary Science Letters* **394**, 70–81 (2014).

Bowen, G. J., Beerling, D. J., Koch, P. L., Zachos, J. C. & Quattlebaum, T. A humid climate state during the Palaeocene/Eocene thermal maximum. *Nature* **432**, 495–499 (2004).

Bowen, G. J. & Beitler Bowen, B. Mechanisms of PETM global change constrained by a new record from central Utah. *Geology* **36**, 379 (2008).

Bowen, G.J., Maibauer, B.J., Kraus, M.J., Röhl, U., Westerhold, T., Steimke, A., Gingerich, P.D., Wing, S.L., Clyde, W.C. Two massive, rapid releases of carbon during the onset of the Palaeocene–Eocene thermal maximum. *Nature Geoscience* **8**, 44–47 (2015).

Bowen, G. J. & Zachos, J. C. Rapid carbon sequestration at the termination of the Palaeocene–Eocene Thermal Maximum. *Nature Geoscience* **3**, 866–869 (2010).

Bown, T. M. & Kraus, M. J. Lower Eocene alluvial paleosols (Willwood Formation, Northwest Wyoming, U.S.A.) and their significance for paleoecology, paleoclimatology, and basin analysis. *Palaeogeography, Palaeoclimatology, Palaeoecology* **34**, 1–30 (1981).

Bown, T. M. & Kraus, M. J. Lower Eocene alluvial paleosols (Willwood Formation, Northwest Wyoming, U.S.A.) and their significance for paleoecology, paleoclimatology, and basin analysis. *Palaeogeography, Palaeoclimatology, Palaeoecology* **34**, 1–30 (1981).

Bump, A. P. & Davis, G. H. Late Cretaceous–early Tertiary Laramide deformation of the northern Colorado Plateau, Utah and Colorado. *Journal of Structural Geology* **25**, 421–440 (2003).

Burger, B. J. & Honey, J. G. Plesiadapidae (Mammalia, Primates) from the late Paleocene Fort Union Formation of the Piceance Creek Basin, Colorado. *Journal of Vertebrate Paleontology* **28**, 816–825 (2008).

Burger, B. J. Northward range extension of a diminutive-sized mammal (Ectocion parvus) and the implication of body size change during the Paleocene–Eocene Thermal Maximum. *Palaeogeography, Palaeoclimatology, Palaeoecology* **363–364**, 144–150 (2012).

Calero, J., Delgado, R., Delgado, G. & Martín-García, J. M. Transformation of categorical field soil morphological properties into numerical properties for the study of chronosequences. *Geoderma* **145**, 278–287 (2008).

Carmichael, M.J., Inglis, G.N., Badger, M.P.S., Naafs, B.D.A., Behrooz, L., Remmelzwaal, S., Monteiro, F.M., Rohrssen, M., Farnsworth, A., Buss, H.L., Dickson, A.J., Valdes, P.J., Lunt, D.J., Pancost, R.D. Hydrological and associated biogeochemical consequences of rapid global warming during the Paleocene-Eocene Thermal Maximum. *Global and Planetary Change* **157**, 114–138 (2017).

Carmichael, M. J., Pancost, R. D. & Lunt, D. J. Changes in the occurrence of extreme precipitation events at the Paleocene–Eocene thermal maximum. *Earth and Planetary Science Letters* **501**, 24–36 (2018).

Cather, S.M., Chapin, C.E., Dickinson, W.R., Klute, M.A., Hayes, M.J., Janecke, S.U., Lundin, E.R., Mckittrick, M.A., Olivares, M.D. Paleogeographic and paleotectonic setting of Laramide sedimentary basins in the central Rocky Mountain region: Alternative interpretation and reply. *Geological Society of America Bulletin* **102**, 256–260 (1990).

Cerling, T. E., Wang, Y. & Quade, J. Expansion of C4 ecosystems as an indicator of global ecological change in the late Miocene. *Nature* **361**, 344–345 (1993).

Chou, C. & Neelin, J. D. Mechanisms of Global Warming Impacts on Regional Tropical Precipitation. *Journal of Climate* **17**, 2688–2701 (2004).

Clyde, W. C., Bartels, W. S., Gunnell, G. F. & Zonneveld, J.-P. 40Ar/39Ar geochronology of the Eocene Green River Formation, Wyoming: Discussion. *Geological Society of America Bulletin* **116**, 251 (2004).

Codron, J., Codron, D., Lee-Thorp, J.A., Sponheimer, M., Bond, W.J., de Ruiter, D., Grant, R. Taxonomic, anatomical, and spatio-temporal variations in the stable carbon and nitrogen isotopic compositions of plants from an African savanna. *Journal of Archaeological Science* **32**, 1757–1772 (2005).

Copeland, P., Lawton, T. L. & Muphy, M. A. Location, Location, Location: The variable lifespan of the Laramide Orogeny and implications for the ancient Grand Canyon hypothesis. (2016). doi:10.1130/abs/2016AM-284975

Crouch, E.M., Dickens, G.R., Brinkhuis, H., Aubry, M.-P., Hollis, C.J., Rogers, K.M., Visscher, H. The Apectodinium acme and terrestrial discharge during the Paleocene–Eocene

thermal maximum: new palynological, geochemical and calcareous nannoplankton observations at Tawanui, New Zealand. *Palaeogeography, Palaeoclimatology, Palaeoecology* **194**, 387–403 (2003).

Dai, A. & Trenberth, K. E. The Diurnal Cycle and Its Depiction in the Community Climate System Model. *Journal of Climate* **17**, 930–951 (2004).

Dawson, T. E., Mambelli, S., Plamboeck, A. H., Templer, P. H. & Tu, K. P. Stable Isotopes in Plant Ecology. *Annual Review of Ecology and Systematics* **33**, 507–559 (2002).

DeCelles, P. G. Late Jurassic to Eocene evolution of the Cordilleran thrust belt and foreland basin system, western U.S.A. *American Journal of Science* **304**, 105–168 (2004).

Deines, P. The isotopic composition of reduced organic carbon. in *The Terrestrial Environment* 329–406 (Elsevier, 1980).

Dickens, G. R. Rethinking the global carbon cycle with a large, dynamic and microbially mediated gas hydrate capacitor. *Earth and Planetary Science Letters* **213**, 169–183 (2003).

Dickens, G. R., Castillo, M. M. & Walker, J. C. G. A blast of gas in the latest Paleocene: Simulating first-order effects of massive dissociation of oceanic methane hydrate. *Geology* **25**, 259 (1997).

Dickinson, W. R. Evolution of the North American Cordillera. *Annual Review of Earth and Planetary Sciences* **32**, 13–45 (2004).

Diefendorf, A. F., Mueller, K. E., Wing, S. L., Koch, P. L. & Freeman, K. H. Global patterns in leaf 13C discrimination and implications for studies of past and future climate. *Proceedings of the National Academy of Sciences* **107**, 5738–5743 (2010).

Diefendorf, A. F., Freeman, K. H., Wing, S. L., Currano, E. D. & Mueller, K. E. Paleogene plants fractionated carbon isotopes similar to modern plants. *Earth and Planetary Science Letters* **429**, 33–44 (2015).

Donnell, J. *Paleocene and lower Eocene units in the southern part of the Piceance Creek basin, Colorado*. U.S. Geological Survey Bulletin **1274**, 1-18 (1969).

Ehleringer, J. R. Carbon and Water Relations in Desert Plants: An Isotopic Perspective. in *Stable Isotopes and Plant Carbon-water Relations* 155–172 (Elsevier, 1993).

Evans, C. V. & Franzmeier, D. P. Saturation, Aeration, and Color Patterns in a Toposequence of Soils in North-central Indiana. **50**, 975 (1986).

Farquhar, G. D., Ehleringer, J. R. & Hubick, K. T. Carbon Isotope Discrimination and Photosynthesis. *Annual Review of Plant Physiology and Plant Molecular Biology* **40**, 503–537 (1989).

Farquhar, G. D., von Caemmerer, S. & Berry, J. A. A biochemical model of photosynthetic CO2 assimilation in leaves of C3 species. *Planta* **149**, 78–90 (1980).

Fielding, C. R. Upper flow regime sheets, lenses and scour fills: Extending the range of architectural elements for fluvial sediment bodies. *Sedimentary Geology* **190**, 227–240 (2006).

Folk, R. L. The distinction between grain size and mineral composition in sedimentary rock nomenclature. *Journal of Geology* **62**, 344–359 (1954).

Foreman, B. Z. Climate-driven generation of a fluvial sheet sand body at the Paleocene-Eocene boundary in north-west Wyoming (USA). *Basin Research* **26**, 225–241 (2014).Foreman, B. Z., Clementz, M. T. & Heller, P. L. Evaluation of paleoclimatic conditions east and west of

the southern Canadian Cordillera in the mid-late Paleocene using bulk organic δ13C records. *Palaeogeography, Palaeoclimatology, Palaeoecology* **376**, 103–113 (2013).

Foreman, B. Z., Heller, P. L. & Clementz, M. T. Fluvial response to abrupt global warming at the Palaeocene/Eocene boundary. *Nature* **491**, 92–95 (2012).

Foreman, B. Z. & Rasmussen, D. M. Provenance Signals In the Piceance Creek Basin: Unroofing of the Sawatch Range and Extent of the Early Paleogene California River System (Colorado, U.S.A.). *Journal of Sedimentary Research* **86**, 1345–1358 (2016).

Gehler, A., Gingerich, P. D. & Pack, A. Temperature and atmospheric CO_2 concentration estimates through the PETM using triple oxygen isotope analysis of mammalian bioapatite. *Proceedings of the National Academy of Sciences* **113**, 7739–7744 (2016).

Gingerich, P. D. Biostratigraphy of the continental Paleocene–Eocene boundary interval on Polecat Bench in the northern Bighorn Basin. *University of Michigan Papers on Paleontology* **33**, 37–71 (2001).

Gingerich, P. D. Mammalian responses to climate change at the Paleocene-Eocene boundary: Polecat Bench record in the northern Bighorn Basin, Wyoming. *Geological Society of America* 463–478 (2003).

Harden, J. W. A quantitative index of soil development from field descriptions: Examples from a chronosequence in central California. *Geoderma* **28**, 1–28 (1982).

Held, I. M. & Soden, B. J. Robust Responses of the Hydrological Cycle to Global Warming. *Journal of Climate* **19**, 5686–5699 (2006).

Heller, P. L., Mathers, G., Dueker, K. & Foreman, B. Far-traveled latest Cretaceous-Paleocene conglomerates of the Southern Rocky Mountains, USA: Record of transient Laramide tectonism. *Geological Society of America Bulletin* **125**, 490–498 (2013).

Hyland, E. G., Sheldon, N. D., Van der Voo, R., Badgley, C. & Abrajevitch, A. A new paleoprecipitation proxy based on soil magnetic properties: Implications for expanding paleoclimate reconstructions. *Geological Society of America Bulletin* **127**, 975-981 (2015). doi:10.1130/B31207.1

IPCC 2007: *Climate change 2007: impacts, adaptation and vulnerability: contribution of Working Group II to the fourth assessment report of the Intergovernmental Panel on Climate Change*. (Cambridge University Press, 2007).

IPCC, 2018: Summary for Policymakers. In: Global warming of 1.5°C. An IPCC Special Report on the impacts of global warming of 1.5°C above pre-industrial levels and related global greenhouse gas emission pathways, in the context of strengthening the global response to the threat of climate change, sustainable development, and efforts to eradicate poverty [V. Masson-Delmotte, P. Zhai, H. O. Pörtner, D. Roberts, J. Skea, P. R. Shukla, A. Pirani, W. Moufouma-Okia, C. Péan, R. Pidcock, S. Connors, J. B. R. Matthews, Y. Chen, X. Zhou, M. I. Gomis, E. Lonnoy, T. Maycock, M. Tignor, T. Waterfield (eds.)]. World Meteorological Organization, Geneva, Switzerland, 32 pp

Jahren, A. H., Arens, N. C. & Harbeson, S. A. Prediction of atmospheric $\delta^{13}CO_2$ using fossil plant tissues. *Reviews of Geophysics* **46** (2008).

John, C.M., Bohaty, S.M., Zachos, J.C., Sluijs, A., Gibbs, S., Brinkhuis, H., Bralower, T.J. North American continental margin records of the Paleocene-Eocene thermal maximum: Implications for global carbon and hydrological cycling: Continental Margin Records of the PETM. *Paleoceanography* **23**, (2008).

Johnson, D. M., Hooper, P. R. & Conrey, R. M. XRF analysis of rocks and minerals for major and trace elements on a single low dilution Li-tetraborate fused bead. *International Centre for Diffraction Data* 843–867 (1999).

Johnson, R. C. & Finn, T. M. Cretaceous through Holocene history of the Douglas Creek Arch, Colorado and Utah. *RMAG Guidebook, New Interpretations of Northwest Colorado Geology* 77–95 (1986).

Johnson, R. C. & Finn, T. M. Cretaceous through Holocene history of the Douglas Creek arch, Colorado and Utah, in Stone, D.S., ed., New interpretations of northwest Colorado geology. *Denver, Colo., Rocky Mountain Association of Geologists* 77–95 (1986).

Johnson, R. C. & Flores, R. M. History of the Piceance Basin from Latest Cretaceous through early Eocene and the characterization of lower Tertiary sandstone reservoirs, in Peterson, K.M., Olson, T.M., and Anderson, D.S., eds., Piceance Basin 2003 guidebook. *Rocky Mountain Association of Geologists Guidebook* 21–61 (2003).

Johnson, R. C. & May, F. Maestrichtian conglomerates in the southwestern Piceance Creek basin: *American Association of Petroleum Geologists-Society of Economic Paleontologists and Mineralogists Annual Meeting, 27th, Rocky Mountain Section* 28 (1978).

Jones, C. H., Farmer, G. L., Sageman, B. & Zhong, S. Hydrodynamic mechanism for the Laramide orogeny. *Geological Society of America* **7(1)**, 183–201 (2011).

Kennett, J. P. & Stott, L. D. Abrupt deep-sea warming, palaeoceanographic changes and benthic extinctions at the end of the Palaeocene. *Nature* **353**, 225–229 (1991).

Kennett, J. P., Houtz, R. E. & et al. *Initial Reports of the Deep Sea Drilling Project, 29*. **29**, (U.S. Government Printing Office, 1975).

Koch, P. L. Isotopic reconstruction of past continental environments. *Annual Review of Earth and Planetary Sciences* **26**, 573–613 (1998).

Koch, P. L., Zachos, J. C. & Gingerich, P. D. Correlation between isotope records in marine and continental carbon reservoirs near the Palaeocene/Eocene boundary. *Nature* **358**, 319–322 (1992).

Kohn, M. J. Carbon isotope compositions of terrestrial C3 plants as indicators of (paleo)ecology and (paleo)climate. *Proceedings of the National Academy of Sciences* **107**, 19691–19695 (2010).

Kraus, M. J. Lower Eocene alluvial paleosols: Pedogenic development, stratigraphic relationships, and paleosol/landscape associations. *Palaeogeography, Palaeoclimatology, Palaeoecology* **129**, 387–406 (1997).

Kraus, M. J., McInerney, F.A., Wing, S.L., Secord, R., Baczynski, A.A., Bloch, J.I. Paleohydrologic response to continental warming during the Paleocene–Eocene Thermal Maximum, Bighorn Basin, Wyoming. *Palaeogeography, Palaeoclimatology, Palaeoecology* **370**, 196–208 (2013).

Kraus, M. J. & Riggins, S. Transient drying during the Paleocene–Eocene Thermal Maximum (PETM): Analysis of paleosols in the bighorn basin, Wyoming. *Palaeogeography, Palaeoclimatology, Palaeoecology* **245**, 444–461 (2007).

Kraus, M. J., Woody, D. T., Smith, J. J. & Dukic, V. Alluvial response to the Paleocene–Eocene Thermal Maximum climatic event, Polecat Bench, Wyoming (U.S.A.). *Palaeogeography, Palaeoclimatology, Palaeoecology* **435**, 177–192 (2015).

Larson, T. E., Heikoop, J. M., Perkins, G., Chipera, S. J. & Hess, M. A. Pretreatment technique for siderite removal for organic carbon isotope and C:N ratio analysis in geological samples. *Rapid Communications in Mass Spectrometry* **22**, 865–872 (2008).

Lawton, T. F. Chapter 12 Laramide Sedimentary Basins. in *Sedimentary Basins of the World* **5**, 429–450 (Elsevier, 2008).

Lorenz, J. C. & Nadon, G. C. Braided-River Deposits in A Muddy Depositional Setting: The Molina Member of the Wasatch Formation (Paleogene), West-Central Colorado, U.S.A. *Journal of Sedimentary Research* **72**, 376–385 (2002).

Lourens, L.J., Sluijs, A., Kroon, D., Zachos, J.C., Thomas, E., Röhl, U., Bowles, J., Raffi, I. Astronomical pacing of late Palaeocene to early Eocene global warming events. *Nature* **435**, 1083–1087 (2005).

Lyons, S.L., Baczynski, A.A., Babila, T.L., Bralower, T.J., Hajek, E.A., Kump, L.R., Polites, E.G., Self-Trail, J.M., Trampush, S.M., Vornlocher, J.R., Zachos, J.C., Freeman, K.H. Palaeocene–Eocene Thermal Maximum prolonged by fossil carbon oxidation. *Nature Geoscience* **12**, 54–60 (2019).

Mack, G. H., James, W. C. & Monger, H. C. Classification of paleosols. *Geological Society of America Bulletin* **105**, 129–136 (1993).

Magioncalda, R., Dupuis, C., Smith, T., Steurbaut, E. & Gingerich, P. D. Paleocene-Eocene carbon isotope excursion in organic carbon and pedogenic carbonate: Direct comparison in a continental stratigraphic section. *Geology* **32**, 553-556 (2004).

Maxbauer, D. P., Feinberg, J. M., Fox, D. L. & Clyde, W. C. Magnetic minerals as recorders of weathering, diagenesis, and paleoclimate: A core–outcrop comparison of Paleocene–

Eocene paleosols in the Bighorn Basin, WY, USA. *Earth and Planetary Science Letters* **452**, 15–26 (2016).

McInerney, F. A. & Wing, S. L. The Paleocene-Eocene Thermal Maximum: A Perturbation of Carbon Cycle, Climate, and Biosphere with Implications for the Future. *Annual Review of Earth and Planetary Sciences* **39**, 489–516 (2011).

McKirdy, D. M. & Powell, T. G. Metamorphic Alteration of Carbon Isotopic Composition in Ancient Sedimentary Organic Matter: New Evidence from Australia and South Africa. *Geology* **2**, 591-595 (1974).

Medina, E., Montes, G., Cuevas, E. & Rokzandic, Z. Profiles of CO2 concentration and δ13C values in tropical rain forests of the upper Rio Negro Basin, Venezuela. *Journal of Tropical Ecology* **2**, 207–217 (1986).

Mercier, T. & Johnson, R. C. *Isopach and isoresource maps for oil shale deposits in the Eocene Green River Formation for the combined Uinta and Piceance Basins, Utah and Colorado*. 1–85 (2012).

Miall, A. D. & Hsü, K. J. *The sedimentary basins of the United States and Canada*. (Elsevier, 2008).

Murphy, B. H., Farley, K. A. & Zachos, J. C. An extraterrestrial 3He-based timescale for the Paleocene–Eocene thermal maximum (PETM) from Walvis Ridge, IODP Site 1266. *Geochimica et Cosmochimica Acta* **74**, 5098–5108 (2010).

Nicolo, M. J., Dickens, G. R., Hollis, C. J. & Zachos, J. C. Multiple early Eocene hyperthermals: Their sedimentary expression on the New Zealand continental margin and in the deep sea. *Geology* **35**, 699 (2007).

Nordt, L. C. & Driese, S. D. New weathering index improves paleorainfall estimates from Vertisols. *Geology* **38**, 407–410 (2010).

Pagani, M., Caldeira, K., Archer, D. & Zachos, J. C. Atmosphere: An Ancient Carbon Mystery. *Science* **314**, 1556–1557 (2006).

Patterson, P. E., Kronmueller, K. & Davies, T. D. Sequence stratigraphy of the Mesa Verde Group and Ohio Creek Conglomerate, Northern Piceance Basin, Colorado. *Piceance Basin 2003 Guidebook: Denver, Colorado, RMAG* 115–128 (2003).

PiPujol, M. D. & Buurman, P. The distinction between ground-water gley and surface-water gley phenomena in Tertiary paleosols of the Ebro basin, NE Spain. *Palaeogeography, Palaeoclimatology, Palaeoecology* **110**, 103–113 (1994).

Plink-Björklund, P. Morphodynamics of rivers strongly affected by monsoon precipitation: Review of depositional style and forcing factors. *Sedimentary Geology* **323**, 110–147 (2015).

Romans, B. W., Castelltort, S., Covault, J. A., Fildani, A. & Walsh, J. P. Environmental signal propagation in sedimentary systems across timescales. *Earth-Science Reviews* **153**, 7–29 (2016).

Sackett, W. M., Nakaparksin, S. & Dalrymple, D. Carbon isotope effects in methane production by thermal cracking. *Advances in Organic Geochemistry* 37–53 (1970). doi: 10.1016/B978-0-08-012758-3.50006-2

Schmidt, D. N., Thomas, E., Authier, E., Saunders, D. & Ridgwell, A. Strategies in times of crisis—insights into the benthic foraminiferal record of the Palaeocene–Eocene Thermal Maximum. *Philosophical Transactions of the Royal Society A: Mathematical, Physical and Engineering Sciences* **376**, 20170328 (2018).

Schmitz, B. & Pujalte, V. Sea-level, humidity, and land-erosion records across the initial Eocene thermal maximum from a continental-marine transect in northern Spain. *Geology* **31**, 689 (2003).

Schmitz, B. & Pujalte, V. Abrupt increase in seasonal extreme precipitation at the Paleocene-Eocene boundary. *Geology* **35**, 215 (2007).

Secord, R., Gingerich, P.D., Smith, M.E., Clyde, W.C., Wilf, P., Singer, B.S. Geochronology and Mammalian Biostratigraphy of Middle and Upper Paleocene Continental Strata, Bighorn Basin, Wyoming. *American Journal of Science* **306**, 211–245 (2006).

Sewall, J. O. & Sloan, L. C. Come a little bit closer: A high-resolution climate study of the early Paleogene Laramide foreland. *Geology* **34**, 81-84 (2006).

Sheldon, N. D., Retallack, G. J. & Tanaka, S. Geochemical Climofunctions from North American Soils and Application to Paleosols across the Eocene-Oligocene Boundary in Oregon. *The Journal of Geology* **110**, 687–696 (2002).

Sluijs, A., Schouten, S., Woltering, M., Brinkhuis, H., Damsté, J.S.S., Dickens, G.R., Huber, M., Reichart, G.-J., Stein, R., Matthiessen, J., Lourens, L.J., Pedentchouk, N., Backman, J., Moran, K. Subtropical Arctic Ocean temperatures during the Palaeocene/Eocene thermal maximum. *Nature* **441**, 610–613 (2006).

Sluijs, A., van Roij, L., Harrington, G.J., Schouten, S., Sessa, J.A., LeVay, L.J., Reichart, G.-J., Slomp, C.P. Warming, euxinia and sea level rise during the Paleocene–Eocene Thermal Maximum on the Gulf Coastal Plain: implications for ocean oxygenation and nutrient cycling. *Climate of the Past* **10**, 1421–1439 (2014).

Sluijs, A., Röhl, U., Schouten, S., Brumsack, H.-J., Sangiorgi, F., Sinninghe Damsté, J.S., Brinkhuis, H. Arctic late Paleocene-early Eocene paleoenvironments with special

emphasis on the Paleocene-Eocene thermal maximum (Lomonosov Ridge, Integrated Ocean Drilling Program Expedition 302): Paleocene-Eocene Artic Environments. *Paleoceanography* **23**, (2008).

Smith, J. J., Hasiotis, S. T., Kraus, M. J. & Woody, D. T. Relationship of Floodplain Ichnocoenoses to Paleopedology, Paleohydrology, and Paleoclimate in the Willwood Formation, Wyoming, During the Paleocene-Eocene Thermal Maximum. *PALAIOS* **23**, 683–699 (2008).

Smith, E., M., Carroll, A. R. & Mueller, E. R. Elevated weathering rates in the Rocky Mountains during the Early Eocene Climatic Optimum. *Nature Geoscience* **1**, 370–374 (2008).

Smith, M. E., Carroll, A. R. & Singer, B. S. Synoptic reconstruction of a major ancient lake system: Eocene Green River Formation, western United States. *Geological Society of America Bulletin* **120**, 54–84 (2008).

Snell, K.E., Thrasher, B.L., Eiler, J.M., Koch, P.L., Sloan, L.C., Tabor, N.J. Hot summers in the Bighorn Basin during the early Paleogene. *Geology* **41**, 55–58 (2013).

Tieszen, L. L. Natural variations in the carbon isotope values of plants: Implications for archaeology, ecology, and paleoecology. *Journal of Archaeological Science* **18**, 227–248 (1991).

Tissot, B., Durand, B., Espitalie, J. & Combaz, A. Influence of Nature and Diagenesis of Organic Matter in Formation of Petroleum. *American Association of Petroleum Geologists* **58**, 499–506 (1974).

Trenberth, K. E. Changes in precipitation with climate change. *Climate Research* **47**, 123–138 (2011).

Tweto, O. Laramide (Late Cretaceous-Early Tertiary) Orogeny in the Southern Rocky Mountains. *Geological Society of America Memoirs* **144**, 1–44 (1975).

.Vidic, N. J. & Lobnlk, F. Rates of soil development of the chronosequence in the Ljubljana Basin, Slovenia. *Geoderma* **76**, 35–64 (1997).

Wedin, D. A., Tieszen, L. L., Dewey, B. & Pastor, J. Carbon Isotope Dynamics During Grass Decomposition and Soil Organic Matter Formation. *Ecology* **76**, 1383–1392 (1995).

Wing, S. L. Causes and consequences of globally warm climates in the early Paleogene. *Geological Society of America* **369**, (2003).

Wing, S. L. Transient Floral Change and Rapid Global Warming at the Paleocene-Eocene Boundary. *Science* **310**, 993–996 (2005).

Wing, S. L. & Currano, E. D. Plant response to a global greenhouse event 56 million years ago. *American Journal of Botany* **100**, 1234–1254 (2013).

Winguth, A., Shellito, C., Shields, C. & Winguth, C. Climate Response at the Paleocene–Eocene Thermal Maximum to Greenhouse Gas Forcing—A Model Study with CCSM3. *Journal of Climate* **23**, 2562–2584 (2010).

Wynn, J. G. Carbon isotope fractionation during decomposition of organic matter in soils and paleosols: Implications for paleoecological interpretations of paleosols. *Palaeogeography, Palaeoclimatology, Palaeoecology* **251**, 437–448 (2007).

Wynn, J. G., Bird, M. I. & Wong, V. N. L. Rayleigh distillation and the depth profile of 13C/12C ratios of soil organic carbon from soils of disparate texture in Iron Range National Park, Far North Queensland, Australia. *Geochimica et Cosmochimica Acta* **69**, 1961–1973 (2005).

Wynn, J. G., Harden, J. W. & Fries, T. L. Stable carbon isotope depth profiles and soil organic carbon dynamics in the lower Mississippi Basin. *Geoderma* **131**, 89–109 (2006).

Yin, A. & Ingersoll, R. V. A Model for Evolution of Laramide Axial Basins in the Southern Rocky Mountains, U.S.A. *International Geology Review* **39**, 1113–1123 (1997).

Zachos, J. Trends, Rhythms, and Aberrations in Global Climate 65 Ma to Present. *Science* **292**, 686–693 (2001).

Zachos, J. C. A Transient Rise in Tropical Sea Surface Temperature During the Paleocene-Eocene Thermal Maximum. *Science* **302**, 1551–1554 (2003).

Zachos, J. C. Rapid Acidification of the Ocean During the Paleocene-Eocene Thermal Maximum. *Science* **308**, 1611–1615 (2005).

Zachos, J. C., Dickens, G. R. & Zeebe, R. E. An early Cenozoic perspective on greenhouse warming and carbon-cycle dynamics. *Nature* **451**, 279–283 (2008).

Zeebe, R. E., Zachos, J. C. & Dickens, G. R. Carbon dioxide forcing alone insufficient to explain Palaeocene–Eocene Thermal Maximum warming. *Nature Geoscience* **2**, 576–580 (2009).

FIGURES

Figure 1. Simplified geologic map of Laramide basins within the Western Interior and locations where the PETM has been identified (Koch et al., 1992; Wing et al., 2005; Bowen and Bowen, 2008; Burger, 2012; Foreman et al., 2012; Baczynski et al. 2013; 2016).

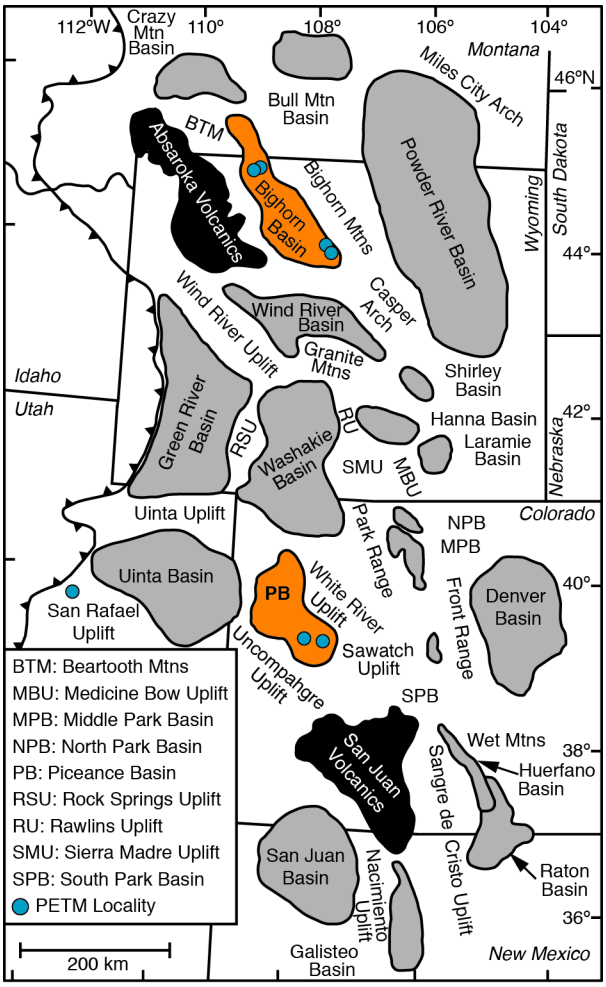

Figure 2. Study area showing locations and simplified stratigraphic sections of Johnson & May (1978) (C,D,E), Burger (2012) (SG), Foreman et al. (2012) (X), and this study (WF). Biostratigraphic, chemostratigraphic, and chronostratigraphic constraints from Johnson & May (1978), Burger (2007; 2009; 2012), and Foreman et al. (2012; in prep.).

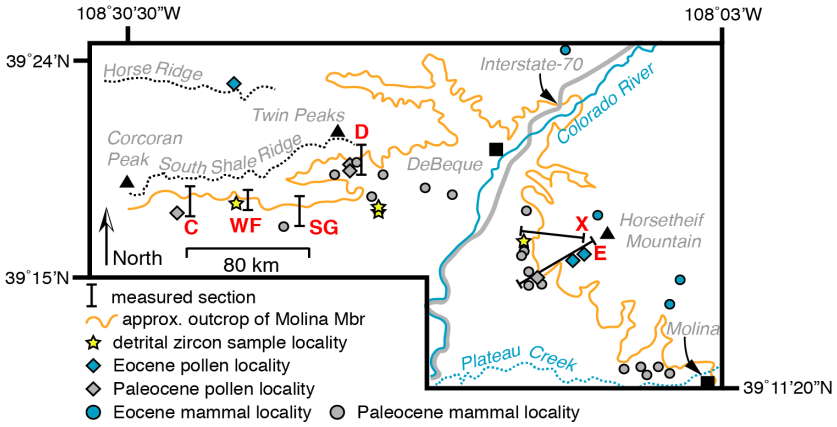

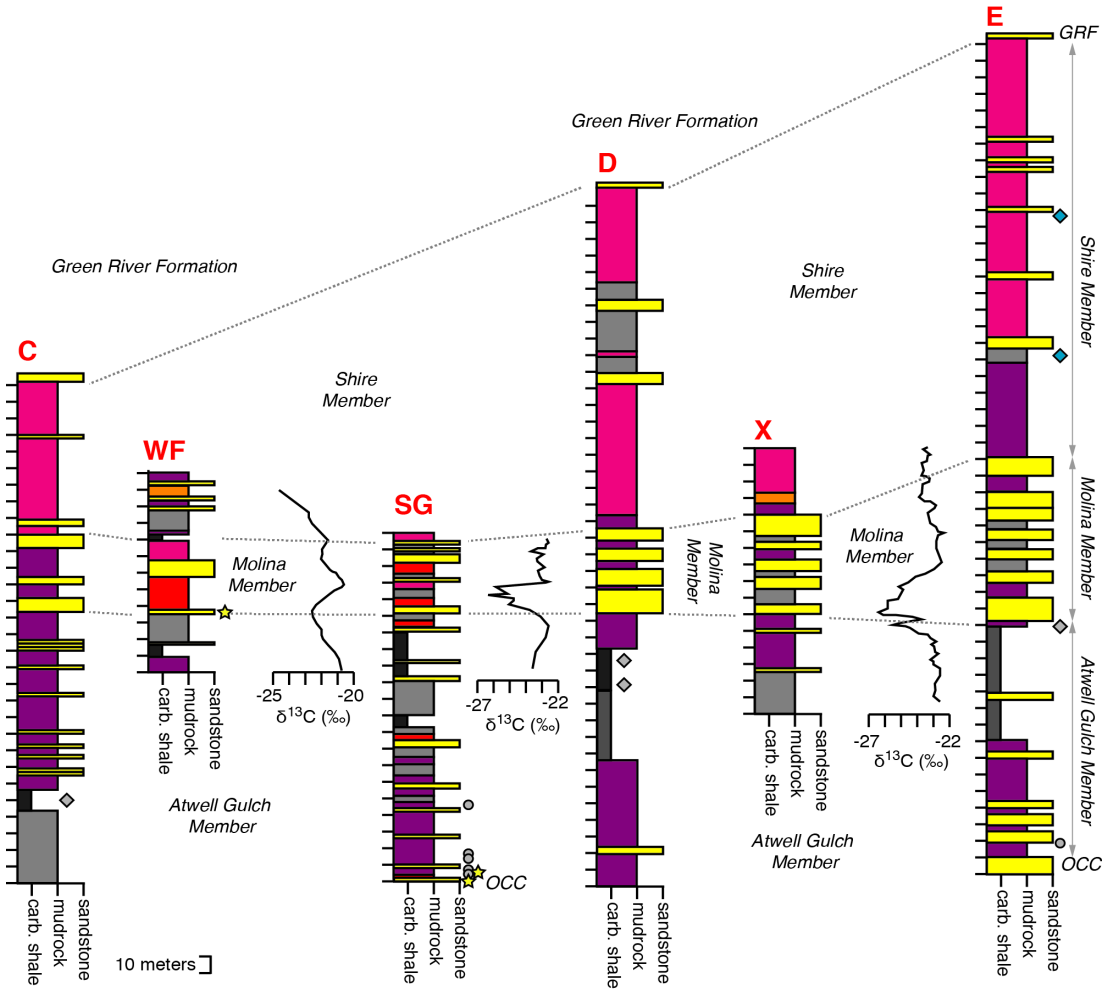

Figure 3. Images of Wasatch Formation in study area. A) Outcrop image of Atwell Gulch Member and overlying Molina Member east of DeBeque near "X" stratigraphic section of Foreman et al. (2012), B) outcrop image east of Winter Flats study area showing the three geologic members of the Wasatch Formation, C) outcrop image of Atwell Gulch Member at Winter Flats stratigraphic section, D) outcrop image of Molina Member equivalent at Winter Flats stratigraphic section, E) columnar ped structures within paleosol horizon, F) yellow mottling overlying red, bioturbated fine sandstone, G) purple mottling and green-gray gley features within paleosol horizon, and H) carbonaceous shale unit.

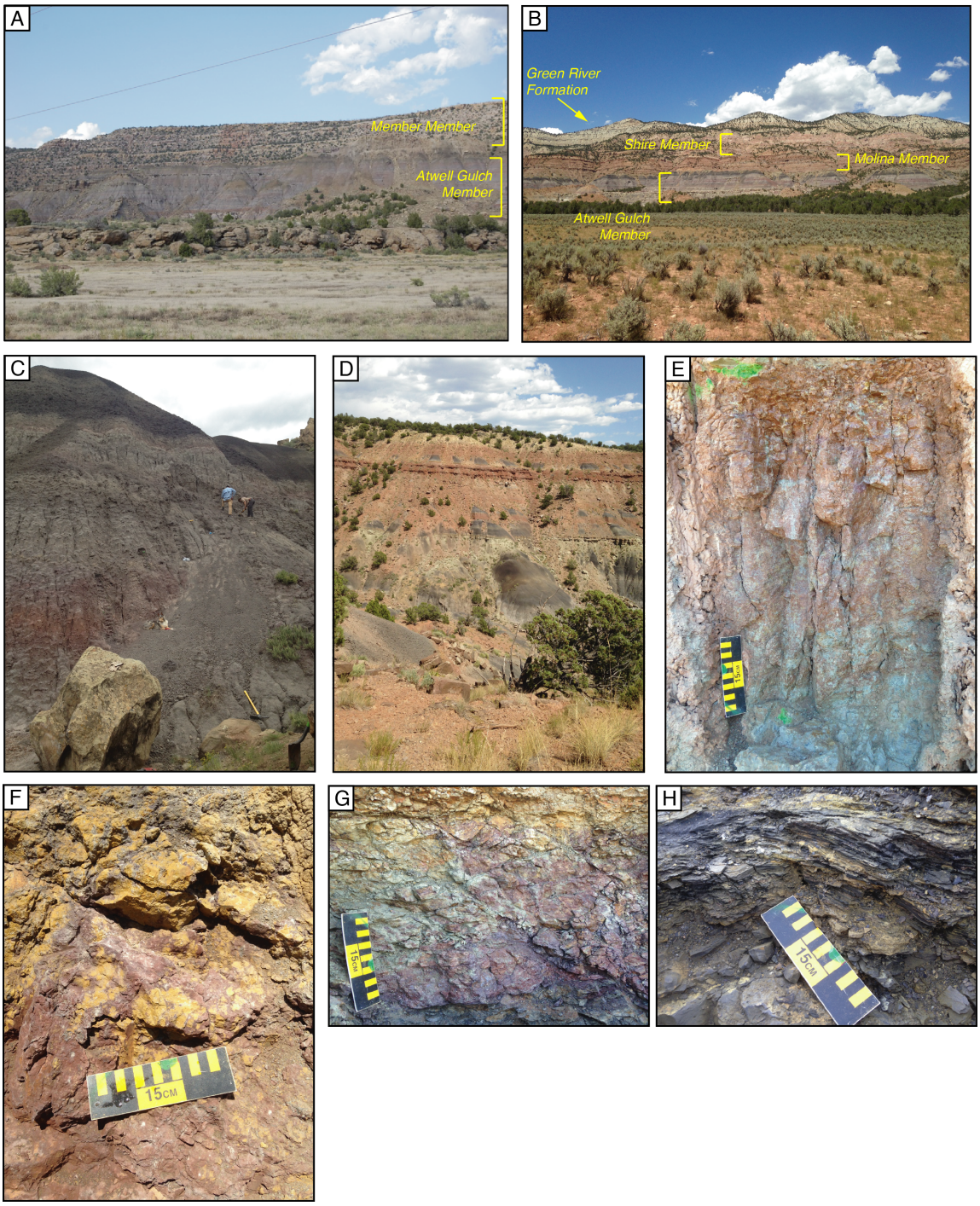
A
Member Member
Atwell Gulch Member
B
Green River Formation
Shire Member
Molina Member
Atwell Gulch Member
C
D
E
F
15CM
G
15CM
H
15CM

Figure 4. Plots of A) bulk organic $\delta^{13}C$ values against carbon content, and B) box plots of bulk organic $\delta^{13}C$ values based on sample lithology. Box defined by 1st and 3rd quartile of the data, middle line the median, whiskers defined by 1.5 times the interquartile range, and outliers shown as individual circles. Sample size for each lithology listed as *n* =.

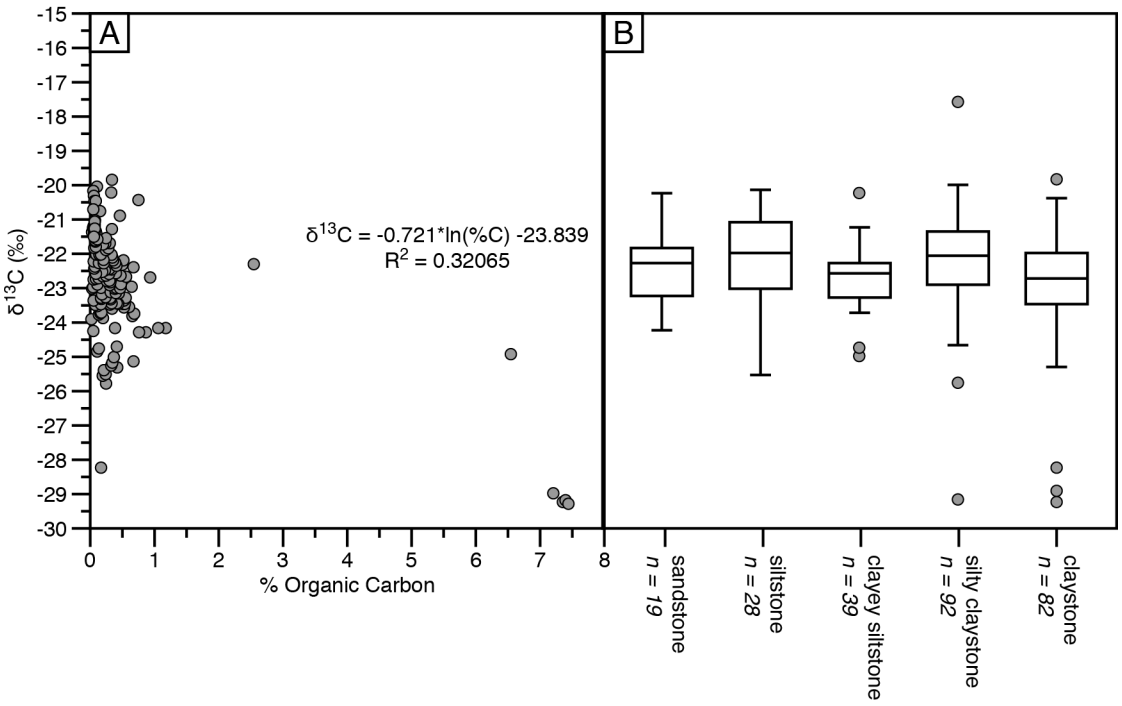

Figure 5. Stratigraphic section at Winter Flats study area with corresponding bulk organic $\delta^{13}C$ record, soil morphology indices, and mean annual precipitation estimates.

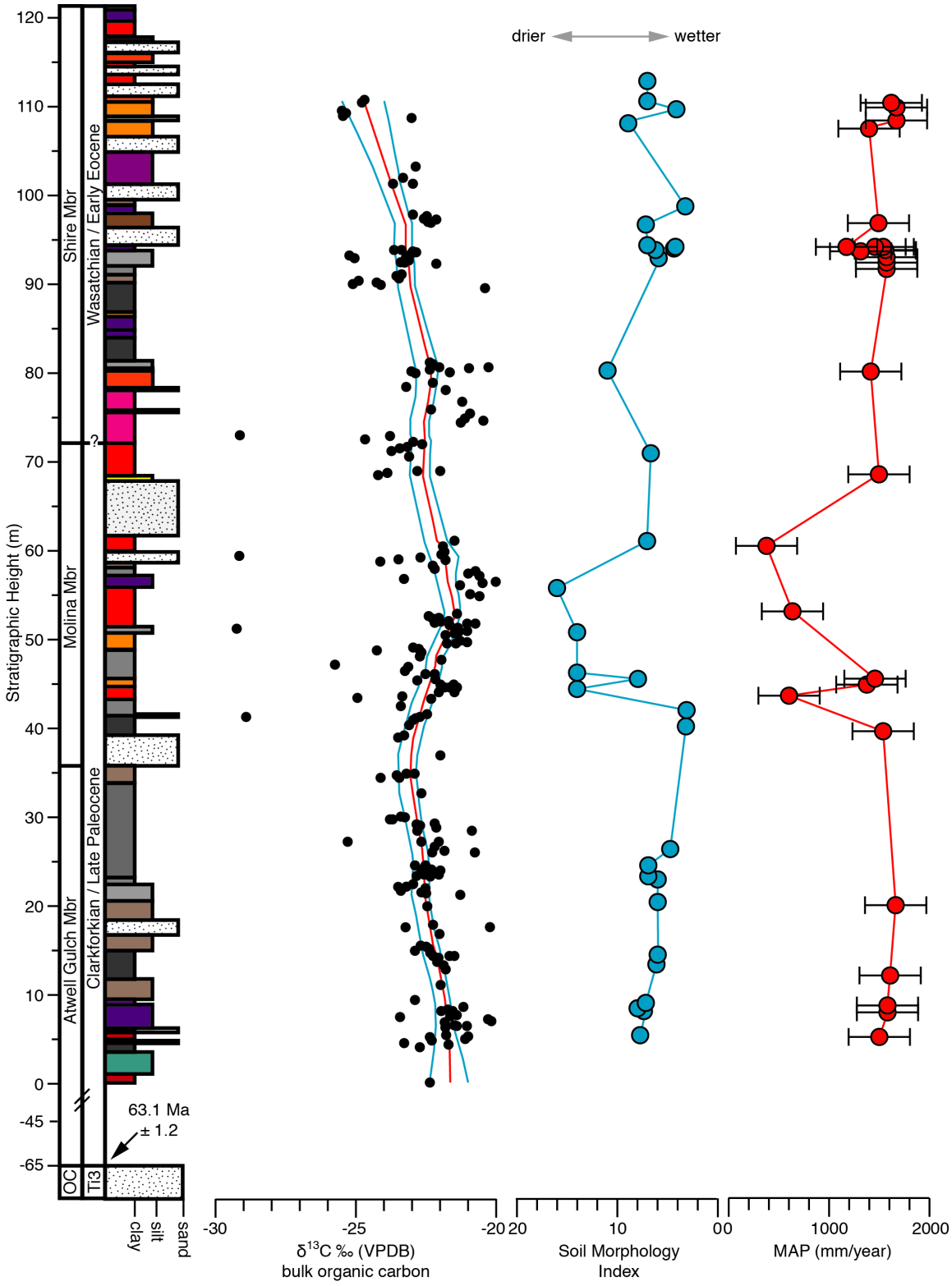

Figure 6. Comparison of soil morphology index and mean annual precipitation spanning the PETM and comparison to this study (data from Bighorn Basin from Kraus et al., 2013).

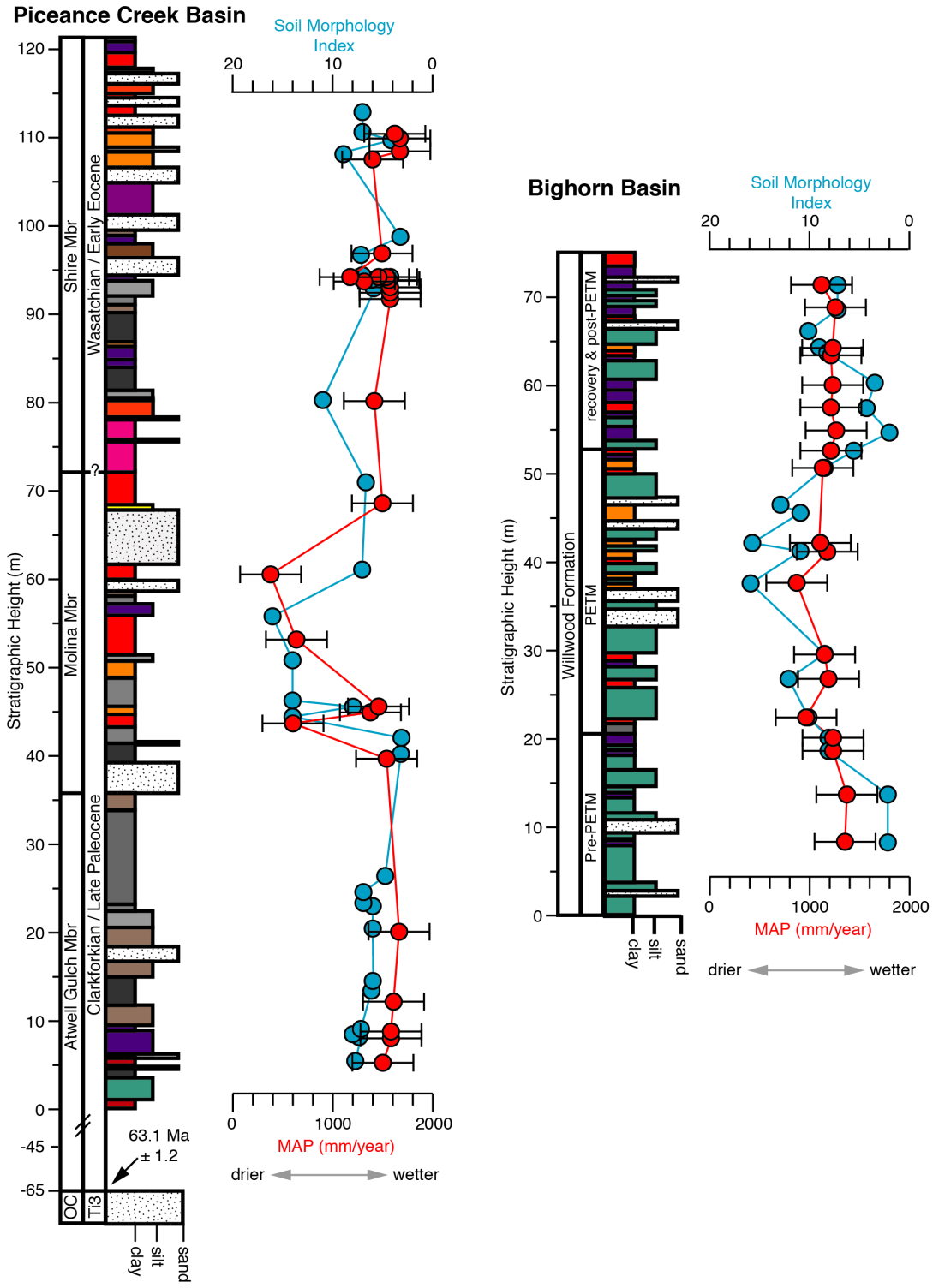

APPENDICES

WF2015	**thru purple soil of purple red cuplet beneath black shale (base of WF-2105)**	**Column1**	**Column2**
UNIT	DESCRIPTION	THICKNESS	SAMPLES
1	siltstone to very fine lower yellow mottling face is really weathered minor rippling bioturbation mm scale tuber	0.53m 0.00-0.53m	PURP2-001>0.43m
2	claystone with minor silt overall color is greyish red purple very minor sharp olive grey mottles, 5Y4/2 there are large slicken sides minor diffuse greenish purple mottles increase in greyish purple up the unit B horizon	0.82m 0.53-1.35m	PURP2-002>0.63m PURP2-003>0.73m PURP3-004>0.83m PURP2-005>0.93m PURP2-006>1.03m PURP2-007>1.13m PURP2-008>1.23m PURP2-009>1.33m
3	claystone with silt greyish purple some reddish purple mottles roots filled in with yellow brown colors ~2mm in diameter contains clay cutans B horizon	0.70m 1.35m-2.05m	PURP2-010>1.45m PURP2-011>1.55m PURP2-012>1.65m PURP2-013>1.75m PURP2-014>1.85m PURP2-015>1.95m PURP2-016>2.04m
4	claystone light grey minor sharp reddish purple mottles yellow brown root traces clay cutans silt near top of unit gradational lower contact likely “A” horizon	0.3m 2.05m-2.35m	PURP2-017>2.10m PURP2-018>2.30m

WF2015 Remeasured			
UNIT	DESCRIPTION	THICKNESS	SAMPLES
1	Muddy siltstone C horizon Fresh color- 10R 4/2weak red Weathered color- 5YR 5/2 Chroma value- 2 Mottling 1- 10R 2/2 minor very dusky red Mottling 2- 10YR	0.21 0-0.21	WF-001>0.00

2	Muddy siltstone Bss horizon Fresh color- 10R ¾ dusky red Weathered color- 10R 5/4 Chroma value- 4 Minor slicks Minor roots Mottling 1- 10YR 6/6 20% brownish yellow Mottling 2- 5P 4/2 7.5% pale red SMI chroma- 4 SMI carb- 0 SMI yb- 6 SMI- 10	0.75 0.21-0.96	WF-002>0.21 WF-003>0.31 WF-004> 0.41 WF-005>0.51 WF-006>0.61 WF-007>0.71 WF-008>0.81 WF-009>0.91
3	Massive fine sandstone Fine sand C horizon Fresh color- 10R 6/2 pale red Weathered- covered Chroma value-2 Mottling 1- 5RP 4/2 minor	0.34 0.96-1.30	WF-010> 1.01 WF-011>1.11
4	Siltstone, clays in upper portion B horizon Fresh color- 10R 2/2 very dusky red Weathered- 5R 4/2 Chroma- 2 Minor clay cutans Mottling 1- 10YR 6/6 5% brownish yellow Mottling 2- 10R 6/2 25% pale red SMI chroma- 2 SMI carb- 0 SMI yb- 6 SMI- 8	1.21 1.30-2.51	WF-012>1.40 WF-013>1.50 WF-014>1.60 WF-015>1.70 WF-016>1.80 WF-017>1.90 WF-018>2.00 WF-019>2.10 WF-020>2.20 WF-021>2.30 WF-022>2.45
5	Siltstone, minor clay A horizon Fresh color- 10R 6/2 pale red Weathered- 10R 6/2 Chroma values- 2 Minor clay cutans Mottling 1- 10YR 5/4 50% yellowish brown SMI chroma- 2 SMI carb- 0 SMI yb- 6 SMI- 8	0.70 2.51-3.21	WF-023>2.55 WF-024>2.65 WF-025>2.75 WF-026>2.85 WF-027>2.95 WF-028>3.05 WF-029>3.15
6	Massive siltstone C horizon Fresh color- 5Y 4/1 dark grey Weathered- 5Y 6/1 gray Chroma value- 1	2.29 3.21-5.50	WF-030>3.25 WF-031>3.50 WF-032>3.75 WF-033>4.00 WF-034>4.25 WF-035>4.50 WF-036>4.75 WF-037>5.00 WF-038>5.25 WF-039>5.50

7	Siltstone B horizon Fresh color- 5YR 6/1 gray Weather- 5YR 6/1 Chroma value- 1 Slicks Clay cutans Mottling 1- 5RP 4/2 20% Mottling 2- 10YR 5/4 15% yellowish brown SMI chroma- 1 SMI carb- 0 SMI yb- 6 SMI- 7	0.5 5.50-6.00	WF-040>5.75 WF-041>6
8	Silty claystone B horizon Fresh color- N3 very dark gray Weathered- 5Y 6/1 gray Chroma value- 0 Weak clay cutans Minor roots Root color- white center with dark yellowish orange outline Borrows Mottling 1- 10YR 6/6 10% brownish yellow SMI chroma- 0 SMI carb- 0 SMI yb- 6 SMI-6	2.01 6.00-8.01	WF-043>6.5 WF-044>6.75 WF-045>7 WF-046>7.25 WF-047>7.5 WF-048>7.75 WF-049>8
9	Silty mudstone B horizon Fresh color- N3 very dark grey Weathered- N6 Chroma value- 0 Mottling 1-5R 3/4 17.5% concentrated Mottling 2-5Y 4/4 7.5% dispersed SMI chroma- 0 SMI carb- 0 SMI yb- 6 SMI- 6	0.72 8.01-8.73	WF-050>8.01 WF-051>8.26 WF-052>8.51 WF-053>8.73
10	Clayey siltstone Fresh color- 5Y 4/1 dark gray Weather- 5Y 6/1 Chroma value- 1 Mottling 1- 10YR 6/6 12.5% brownish yellow	1.75 8.73-10.48	WF-054>8.98 WF-055>9.23 WF-056>9.48 WF-057>9.73 WF-058>9.98 WF-059>10.23 WF-060>10.48
11	Massive fine sandstone Fine sands, fines upward and gains silt at top Fresh color- 5GY 8/1light greenish gray Weathered- 5Gy 8/1 Chroma value- 1 Mottling 1- 5RP 4/2 SMI crhoma-0 SMI carb-0 SMI yb- 0	1.68 10.48-12.16	WF-061>10.73 WF-062>10.98 WF-063>11.23 WF-064>11.48

12	Siltstone, clays in upper portion B horizon Fresh color- N4 dark gray Weathered- 5Y 4/1 Chroma value- 0 Minor slicks Roots Burrows Mottling 1- 10YR 6/6 22.5% brownish yellow SMI chroma- 0 SMI carb- 0 SMI yb- 6 SMI- 6	2.16 12.16-14.32	WF-065>13.57 WF-066>13.82 WF-067>14.07 WF-068>14.32
13	Massive siltstone with minor clay Fresh color- N4 dark gray Weather- 5Y 4/1 Chroma value- 0	1.85 14.32-16.17	WF-069>14.57 WF-070>14.82 WF-071>15.07 WF-072>15.32 WF-073>15.57 WF-074>15.82 WF-075>16.07
14	Claystone B horizon Fresh color- N4 dark gray Weathered- 5Y 5/2 Chroma value- 0 Minor roots Minor burrows Mottling 1- 10YR 6/6 25% brownish yellow SMI chroma- 0 SMI chroma- 0 SMI yb- 6 SMI- 6	1.85 16.17-16.95	WF-076>16.22 WF-077>16.47 WF-078>16.72
15	Claystone B horizon Fresh color- 5YR 4/1dark gray Weather- 10R 4/2 Chroma value- 1 Slicks Minor clay cutans Minor roots Minor burrows Mottle 1- 5YR 5/6 10-15% yellowish red, with mottle 2 Mottle 2- 10YR 6/6 brownish yellow SMI chroma- 1 SMI carb- 0 SMI yb- 6 SMI-7	0.9 16.95-17.85	WF-079>16.97 WF-080>17.22 WF-081>17.47 WF-082>17.72
16	Silty claystone Fresh color- 5 YR 4/1 dark gray Weather- 10R 6/2 Chroma value- 1 Clay cutans Mottling 1- 5YR 5/6 15% combined yellowish red Mottling 2- 5YR 4/4 reddish brown SMI chroma-1 SMI carb- 0	0.4 17.85-18.25	WF-083>17.97 WF-084>18.22

	SMI yb- 6 SMI- 7		
17	Muddy siltstone Increase in clay towards top Fresh color- 5YR 4/1 to N3 dark gray-very dark gray Weathered- 10R 6/2 Chroma value- 1 Minor clay cutans Mottling 1- 10YR 6/6 <10% brownish yellow SMI chroma- 0.5 SMI carb- 0 SMI yb- 6 SMI- 6.5	0.83 18.25-19.08	WF-085>18.5 WF-086>18.75 WF-087>19
18	Claystone B horizon Yb nodules- yes, mottle 2 color. Fresh color- 5Y 4/1 dark gray Weathered- 5YR 5/2 Chroma value- 1 Slicks Clay cutans Abundant burrows Mottling 1- 10YR 6/6, associated with burrows brownish yellow Mottling 2- 5RP 4/2 50% SMI chroma- 1 SMI carb-0 SMI yb-3 SMI-4	2.53 19.08-21.61	WF-088>19.33 WF-089>19.58 WF-090>19.83 WF-091>20.08 WF-092>20.33 WF-093>20.58 WF-094>20.83 WF-095>21.08 WF-096>21.33 WF-097>21.58
19	Claystone Fresh color- N3 very dark gray Weathered- 5YR 2/1 Chroma value- 0 Minor slicks Minor clay cutans Mottling 1- 10YR 5/4 5% yellowish brown	4.85 21.61-26.46	WF-098>21.86 WF-099>22.11 WF-100>22.36 WF-101>22.61 WF-102>22.86 WF-103>23.36 WF-104>23.61 WF-105>23.86 WF-106>25.81 WF-107>26.03 WF-108>26.15 WF-109>26.31
20	Silty claystone Fresh color- N3 very dark gray Weathered- N1 Chroma value- 0 Mottling 1- 10YR 5/4 <5% yellowish brown	1.1 26.46-27.56	WF-110>26.46 WF-111>26.71

21	Claystone Fresh color- 5Y 4/1 dark gray Weathered- 5Y 4/1 Chroma value- 1 Slicks Clay cutans Mottling 1- 10YR 4/2 15% dark grayish brown	1.95 27.56-29.51	WF-112>28.01 WF-113>28.26 WF-114>28.51 WF-115>28.76 WF-116>29.01 WF-117>29.26 WF-118>29.51
22	Fined grained sandstone with layered silty claystone B horizon, incipient soil layer Fresh color- ss, 10R 5/4 weak red Silty clay 10R 4/2 weak red Weathered- 5GY 5/2 Chroma value- 2 Roots, brown Mottling 1- 5GY 7/2 17.5% light greenish gray SMI chroma- 2 SMI carb- 0 SMI yb- 6 SMI-8	2.95 29.51-32.46	WF-119>29.76 WF-120>30.01 WF-121>20.26 WF-122>30.51
23	Fine to very fine ss Fines upwards C horizon Fresh color- 10Y6/2 Weathered- 5Y 7/2 light gray Chroma value- 2 Bioturbation Mottling 1- 5RP 2/2 12.5% Mottling 2- 10YR 5/4 5% yellowish brown	0.51 32.46-32.96	WF-123>32.61 WF-124>32.87
24	Claystone Bss horizon Yb nodules- mottles Fresh color- N4 dark gray Weathered- N3 Chroma value- 0 Slicks- yes Clay cutans Roots- yellow brown Mottling 1- 10YR 5/4 2% yellowish brown SMI chroma- 0 SMI carb- 0 SMI yb- 3 SMI- 3	2.2 32.96-35.17	WF-125>32.97 WF-126>33.22 WF-127>33.47 WF-128>33.72 WF-129>33.97 WF-130>34.22 WF-131>34.47 WF-132>34.72 WF-133>34.97
25	Silty vf sandstone Fresh color- 5Y 6/1 gray Weathered- 5Y 6/1 Chroma value-1 Bioturbation	0.35 35.17-35.52	WF-134>35.17 WF-135>35.42

26	See description for unit 24 gray SMI chroma-0 SMI carb-0 SMI yb- 3 SMI-3	0.64 35.52-36.16	WF-136>35.57 WF-137>35.82 WF-138>36.02
27	Claystone Fresh color- N2 Weathered- 5Y 4/1 Chroma value- 0 Slicks Clay cutans Mottling 1- 10YR 5/4 weak	1.28 36.16-37.44	WF-139>36.31 WF-140>36.56 WF-141>36.81 WF-142>37.06 WF-143>37.29
28	Silty claystone B horizon Carbonate Fresh color- 10R 4/2 weak red Weather- 10R 5/4 Chroma value- 2 Roots in upper 6 samples Mottling 1-10YR 6/6 15% brownish yellow Mottling 2- 5Y6/1 associated with roots gray SMI chroma- 2 SMI carb- 6 SMI yb- 6 SMI- 14	1.44 37.44-38.88 Start of the PETM? This is the onset of the "rainbow" paleosols. Is this the start of the Molina?	WF-144>37.54 WF-145>37.64 WF-146>37.74 WF-147>37.84 WF-148>37.94 WF-149>38.04 WF-150>38.14 WF-151>38.24 WF-152>38.34 WF-153>38.44 WF-154>38.54 WF-155>38.64 WF-156>38.74 WF-157>38.84
29	Claystone B (maybe B and A at top) horizon Fresh color- 5R 4/2 at base, 5RP 4/2 at top Weathered- 10R 7/4 Chroma value- 2 Clay cutans Mottling 1- 5Y 6/1 at base, 10YR 6/6 near top 15% Mottling 2- 10YR 5.4 and 5G 7/2, both near top 15 and 20% respectively SMI chroma- 2 SMI carb – 0 SMI yb- 6 SMI- 8	0.38 38.88-39.26	WF-158>38.94 WF-159>39.04 WF-160>39.14 WF-161>39.24
30	Silty claystone B horizon Carbonate- yes, at base Fresh color- 5RP 4/2 Weathered- 10R 7/4 Chroma value- 2 Weak slicks Mottling- yes, blocky and concentrated Mottling 1- 10YR 6/6 32.5% Mottling 2- 5GY 6/1 17.5% SMI chroma- 2 SMI carb- 6 SMI yb- 6 SMI-14	0.6 39.26-39.86 brick red nodules are present at this level, large slicks	WF-162>39.36 WF-163>39.46 WF-164>39.56 WF-165>39.66 WF-166>39.76 WF-167>39.86

31	Silty claystone Fresh color- N6 Weathered- 5YR 5/2 Chroma value- 0 Mottling 1- 10YR 6/6 10%	0.3 39.86-40.16	WF-168>40.01 WF-169>40.16
32	Claystone with silt See description for unit 24, also see notes at right SMI chroma- 0 SMI carb- 0 SMI yb- 3 SMI- 3 Notes mention that burrows are present but rare, in the upper 1m	2.9 40.16-43.06	WF-170>40.41 WF-171>40.66 WF-172>41.01 WF-173>41.26 WF-174>41.61 WF-175>41.76 WF-176>42.01 WF-177>42.36 WF-178>42.51 WF-179>42.76

33	Primarily follows description for unit 28, becomes siltier as you go up section and at the top (WF-201) it is essentially a fine ss w/ a pale brown primary color (5YR 5/2) with similar mottling	2.2 45.26	WF-180>43.06 WF-181>43.16 WF-182>43.26 WF-183>43.36 WF-184>43.46 WF-185>43.56 WF-186>43.66 WF-187>43.76 WF-188>43.86 WF-189>44.06 WF-190>44.16 WF-191>44.26 WF-192>44.36 WF-193>44.46 WF-194>44.56 WF-195>44.66 WF-196>44.76 WF-197>44.86 WF-198>44.96 WF-199>45.06 WF-200>45.16 WF-201>45.26
34	Similar to unit 30, fine ss, no slickensides, upper and lower contact gradational SMI Chroma- 2 SMI carb-0 SMI yb- 6 SMI- 8	0.3 45.26-45.56 no carbonate, another diff w/ unit 30	WF-202>45.36 WF-203>45.46 WF-204>45.56
35	Siltstone with minor clay similar to unit 24, orange mottles (30%), weak red purple mottles (5%), clay cutans SMI chroma- 0 SMI carb- 0 SMI yb- 3 SMI- 3	0.22 45.56-45.78	WF205>45.76
36	Basically the same as unit 35 above, but w/o burrows and only minimal orange mottles (1-2%) SMI chroma- 0	0.12 45.78-45.90	WF-206>45.84

	SMI carb- 0 SMI yb- 3 SMI- 3		
37	Siltstone with minor clay Horizon Chroma value- 0 Fresh color- N4 Clay cutans Mottling 1- dark yellowish orange 17.5% Sharp lower and gradational upper contacts	0.07 45.90-45.97	WF-207>45.93
38	Claystone Horizon B? Fresh color- 10R 2/2 very dusky red Chroma value- 2 Slicks Mottling 1- medium dark grey 30% Mottling 2- orange 5% SMI chroma-0 SMI carb- 0 SMI yb- 6 SMI-8	45.97-46.25	WF-208>46.02 WF-209>46.12 WF-210>46.17
39	Silty claystone Horizon C See unit 35 SMI chroma- 0 SMI carb- 0 SMI yb-3 SMI-3 no mottles, sharp upper contact	0.08 46.25- 46.33	WF-211>46.29
40	Silty claystone Horizon B Carbonate present Fresh color- 10R3/4 Chroma value- 4 Mottling 1- 10YR5/4 see notes Mottling 2- N5 12.5% SMI chroma- 4 SMI carb- 6 SMI yb- 6 SMI 16 the main color, 10R 3/4 (dark reddish brown) is the main color for lower 30 cm and then becomes a mottle color. The mottle_1 color is a mottle at base and becomes dominant in the upper portion	4.1 46.33-50.43	WF-212>46.58 WF-213>48.43 WF-214>48.68 WF-215>48.93 WF-216>49.43 WF-217>49.68 WF-218>49.93 WF-219>50.18
41	silty claystone at base and coarsens upwards into a fine ss clay to fine sand B + splay? Fresh color- 5RP 4/2 at base, 5Y 6/1 Weather- dark yellowish orange at base, 5Y 6/1 at top Chroma value- 1.5 Weak clay cutans Mottling 1- 10YR 6/6 30% Mottling 2- 5GY 6/1 10% SMI chroma- 1.5 SMI carb- 0 SMI yb- 6 SMI-7.5 modern roots present	1.3 50.43-51.73	WF-220>50.43 WF-221>50.73 WF-222>51.03 WF-223>51.33 WF-224>51.63
42	siltstone or shale	0.9	WF-225>51.83

	silt grades to shale at top Fresh color-N3 Weathered- 5Y 4/1 Chroma value-0 modern roots	51.73-52.63	WF-226>52.08 WF-227>52.33 WF-228>52.58
43	claystone clay Fresh color- 5Y 4/4 lower half, 5GY 7/2 upper half Weathered- 10YR 5/4 Chroma value- 3 Slicks are weak in lower half Mottling 1-5GY 7/2 2% roots	0.55 52.63-53.18	WF-229>52.78 WF-230>53.03
44	medium to fine ss grades up into claystone clay to medium sand splay + soil development Fresh color- 10Y 6/2 in sand, 5Y 5/2 is clay Weathered- 5Y 7/2 2 Mottling 1- 5G 6/1 5% large splay capped by soil development?	1.2 53.18-54.38	WF-231>53.28 WF-232>53.53 WF-233>53.78 WF-234>54.03 WF-235>54.28
45	silty claystone silt and clay Fresh color- 5GY 6/1 Chroma value- 1 Fresh color- 10R 4/2 25%, combo Weathered- 10R ¾ %25, combo	0.5 54.38-54.88	WF-236>54.48 WF-237>54.73
46	siltstone to claystone silt and clay similar to unit 44, pale red (5R 6/2) mottling becomes more common up section until it dominates, somewhat fissile in middle and laminated	1.21 54.88-56.09	WF-238>54.98 WF-239>55.23 WF-240>55.33 WF-241>55.58 WF-242>55.83
47	fine to medium ss fine to medium sand Fresh color-N7 ripple laminations	0.35 56.09-56.44	WF-243>56.29
48	"Molina sand" rusty unit. This unit is common throughout the "rainbow paleosol" zone and can be continuous for 50+ meters. In places it is extensively bioturbated or massive. But, also displays large scale ripple laminations. Outcrop color is dark reddish brown (10R 3/4) medium grained sandstone. Appears to be zones of crevasse splays or shallow channels. Forms oblate lens in zones. The reported thickness is a "splay" zone that include siltstones that are vegitated adn we did not dig through. Sand intervals have spaly in thicknesses of a few cm to 1 meter. Start of Molina?	5.4 56.44-61.84	
49	medium ss medium sand Fresh color-5P 6/2 Weathered- 5P 6/2 2 Heavy burrows Mottling- 10R 4/2 surround mottle_2 Mottling 2- 10YR 6/6 40%, combo	0.4 61.84-62.24	WF-244>62.14
50	fine ss to siltstone silt to fine sand Fresh color- 10R 5/4	0.4 62.24-62.44	WF-245>62.34

	Weathered- 10R 5/4 Chroma value- 4 Mottling 1- 5GY 8/1 interior, 5P 6/2 exterior 30% Mottling 2- 10YR 6/6 interior, 10R 4/2 exterior		
51	ss? Fresh color- 10YR 6/6 Chroma value- 6 Mottling 1- see unit 50 Yellow bed	0.4 62.44-62.84	WF-246>62.59 WF-247>62.84
52	silty claystone silt and clay Fresh color- N3 Weathered- 10R 6/2 Chroma value- 0 Slicks- yes, up section mild bioturbation Mottling 1- 10YR 6/6 weak Mottling 2- 10YR 5/4 weak	3.8 62.84-66.64	WF-248>62.9 WF-249>63.15 WF-250>63.4 WF-251>63.65 WF-252>63.9 WF-253>64.15 WF-254>64.4 WF-255>64.65 WF-256>64.9 WF-257>65.15 WF-258>65.4 WF-259>65.65 WF-260>65.9 WF-261>66.15 WF-262>66.4 WF-263>66.64
53	mudstonemud Fresh color- 5Y 5/6olive Weathered- 10R 7/4 Chroma value- 6 Mottling 1-N7 35% Mottling 2- 5R 3/4 rims around mottle 1	0.85 66.64-67.49	WF-264>66.89 WF-265>67.14 WF-266>67.39
54	repeating units: 1) silty mudstone, 2) mottled silty mudstone, 3)fine ss Fresh color- 5R 6/2 Weathered- 10R 8/2 Chroma value- 2 Minor slicks see field notes for this description	2.6 67.49-70.9	WF-267>67.74 WF-268>67.99 WF-269>68.24 WF-270>68.49 WF-271>68.74 WF-272>68.99 WF-273>69.24 WF-274>69.49 WF-275>69.74
55	fine to medium sandstone, lenticular sand body, significant subvertical bioturbation (1.cm in diameter and ~13cm long burrows), sand body piches out over ~20 meters, weak cross-bedding, took thin section sample for rusty coloration	0.3 70.09-70.39	
56	same as unit 54	2.23 70.39-72.62	WF-276>70.39 WF-277>70.64 WF-278>70.89 WF-279>71.14 WF-280>71.39 WF-281>71.64 WF-282>71.89 WF-283>72.14 WF-284>72.39

57	same as 55, rusty sandstone w/ ripple cross lamination, edge of sand body lense. Took thin section sample	0.31 72.62-72.93	WF-285>72.77
58	Covered interval	0.6 72.93-73.53	
59	silty fine ss fine sand and silt B? Carbonate present Fresh color- 10R 4/2 Weathered- 10R 5/4 and 10YR 6/6 splotch Chroma value- 2 Mottling 1- 10YR 6/6 40% Mottling 2- 5GY 8/1 rims mottle 1 SMI Chroma- 2 SMI Carb- 6 SMI yb- 6 SMI- 14 beginning of the Shire Member	0.39 73.53-73.92	WF-286>73.53 WF-287>73.63 WF-288>73.73 WF-289>73.83 WF-290>73.92
60	silty fine ss fine sand and silt B Horizon Carbonate present Fresh color- 5RP 4/2 Weathered- 10R 4/2 Chroma value- 2 Roots- yellowish grey with pale purple and yellow brown rims Mottle 1- 10YR 6/2 surrounds rhizolith Mottle 2- 5P 6/2 surrounds rhizoliths SMI chroma- 2 SMI carb- 6 SMI yb- 6 SMI- 14	0.3 73.93-74.22	WF-291>74.02 WF-292>74.12 WF-293>74.2
61	clayey siltstone silt and clay B or E? Fresh color- N5 and N6 Weather- N7 Chroma value- 0 Slicks- yes, near base Clay cutans- yes, near base Mottling 1-10YR 6/6 10%, at base SMI chroma-0 SMI carb-0 SMI yb- 6 SMI-6	0.62 74.22-74.84	WF-294>74.27 WF-295>74.37 WF-296>74.47 WF-297>74.57 WF-298>74.67 WF-299>74.77
62	clayey siltstone silt and clay A? Fresh colore- N3 Weathered- N4 Soil chroma-0 SMI chroma- 0 SMI carb-0 SMI yb-6 SMI-6 appears organic rich, gradational lower contact some modern roots and/or weathering	0.22 74.84-75.06	WF-300>74.89 WF-301>74.99

WF2			
UNIT	DESCRIPTION	THICKNESS	SAMPLE
1	mostly covered deeply weathered claystones/siltstone vegetated slope unable to sample the base is the pink paleosole from WF-2015 Top is a thin rusty sandstone ledge black shale layer in the middle reddish paleosole near the top sandstone is fine-upper to medium-lower, 4/3 weak red modeling	2.6m 0-2.6m	
2	siltstone 10y/7.1 light greenish gray 10R 5/3 weak red two colors are subequal proportions and they're mottles top half is mottled with a greyish-purple and a light olive-brown 2.5y 5/4 mottles near the top there is a light greenish grey along with distorted pillow structures and weak mukkara carbonate nodules located at the middle and top of unit	0.38m 2.6m-2.98m	WF2-001>2.6m WF2-002>2.8m WF2-003>2.95m
3	silty claystone large carbonate nodules in the middle of the unit clay cutans higher percent of greenish purple subject to modern weathering	0.49m 2.98-3.47m	WF2-004>3.25m WF2-005>3.44m
4	clay siltstone 10y 6/1, greenish grey for the entire unit massive structure	0.36m 3.47m-3.83m	WF2-006>3.65m
5	same as unit 3 very fryable dark yellowish orange mottle subequal with light greenish grey, and purple burrows are present upper contact is gradational	1.13m 3.83m-4.96m	WF2-007>4.93m
6	claystone ~80% dark yellowish orange mottles 10% light greenish grey and greyish purple clay cutans blocky heads	0.52m 4.96m-5.48m	WF2-008>5.22m
7	partially covered interval grey siltstone in places black shale where measured deep modern weathering no samples possible	1.85m 5.48m-7.33m	

8	claystoneminor silt near topclay cutansslickensidespowdered jarositecoalified organic materialdark greyweak mottling near base 7.5YR 5/6, strong brownhalf way up there are "pebbly" zones, friable individual rounded clay particles less than 1mm in size (wrapped in WF2-009 bag)	0.85m7.33m-8.18m	WF2-009>7.93mWF2-010>8.17m
9	claystone blocky breakage roots and organic matter are uncommon minor slicken sides	0.35m 8.18m-8.53m	WF2-011>8.38m WF2-012>8.52m
10	claystone black finely laminated <1mm abundant organic matter coalified material abundant jarosite palm fronds clay cutans upper contact is gradational	0.26m 8.53m-8.79m	WF2-013>8.55m WF2-014>8.77m
11	claystone clay cutans medium grey olive grey SY 4/2 mottles minor olive yellow 2.5Y 6/8 mottles blocky breakage pattern minor jarosite	0.9m 8.79m-9.69m	WF2-015>8.99m WF2-016>9.19m WF2-017>9.39m WF2-018>9.59m WF2-019>9.68m
12	dark grey very friable deeply weathered not able to sample	1.08m 9.69m-10.77m	

13	siltstonedark greyweak local clay cutans WF2-024>10y 3/1 WF2-025>N 3/1 WF2-026>N3/1 WF2-027>N2.5	1.70m10.77-12.47m	WF2-020>10.87mWF2-021>10.97m - clayey siltstoneWF2-022>11.07m - clayey siltstone - clay cutansWF2-023>11.17M - same but with mottles -dark olive gray SY-3/2WF2-024>11.27m - same grain size and mottlingWF2-025>11.37mWF2-026>11.47m - larger slicken sides -very minor yellow brown mottles -mm scaleWF2-027>11.57m - claystone with minor silt -slicken sides - blocky/angular peds -very minor yellow brown mottles -faint, light gray root traces (linear)
14	claystone black appears carbonaceous minor thin laminations clay cutans small A-horizon? sharp lower contact	0.02m 12.47m-12.49m	WF2-037>12.475
15	claystone slick and sides diffuse, amorphous, gleyed zone, green-gray ~30%-40% grayish purple mottles surround gley zone minor yellow brown mottles, ~10%-20% iron oxide nodules WF2-038>10YR 3/1 very dark gray WF2-039> 2.5YR 4/2 weak red WF2-040> 2.5YR 4/1 dark reddish gray	0.15m 12.49m-12.64m	WF2-038>12.50m WF2-039>12.56m WF2-040>12.63m -nice blocky, small columnar peds ~1cm by 2cm -B horizon (Bt)? -sharp lower contact
16	claystone Bg? increased proportion of green-gray gley, ~60% increased yellow brown mottles a lot of clay cutans not many big slicken sides yellow brown surrounded by purple surrounded by grey green gradational lower contact WF2-041> 10Y 6/1 greenish gray WF2-042> 5YR 4/1 dark gray	0.25m 12.64m-12.89m	WF2-041>12.68m *iron oxide nodules WF2-042>>12.85m

17	clayey siltstone 10Y-6/1, greenish-greymottled ~30%, 7.5YR-4/3 browncutansgradational lower contactminor grayish purple (dusky?)	0.14m12.89m-13.03m	WF2-043>12.92mWF2-044>13.00m
18	sandstone green sharp lower contact fine upper-medium lower large cross stratification at base thins over 30m before obscured by modern weathers fines upward and is massive near top thin (1-3m) layers of siltstone and minor clay yellow brown mottles (circular) surrounded by grey and the dusky purple yellow brown mottles at top minor pedogenesis on splays?	1.44m 13.03m-14.47m	WF2-045>13.28m WF2-046>13.53m WF2-047>14.07m
19	fine-grained sandstone with silt mottled with yellow brown, ~20% glay 10Y-6/1 greenish grey, main color probable soil horizon on top of underline sandstone yellow mottles increase up-section	0.53m 14.47m-15.00m	WF2-048>14.72m WF2-049>14.97m WF2-050>15.22m
20	siltstone with clay medium dark grey no slick and sides at base	1.6m 15.22m-16.82m	WF2-051>15.42m -minor clay cutans -pale olive and brown mottles WF2-052>15.62m -no mottles or slick and sides -minor cutans WF2-053>15.82m -same as below WF2-054>16.02m -Slick and sides -some brown mottling WF2-055>16.22m -same as below WF2-056>16.42m -no more mottling WF2-057>16.62m -slick and sides WF2-058>16.82m -same as above
21	claystone with silt yellow brown mottles that are surrounded by a pale olive mottle yellow brown roots dusky purple, ~30% yellow brown nodules consentric roots are filled in with clay and yellow brown nodules wetter conditions than calcite nodules? clay cutans	0.9m 16.82m-17.72m	WF2-059>17.02m WF2-060>17.22m -more intense yellow roots WF2-061>17.42m WF2-062>17.62m WF2-063>17.69m

	WF2-062>5PB 3/1 dark bluish gray WF2-063>N3 very dark gray		
22	claystonedark olive brown mottlingmedium grey, main colorslick and sides near base minor yellow brown mottling	0.59m17.72m-18.31m	WF2-064>18.015mWF2-065>18.30m
23	sandstone rusty color medium lower to fine upper grain size near the base trough cross bedding laminated ripples in middle and upper unit sharp lower contact thins laterally over a few tens of meters thin section sample: rusty red is surface discoloration, white on the inside	1.74m 18.31m-20.05m	
24	siltstone with clay weathers onto recessive vegetative surface in outcrop it's a rusty red fresh color is a weak red, 10R-5/3 massive	0.35m 20.05m-20.40m	WF2-066>19.9m WF2-067>20.04m
25	siltstone fine-grained clay-rich same color as below minor yellow brown mottles surrounded by greyish purple mottles submilimeter burrows	0.45m 20.40m-20.85m	WF2-068>20.60m WF2-069>20.8m
26	silty claystone same colors as below	1.1m 20.85m-21.95m	WF2-070>21.00m WF2-071>21.8m
27	silty claystone same colors as below massive	0.8m 21.95m-22.75m	WF2-072>22.20m WF2-073>22.5m WF2-074>22.65m *carbonate nodule from ground *added unknown small sample
28	siltstone with fine grain sand same/or darker red than below has yellow and brown mottles green grey gley which is minor	0.47m 22.75m-23.22m	WF2-075>22.8m WF2-076>22.95m -clay cutans -soil B horizon WF2-077>23.15m

29	sandstone, rusty, lenticular weathered, pale red contains large scale trough cross beds at base massive near the top red mud rip ups minor ripple lamination medium lower to fine upper grain size	1.8m 23.22-25.02m	
30	base is partially covered claystone, minor siltmostly dusky red, 10R-3/3, ~60%greenish grey root traves, ~10%yellow brown mottles, ~30% (appears blocky)this is a B horizongreyish red, ~40%yellow, ~50%grey, ~10%burrow or roots have a green grey halo with yellow brown in center	1.75m25.02m-26.77m	WF2-078>26.27m - example of burrows -also some nesting vertical burrows 10cm long and 3cm wide at the bottomWF2-079>26.37mWF2-080>26.47mWF2-081>26.57mWF2-082>26.67mWF2-083>26.76m
31	fine grained sandstone with silt massive minor yellow brown mottles and burrow fills burrows are cylindrical 1/2cm or less in diameter most of the unit is green grey color probably Bg zone WF2-084>5GY 7/1 light greenish gray WF2-085>10Y 7/1 light greenish gray	0.22m 26.77m-26.99m	WF2-084>26.87m -one piece saved for thin section sample WF2-085>26.97m -minor diffuse purple mottles -gradational lower contact
32	same as below but more yellow brown mottling vertical burrows abundant tiny spheres fine sand to silt potentially A horizon	0.25m 26.99m-27.24m	WF2-086>27.04m WF2-087>27.15m -slicken sides on sample -potential carbonate nodules -also dark grey roots above/penetrating sample WF2-088>27.22m -this sample has no slicken sides
33	siltstone, light grey with minor yellow brown some sand	0.16m 27.24m-27.40m	WF2-089>27.29m WF2-090>27.37m
34	siltstone overall color is grey fine laminations near the base, otherwise massive one slicken side near the top	0.85m 27.40m-28.25m	WF2-091>27.60m WF2-092>27.80m WF2-093>28.00m WF2-094>28.20m
35	siltstone with some clay light grey with pale orange mottles that are ~50% diffuse boundaries slicken side	0.6m 28.25m-28.85m	WF2-095>28.45m WF2-096>28.65m
36	siltstone with clay greenish grey, ~40% 10R-6/1 ~60% weak red mottles, 10R-4./4 some of the green grey is wispy	0.64m 28.85m-29.49	WF2-097>29.05m WF2-098>29.25m

37	crevasse splay zone fine lower to medium lower splay is 5.17cm, 1cm thick interbedded siltstone fine laminations 3cm tall ripple lamination sharp lower contact	1.35m 29.99m-30.84m	
38	claystone with minor silt light grey lower contact is gradual clay cutans very minor diffuse light brown mottles	0.2m 30.84m-31.04m	WF2-099>30.89m WF2-100>30.99m
39	claystonegreenish grey glay, 5GY-6/1, ~60% near basedusky red mottling, 10R-3/4, ~40% near basegradual increase from bottom to top ending in near 100% redroot traces, some are wispyminor yellow brown mottling in the centerslicken side in the middlelower contact of the unit is gradational	0.9m31.04m-31.94m	WF2-101>31.14mWF2-102>31.34mWF2-103>31.54mWF2-104>31.74m -columnar ped: has 5 sides to it, ~7cm in diameterWF2-105>31.84m -has greyish purple mottles -root traces are yellow brownWF2-106>31.92m
40	crevasse display unit	0.91m 31.94m-32.85m	
41	claystone main color is reddish brown, 2.5YR-4/3 has minor greenish grey mottles (distinct) clay cutans has slicken sides	0.21m 32.85m-33.06m	WF2-107>32.95m
42	siltstone same reddish color as below minor green grey root traces faint laminations laterally equivalent to minor crevasse splays	0.28m 33.06m-33.34m	WF2-108>33.20m
43	siltstone with clay reddish brown, ~80% greenish grey,~20% more greenish grey towards the top of the unit wispy mottles	0.99m 33.34m-34.33m	WF2-109>33.44m WF2-110>33.64m -clay cutans -slicken sides WF2-111>34.14m WF2-112>34.31m
44	siltstone with fine grained sand weakly laminated probably a splay deposit	0.34m 34.33m-34.67m	WF2-113>34.48m
45	crevasse splay unit thicker beds 15cm-20cm thick	0.82m 34.67m-35.49m	
46	siltstone with clay-mostly reddish brown greyish purple mottles in lower half ~10% greenish grey glay minor yellow brown mottles thin layer of greenish grey glay ~2/3 up from base	0.43m 35.49m-35.92m	WF2-114>35.64m WF2-115>35.79m WF2-116>35.90m

47	claystone reddish brown coloring, ~80% green greyish mottles, ~20% slicken sides (large) organic matter within green grey mottles the green grey has orange diffuse surrounding it pedotuble some wispy green grey mottles	1.27m 35.92m-37.19m	WF2-117>36.12m WF2-118>36.32m WF2-119>36.52m WF2-120>36.72m WF2-121>36.92m WF2-122>37.18m
48	claystone interbedded with fine grained sandstonelayers are 0.5m to 10cm thick claystone is reddish brown and greenish purplethere are yellow brown mottles (minor)clay cutansmottles are mostly diffusewispy roots have iron oxide in themfine grained sandstone are greenish grey and massivegradational lower contact	0.44m37.19m-37.63m	WF2-123>37.29mWF2-124>37.58m
49	sandstone fine upper interbedded with purple claystone bed thickness decreases up section more clay up section sandstones mostly massive some ripples Claystones have yellow brown mottles surrounded by green grey bottom sand is 0.4m thick other units are 1cm-5cm thick sharp lower contact splay sequence		
50	very finely laminated claystone medium grey at base, light grey in muddle, and pale olive at top sharp lower contact sharp upper contact unit above is very thick sandstone yellow in outcrop	0.45m 38.85m-39.30m	WF2-125>38.90m -minor clay cutans -potential pollen sample WF2-126>38.97m

WF3			
UNIT	DESCRIPTION	THICKNESS	SAMPLE
1	-silty claystone -dusty red mottling (diffuse), moderate (~50%) -main color is dark greenish gray -very minor yellow brown (orangish) mottles with green gray halos	0.3m 0.0m-0.3m	WF3-001>0.1m WF3-002>0.2m -base not exposed
2	silty claystone similar colors but dusky red mottles are 10percent orange mottles slicken sides	0.3m 0.3m-0.6m	WF3-003>0.4m WF3-004>0.5m
3	siltstone with clay slicken sides at the base grayish purple mottles gradational lower contact major color is greenish gray, 10G 5/1 clay cutans	0.36m 0.6m-0.96m	WF3-005>0.7m WF3-006>0.8m WF3-007>0.9m -vein like mottles
4	siltstone -dusky red and greenish grey, ~40-60% -very minor olive mottles near base	0.24m 0.96m-1.20m	WF3-008>1.06m -thin section WF3-009>1.16m -small (2cm diameter) peds
5	clayey siltstone -greenish gray with dusky red mottle (~40%) diffuse but surrounded by green gray -very minor dark yellow/orange mottles ~1-3mm in diameters	0.35m 1.20m-1.55m	WF3-010>1.30m WF3-011>1.40m
6	siltstone with minor clay greenish gray 10Y 6/1 around yellow orange sharp mottles light grayish purple to light gray is majority	1.27m 1.55m-2.83m	WF3-012>1.95m WF3-013>2.15m WF3-014>2.35m WF3-015>2.55m WF3-016>2.75m
7	Siltstone with minor clay Greenish gray to light gray Minor yellow orange mottle , sharp Very very light gray purple Gradational lower contact	0.61m 2.83m-3.44m	WF3-017>3.03m WF3-018>3.23m WF3-019>3.43m

8	ClaystoneMinor siltVery dark gray N3Clay cutansMinor pale olive mottlesGrayish/dusky purple mottles	0.8m3.44m-4.24m	WF3-20>3.54WF3-21>3.64WF3-22>3.74WF3-23>3.84WF3-24>3.94WF3-25>4.04WF3-26>4.14WF3-27>4.23
9	Claystone Clay cutans Mottled dusky red 10R 3/2 ~80% Dark gray ~20% N4 Gradational lower contact	0.3 4.24m-4.54m	WF3-28>4.34m WF3-29>4.44m
10	Sandstone Very fine upper to fine lower Ripple laminations to mostly massive Crevasse splay Sharp lower contact Bioturbation on top	0.3 4.45-4.84	WF3-30>4.65m
11	Siltstone Minor clay Dusky red mottling (10%) Dark gray (90%)	0.26 4.84-5.10	WF3-031>4.90 WF3-032>5.05 -BC horizon? -sharp lower contact pale olive mottles toward top
12	Claystone Gradational lower contact Weak red 10R 4/2 90% Minor green gray mottles and yellow orangish brown mottles Clay cutans More green gray up-section to about 40%	0.36 5.10-5.46	WF3-033>5.20 WF3-034>5.30 WF3-035>5.40
13	Claystone Minor silt Weak red mottles (mostly) Minor yellow orangish brown mottles Platy breakage Dark greenish gray mottles (very very minor) WF3-036>10R 3/2 WF3-037>10R 4/1 dark reddish gray	0.25 5.46-5.71	WF3-036>5.53m WF3-037>5.61m *lower red of double purple/red of WF 2015 section

14	Sandstone Crevasse splayMassive bioturbated Very fine upper to fine lower grainsize	0.485.71-6.19	
15	Siltstone Minor clay Weak red mottle 80-90% Sharp yellow orangish brown mottles (no halos) Circular green gray mottles (~4mm in diameter)	0.2 6.19-6.39	WF3-038>6.29
16	Siltone Very minor clay Weak red 70% Greenish grey 30% Diffuse Greenish grey root traces	0.29 6.39-6.68	WF3-039>6.44 WF3-040>6.54 WF3-041>6.64
17	Siltstone with minor clay Dark reddish gray 10R 4/1 (90%+) Very minor diffuse green gray Yellow brown mottles Clay cutans	0.8 6.68-7.48	WF3-042>6.78 WF3-043>6.88 WF3-044>6.98 WF3-045>7.08 WF3-046>7.18 WF3-047>7.28 WF3-048>7.38 WF3-049>7.47
18	Siltstone Minor clay Light gray Massive Sharp lower contact WF3-050>N5 gray WF3-051>N5 gray	0.15 7.48-7.63	WF3-050>7.53 WF3-051>7.59 Rare clay cutans Probably a C or Bc Horizon
19	Claystone with minor silt Gradational lower contact Purple gray ~70% Weak red ~20% Diffuse and sharp Greenish gray Large slicken sides Yellow brown mottles (stringers like roots with green grey halos) WF3-052>5PB 3/1 dark bluish gray WF3-053> 2.5YR 5/1 reddish gray WF3-054> N5 WF3-055>5PB 4/1 WF3-056>5YR 5/1 gray WF3-057>5YR 6/1 gray WF3-058>	0.84 7.63-8.47	WF3-052>7.73 WF3-053>7.83 WF3-054>7.93 WF3-055>8.03 WF3-056>8.13 WF3-057>8.23 WF3-058>8.33 WF3-059>8.43

20	Siltstone Greyish purple 60% Light greenish grey 40% Very minor olive mottles Upper and lower gradational contact	0.39 8.47-8.86	WF3-060>8.57 WF3-061>8.67 WF3-062>8.77
21	Claystone Minor silt Purple grey mottles ~70% Light grey mottles ~30% *top of red-purple double paleosol at base of WF 2015	0.62 8.86-9.48	WF3-063>8.90 WF3-064>9.15 WF3-065>9.40 WF3-066>9.46

Sample Number	corrected height	Horzion	Lithology	Y/B nodles 0=common,3=rare,6=absent	carbonate noodles (0=absent; 3=rare/small; 6 = abundant)	Chroma	Soil Morph Index	Average SMI	Median Corrected Height
WF2-106	113.31	B	claystone	6	0	1	7	7	113.03
WF2-105	113.23	B	claystone	6	0	1	7		
WF2-104	113.13	B	claystone	6	0	1	7		
WF2-103	112.93	B	claystone	6	0	1	7		
WF2-102	112.73	B	claystone	6	0	1	7		
WF2-101	112.53	B	claystone	6	0	1	7		
WF2-098	110.64	B	clayey siltstone	6	0	1	7	7	110.54
WF2-097	110.44	B	clayey siltstone	6	0	1	7		
WF2-096	110.04	Bg	clayey siltstone	6	0	1	7	4	109.94
WF2-095	109.84	Bg	clayey siltstone	6	0	1	7		
WF2-085	108.36	Bg	sandstone	0	0	1	1		108.31
WF2-084	108.26	Bg	sandstone	0	0	1	1		
WF2-083	108.15	B	silty claystone	6	0	3	9	9	107.91
WF2-082	108.06	B	silty claystone	6	0	3	9		
WF2-081	107.96	B	silty claystone	6	0	3	9		
WF2-080	107.86	B	silty claystone	6	0	3	9		
WF2-079	107.76	B	silty claystone	6	0	3	9		

WF2-078	107.66	B	silty claystone	6	0	3	9		
WF2-063	99.08	B	claystone	0	0	0	0	0.2	98.81
WF2-062	99.01	B	claystone	0	0	1	1		
WF2-061	98.81	B	claystone	0	0	0	0		
WF2-060	98.61	B	claystone	0	0	0	0		
WF2-059	98.41	B	claystone	0	0	0	0		
WF2-050	96.61	B	silty sandstone	6	0	1	7	7	96.36
WF2-049	96.36	B	silty sandstone	6	0	1	7		
WF2-048	96.11	B	silty sandstone	6	0	1	7		
WF2-044	94.39	B	clayey siltstone	6	0	1	7	7	94.35
WF2-043	94.31	B	clayey siltstone	6	0	1	7		
WF2-042	94.24	Bg	claystone	0	0	1	1	1	94.155
WF2-041	94.07	Bg	claystone	0	0	1	1		
WF2-040	94.02	Bt?	claystone	0	0	1	1	1.333333333	93.95
WF2-039	93.95	Bt?	claystone	0	0	2	2		
WF2-038	93.89	Bt?	claystone	0	0	1	1		
WF2-036	93.86	Bss	silty claystone	6	0	1	7	6.333333333	93.76
WF2-035	93.76	Bss	silty claystone	6	0	0	6		
WF2-034	93.66	Bss	silty claystone	6	0	0	6		
WF2-033	93.56	B	silty claystone	6	0	0	6	6	93.06
WF2-032	93.46	B?	silty claystone	6	0	0	6		
WF2-031	93.36	B?	claystone	6	0	0	6		
WF2-030	93.26	B	claystone	6	0	0	6		
WF2-029	93.16	B	claystone	6	0	0	6		
WF2-028	93.06	Bss	claystone	6	0	1	7		
WF2-027	92.96	B roottraces A?	claystone	3	0	0	3		
WF2-026	92.86	Bss	clayey siltstone	3	0	1	4		
WF2-025	92.76	Bss	clayey siltstone	6	0	1	7		
WF2-024	92.66	B	clayey siltstone	6	0	1	7		
WF2-023	92.56	B	clayey siltstone	6	0	2	8		
WF-293	80.59	B	sandy siltstone	6	6	2	14	14	80.265
WF-292	80.51	B	sandy siltstone	6	6	2	14		
WF-291	80.41	B	sandy siltstone	6	6	2	14		
WF-290	80.31	B	sandstone	6	6	2	14		
WF-289	80.22	B	sandstone	6	6	2	14		
WF-288	80.12	B	sandstone	6	6	2	14		
WF-287	80.02	B	sandstone	6	6	2	14		

WF-286	79.92	B	sandstone	6	6	2	14		
WF-263	73.03	B	silty claystone	6	0	0	6	6.666666667	70.915
WF-262	72.79	B	silty claystone	6	0	0	6		
WF-261	72.54	B	silty claystone	6	0	0	6		
WF-260	72.29	B	silty claystone	6	0	0	6		
WF-259	72.04	B	silty claystone	6	0	0	6		
WF-258	71.79	B	silty claystone	6	0	0	6		
WF-257	71.54	B	silty claystone	6	0	0	6		
WF-256	71.29	B	silty claystone	6	0	0	6		
WF-255	71.04	B	silty claystone	6	0	0	6		
WF-254	70.79	B	silty claystone	6	0	0	6		
WF-253	70.54	B	silty claystone	6	0	0	6		
WF-252	70.29	B	silty claystone	6	0	0	6		
WF-251	70.04	B	silty claystone	6	0	0	6		
WF-250	69.79	B	silty claystone	6	0	0	6		
WF-249	69.54	B	silty claystone	6	0	0	6		
WF-248	69.29	B	silty claystone	6	0	0	6		
WF-247	69.23	B	siltstone	6	0	6	12		
WF-246	68.98	B	siltstone	6	0	6	12		
WF-237	61.12	B	silty claystone	6	6	4	16	16	60.995
WF-236	60.87	B	silty claystone	6	6	4	16		
WF-219	56.57	B	silty claystone	6	6	4	16	16	55.57
WF-218	56.32	B	silty claystone	6	6	4	16		
WF-217	56.07	B	silty claystone	6	6	4	16		
WF-216	55.82	B	silty claystone	6	6	4	16		
WF-215	55.32	B	silty claystone	6	6	4	16		
WF-214	55.07	B	silty claystone	6	6	4	16		
WF-213	54.82	B	silty claystone	6	6	4	16		
WF-212	52.97	B	silty claystone	6	6	4	16		
WF-201	51.65	B	silty claystone	6	6	2	14	14	50.6
WF-200	51.55	B	silty claystone	6	6	2	14		
WF-199	51.45	B	silty claystone	6	6	2	14		
WF-198	51.35	B	silty claystone	6	6	2	14		
WF-197	51.25	B	silty claystone	6	6	2	14		
WF-196	51.15	B	silty claystone	6	6	2	14		

WF-195	51.05	B	silty claystone	6	6	2	14		
WF-194	50.95	B	silty claystone	6	6	2	14		
WF-193	50.85	B	silty claystone	6	6	2	14		
WF-192	50.75	B	silty claystone	6	6	2	14		
WF-191	50.65	B	silty claystone	6	6	2	14		
WF-190	50.55	B	silty claystone	6	6	2	14		
WF-189	50.45	B	silty claystone	6	6	2	14		
WF-188	50.25	B	silty claystone	6	6	2	14		
WF-187	50.15	B	silty claystone	6	6	2	14		
WF-186	50.05	B	silty claystone	6	6	2	14		
WF-185	49.95	B	silty claystone	6	6	2	14		
WF-184	49.85	B	silty claystone	6	6	2	14		
WF-183	49.75	B	silty claystone	6	6	2	14		
WF-182	49.65	B	silty claystone	6	6	2	14		
WF-181	49.55	B	silty claystone	6	6	2	14		
WF-180	49.45	B	silty claystone	6	6	2	14		
WF-169	46.55	A/B	silty claystone	6	0	0	6	12	46.1
WF-168	46.4	A/B	silty claystone	6	0	0	6		
WF-167	46.25	B	silty claystone	6	6	2	14		
WF-166	46.15	B	silty claystone	6	6	2	14		
WF-165	46.05	B	silty claystone	6	6	2	14		
WF-164	45.95	B	silty claystone	6	6	2	14		
WF-163	45.85	B	silty claystone	6	6	2	14		
WF-162	45.75	B	silty claystone	6	6	2	14		
WF-161	45.63	B1	claystone	6	0	2	8	8	45.48
WF-160	45.53	B1	claystone	6	0	2	8		
WF-159	45.43	B1	claystone	6	0	2	8		
WF-158	45.33	B1	claystone	6	0	2	8		
WF-157	45.23	B	silty claystone	6	6	2	14	14	44.58
WF-156	45.13	B	silty claystone	6	6	2	14		
WF-155	45.03	B	silty claystone	6	6	2	14		
WF-154	44.93	B	silty claystone	6	6	2	14		
WF-153	44.83	B	silty claystone	6	6	2	14		
WF-152	44.73	B	silty claystone	6	6	2	14		
WF-151	44.63	B	silty claystone	6	6	2	14		

WF-150	44.53	B	silty claystone	6	6	2	14		
WF-149	44.43	B	silty claystone	6	6	2	14		
WF-148	44.33	B	silty claystone	6	6	2	14		
WF-147	44.23	B	silty claystone	6	6	2	14		
WF-146	44.13	B	silty claystone	6	6	2	14		
WF-145	44.03	B	silty claystone	6	6	2	14		
WF-144	43.93	B	silty claystone	6	6	2	14		
WF-133	41.36	B	claystone	3	0	0	3	3	40.36
WF-132	41.11	B	claystone	3	0	0	3		
WF-131	40.86	B	claystone	3	0	0	3		
WF-130	40.61	B	claystone	3	0	0	3		
WF-129	40.36	B	claystone	3	0	0	3		
WF-128	40.11	B	claystone	3	0	0	3		
WF-127	39.86	B	claystone	3	0	0	3		
WF-126	39.61	B	claystone	3	0	0	3		
WF-125	39.36	B	claystone	3	0	0	3		
WF-096	27.72	B	claystone	3	0	1	4	4.625	26.345
WF-095	27.47	B	claystone	3	0	1	4		
WF-094	27.22	B	claystone	3	0	1	4		
WF-093	26.97	B	claystone	3	0	1	4		
WF-092	26.72	B	claystone	3	0	1	4		
WF-091	26.47	B	claystone	3	0	1	4		
WF-090	26.22	B	claystone	3	0	1	4		
WF-089	25.97	B	claystone	3	0	1	4		
WF-088	25.72	B	claystone	3	0	1	4		
WF-087	25.39	B?	clayey siltstone	6	0	0.5	6.5		
WF-086	25.14	B?	clayey siltstone	6	0	0.5	6.5		
WF-085	24.89	B?	clayey siltstone	6	0	0.5	6.5		
WF-068	20.71	B	clayey siltstone	6	0	0	6	6	20.335
WF-067	20.46	B	clayey siltstone	6	0	0	6		
WF-066	20.21	B	clayey siltstone	6	0	0	6		
WF-065	19.96	B	clayey siltstone	6	0	0	6		
WF-049	14.39	A?	silty claystone	6	0	0	6	6.2	13.265
WF-048	14.14	B?	silty claystone	6	0	0	6		
WF-047	13.89	B?	silty claystone	6	0	0	6		
WF-046	13.64	B?	silty claystone	6	0	0	6		
WF-045	13.39	B?	silty claystone	6	0	0	6		
WF-044	13.14	B?	silty claystone	6	0	0	6		

WF-043	12.89	B?	silty claystone	6	0	0	6		
WF-042	12.64	B?	silty claystone	6	0	0	6		
WF-041	12.39	B	clayey siltstone	6	0	1	7		
WF-040	12.14	B	clayey siltstone	6	0	1	7		
WF-022	8.84	B	siltstone	6	0	2	8	8	8.29
WF-021	8.69	B	siltstone	6	0	2	8		
WF-020	8.59	B	siltstone	6	0	2	8		
WF-019	8.49	B	siltstone	6	0	2	8		
WF-018	8.39	B	siltstone	6	0	2	8		
WF-017	8.29	B	siltstone	6	0	2	8		
WF-016	8.19	B	siltstone	6	0	2	8		
WF-015	8.09	B	siltstone	6	0	2	8		
WF-014	7.99	B	siltstone	6	0	2	8		
WF-013	7.89	B	siltstone	6	0	2	8		
WF-012	7.79	B	siltstone	6	0	2	8		
WF3-066	9.46	Bg	claystone	6	0	1	7	7	8.9
WF3-065	9.4	Bg	claystone	6	0	0	6		
WF3-064	9.15	Bg	claystone	6	0	1	7		
WF3-063	8.9	Bg	claystone	6	0	1	7		
WF3-062	8.77	Bg	siltstone	6	0	1	7		
WF3-061	8.67	Bg	siltstone	6	0	1	7		
WF3-060	8.57	Bg	siltstone	6	0	2	8		
WF3-059	8.43	Bss	claystone	6	0	2	8	7.375	8.08
WF3-058	8.33	Bss	claystone	6	0	4	10		
WF3-057	8.23	Bss	claystone	6	0	1	7		
WF3-056	8.13	Bss	claystone	6	0	1	7		
WF3-055	8.03	Bss	claystone	6	0	1	7		
WF3-054	7.93	Bss	claystone	6	0	0	6		
WF3-053	7.83	Bss	claystone	6	0	1	7		
WF3-052	7.73	Bss	claystone	6	0	1	7		
WF3-037	6.61	B	claystone	6	0	1	7	7.8	5.4
WF3-036	5.53	B	claystone	6	0	2	8		
WF3-035	5.4	B	claystone	6	0	2	8		
WF3-034	5.3	B	claystone	6	0	2	8		
WF3-033	5.2	B	claystone	6	0	2	8		
Standard Devation	4.285853622								

Sample Number	corrected height	Horzion	Lithology	Y/B nodles 0=common,3=rare, 6=absent	carbonate noodles (0=absent; 3=rare/small; 6 = abundant)	Chroma	Soil Morph Index	Average SMI	Median Corrected Height
WF2-106	113.31	B	claystone	6	0	1	7	7	113.03
WF2-105	113.23	B	claystone	6	0	1	7		
WF2-104	113.13	B	claystone	6	0	1	7		
WF2-103	112.93	B	claystone	6	0	1	7		
WF2-102	112.73	B	claystone	6	0	1	7		
WF2-101	112.53	B	claystone	6	0	1	7		
WF2-098	110.64	B	clayey siltstone	6	0	1	7	7	110.54
WF2-097	110.44	B	clayey siltstone	6	0	1	7		
WF2-096	110.04	Bg	clayey siltstone	6	0	1	7	4	109.94
WF2-095	109.84	Bg	clayey siltstone	6	0	1	7		
WF2-085	108.36	Bg	sandstone	0	0	1	1		108.31
WF2-084	108.26	Bg	sandstone	0	0	1	1		
WF2-083	108.15	B	silty claystone	6	0	3	9	9	107.91
WF2-082	108.06	B	silty claystone	6	0	3	9		
WF2-081	107.96	B	silty claystone	6	0	3	9		
WF2-080	107.86	B	silty claystone	6	0	3	9		
WF2-079	107.76	B	silty claystone	6	0	3	9		

WF2-078	107.66	B	silty claystone	6	0	3	9		
WF2-063	99.08	B	claystone	0	0	0	0	0.2	98.81
WF2-062	99.01	B	claystone	0	0	1	1		
WF2-061	98.81	B	claystone	0	0	0	0		
WF2-060	98.61	B	claystone	0	0	0	0		
WF2-059	98.41	B	claystone	0	0	0	0		
WF2-050	96.61	B	silty sandstone	6	0	1	7	7	96.36
WF2-049	96.36	B	silty sandstone	6	0	1	7		
WF2-048	96.11	B	silty sandstone	6	0	1	7		
WF2-044	94.39	B	clayey siltstone	6	0	1	7	7	94.35
WF2-043	94.31	B	clayey siltstone	6	0	1	7		
WF2-042	94.24	Bg	claystone	0	0	1	1	1	94.155
WF2-041	94.07	Bg	claystone	0	0	1	1		
WF2-040	94.02	Bt?	claystone	0	0	1	1	1.3333	93.95
WF2-039	93.95	Bt?	claystone	0	0	2	2		
WF2-038	93.89	Bt?	claystone	0	0	1	1		
WF2-036	93.86	Bss	silty claystone	6	0	1	7	6.3333	93.76
WF2-035	93.76	Bss	silty claystone	6	0	0	6		

WF2-034	93.66	Bss	silty claystone	6	0	0	6		
WF2-033	93.56	B	silty claystone	6	0	0	6	6	93.06
WF2-032	93.46	B?	silty claystone	6	0	0	6		
WF2-031	93.36	B?	claystone	6	0	0	6		
WF2-030	93.26	B	claystone	6	0	0	6		
WF2-029	93.16	B	claystone	6	0	0	6		
WF2-028	93.06	Bss	claystone	6	0	1	7		
WF2-027	92.96	B roottraces A?	claystone	3	0	0	3		
WF2-026	92.86	Bss	clayey siltstone	3	0	1	4		
WF2-025	92.76	Bss	clayey siltstone	6	0	1	7		
WF2-024	92.66	B	clayey siltstone	6	0	1	7		
WF2-023	92.56	B	clayey siltstone	6	0	2	8		
WF-293	80.59	B	sandy siltstone	6	6	2	14	14	80.265
WF-292	80.51	B	sandy siltstone	6	6	2	14		
WF-291	80.41	B	sandy siltstone	6	6	2	14		
WF-290	80.31	B	sandstone	6	6	2	14		
WF-289	80.22	B	sandstone	6	6	2	14		
WF-288	80.12	B	sandstone	6	6	2	14		

WF-287	80.02	B	sandstone	6	6	2	14		
WF-286	79.92	B	sandstone	6	6	2	14		
WF-263	73.03	B	silty claystone	6	0	0	6	6.6667	70.915
WF-262	72.79	B	silty claystone	6	0	0	6		
WF-261	72.54	B	silty claystone	6	0	0	6		
WF-260	72.29	B	silty claystone	6	0	0	6		
WF-259	72.04	B	silty claystone	6	0	0	6		
WF-258	71.79	B	silty claystone	6	0	0	6		
WF-257	71.54	B	silty claystone	6	0	0	6		
WF-256	71.29	B	silty claystone	6	0	0	6		
WF-255	71.04	B	silty claystone	6	0	0	6		
WF-254	70.79	B	silty claystone	6	0	0	6		
WF-253	70.54	B	silty claystone	6	0	0	6		
WF-252	70.29	B	silty claystone	6	0	0	6		
WF-251	70.04	B	silty claystone	6	0	0	6		
WF-250	69.79	B	silty claystone	6	0	0	6		
WF-249	69.54	B	silty claystone	6	0	0	6		
WF-248	69.29	B	silty claystone	6	0	0	6		

WF-247	69.23	B	siltstone	6	0	6	12		
WF-246	68.98	B	siltstone	6	0	6	12		
WF-237	61.12	B	silty claystone	6	6	4	16	16	60.995
WF-236	60.87	B	silty claystone	6	6	4	16		
WF-219	56.57	B	silty claystone	6	6	4	16	16	55.57
WF-218	56.32	B	silty claystone	6	6	4	16		
WF-217	56.07	B	silty claystone	6	6	4	16		
WF-216	55.82	B	silty claystone	6	6	4	16		
WF-215	55.32	B	silty claystone	6	6	4	16		
WF-214	55.07	B	silty claystone	6	6	4	16		
WF-213	54.82	B	silty claystone	6	6	4	16		
WF-212	52.97	B	silty claystone	6	6	4	16		
WF-201	51.65	B	silty claystone	6	6	2	14	14	50.6
WF-200	51.55	B	silty claystone	6	6	2	14		
WF-199	51.45	B	silty claystone	6	6	2	14		
WF-198	51.35	B	silty claystone	6	6	2	14		
WF-197	51.25	B	silty claystone	6	6	2	14		
WF-196	51.15	B	silty claystone	6	6	2	14		

WF-195	51.05	B	silty claystone	6	6	2	14		
WF-194	50.95	B	silty claystone	6	6	2	14		
WF-193	50.85	B	silty claystone	6	6	2	14		
WF-192	50.75	B	silty claystone	6	6	2	14		
WF-191	50.65	B	silty claystone	6	6	2	14		
WF-190	50.55	B	silty claystone	6	6	2	14		
WF-189	50.45	B	silty claystone	6	6	2	14		
WF-188	50.25	B	silty claystone	6	6	2	14		
WF-187	50.15	B	silty claystone	6	6	2	14		
WF-186	50.05	B	silty claystone	6	6	2	14		
WF-185	49.95	B	silty claystone	6	6	2	14		
WF-184	49.85	B	silty claystone	6	6	2	14		
WF-183	49.75	B	silty claystone	6	6	2	14		
WF-182	49.65	B	silty claystone	6	6	2	14		
WF-181	49.55	B	silty claystone	6	6	2	14		
WF-180	49.45	B	silty claystone	6	6	2	14		
WF-169	46.55	A/B	silty claystone	6	0	0	6	12	46.1
WF-168	46.4	A/B	silty claystone	6	0	0	6		

WF-167	46.25	B	silty claystone	6	6	2	14		
WF-166	46.15	B	silty claystone	6	6	2	14		
WF-165	46.05	B	silty claystone	6	6	2	14		
WF-164	45.95	B	silty claystone	6	6	2	14		
WF-163	45.85	B	silty claystone	6	6	2	14		
WF-162	45.75	B	silty claystone	6	6	2	14		
WF-161	45.63	B1	claystone	6	0	2	8	8	45.48
WF-160	45.53	B1	claystone	6	0	2	8		
WF-159	45.43	B1	claystone	6	0	2	8		
WF-158	45.33	B1	claystone	6	0	2	8		
WF-157	45.23	B	silty claystone	6	6	2	14	14	44.58
WF-156	45.13	B	silty claystone	6	6	2	14		
WF-155	45.03	B	silty claystone	6	6	2	14		
WF-154	44.93	B	silty claystone	6	6	2	14		
WF-153	44.83	B	silty claystone	6	6	2	14		
WF-152	44.73	B	silty claystone	6	6	2	14		
WF-151	44.63	B	silty claystone	6	6	2	14		
WF-150	44.53	B	silty claystone	6	6	2	14		

WF-149	44.43	B	silty claystone	6	6	2	14		
WF-148	44.33	B	silty claystone	6	6	2	14		
WF-147	44.23	B	silty claystone	6	6	2	14		
WF-146	44.13	B	silty claystone	6	6	2	14		
WF-145	44.03	B	silty claystone	6	6	2	14		
WF-144	43.93	B	silty claystone	6	6	2	14		
WF-133	41.36	B	claystone	3	0	0	3	3	40.36
WF-132	41.11	B	claystone	3	0	0	3		
WF-131	40.86	B	claystone	3	0	0	3		
WF-130	40.61	B	claystone	3	0	0	3		
WF-129	40.36	B	claystone	3	0	0	3		
WF-128	40.11	B	claystone	3	0	0	3		
WF-127	39.86	B	claystone	3	0	0	3		
WF-126	39.61	B	claystone	3	0	0	3		
WF-125	39.36	B	claystone	3	0	0	3		
WF-096	27.72	B	claystone	3	0	1	4	4.625	26.345
WF-095	27.47	B	claystone	3	0	1	4		
WF-094	27.22	B	claystone	3	0	1	4		

WF-093	26.97	B	claystone	3	0	1	4		
WF-092	26.72	B	claystone	3	0	1	4		
WF-091	26.47	B	claystone	3	0	1	4		
WF-090	26.22	B	claystone	3	0	1	4		
WF-089	25.97	B	claystone	3	0	1	4		
WF-088	25.72	B	claystone	3	0	1	4		
WF-087	25.39	B?	clayey siltstone	6	0	0.5	6.5		
WF-086	25.14	B?	clayey siltstone	6	0	0.5	6.5		
WF-085	24.89	B?	clayey siltstone	6	0	0.5	6.5		
WF-068	20.71	B	clayey siltstone	6	0	0	6	6	20.335
WF-067	20.46	B	clayey siltstone	6	0	0	6		
WF-066	20.21	B	clayey siltstone	6	0	0	6		
WF-065	19.96	B	clayey siltstone	6	0	0	6		
WF-049	14.39	A?	silty claystone	6	0	0	6	6.2	13.265
WF-048	14.14	B?	silty claystone	6	0	0	6		
WF-047	13.89	B?	silty claystone	6	0	0	6		
WF-046	13.64	B?	silty claystone	6	0	0	6		
WF-045	13.39	B?	silty claystone	6	0	0	6		

WF-044	13.14	B?	silty claystone	6	0	0	6		
WF-043	12.89	B?	silty claystone	6	0	0	6		
WF-042	12.64	B?	silty claystone	6	0	0	6		
WF-041	12.39	B	clayey siltstone	6	0	1	7		
WF-040	12.14	B	clayey siltstone	6	0	1	7		
WF-022	8.84	B	siltstone	6	0	2	8	8	8.29
WF-021	8.69	B	siltstone	6	0	2	8		
WF-020	8.59	B	siltstone	6	0	2	8		
WF-019	8.49	B	siltstone	6	0	2	8		
WF-018	8.39	B	siltstone	6	0	2	8		
WF-017	8.29	B	siltstone	6	0	2	8		
WF-016	8.19	B	siltstone	6	0	2	8		
WF-015	8.09	B	siltstone	6	0	2	8		
WF-014	7.99	B	siltstone	6	0	2	8		
WF-013	7.89	B	siltstone	6	0	2	8		
WF-012	7.79	B	siltstone	6	0	2	8		
WF3-066	9.46	Bg	claystone	6	0	1	7	7	8.9
WF3-065	9.4	Bg	claystone	6	0	0	6		

WF3-064	9.15	Bg	claystone	6	0	1	7		
WF3-063	8.9	Bg	claystone	6	0	1	7		
WF3-062	8.77	Bg	siltstone	6	0	1	7		
WF3-061	8.67	Bg	siltstone	6	0	1	7		
WF3-060	8.57	Bg	siltstone	6	0	2	8		
WF3-059	8.43	Bss	claystone	6	0	2	8	7.375	8.08
WF3-058	8.33	Bss	claystone	6	0	4	10		
WF3-057	8.23	Bss	claystone	6	0	1	7		
WF3-056	8.13	Bss	claystone	6	0	1	7		
WF3-055	8.03	Bss	claystone	6	0	1	7		
WF3-054	7.93	Bss	claystone	6	0	0	6		
WF3-053	7.83	Bss	claystone	6	0	1	7		
WF3-052	7.73	Bss	claystone	6	0	1	7		
WF3-037	6.61	B	claystone	6	0	1	7	7.8	5.4
WF3-036	5.53	B	claystone	6	0	2	8		
WF3-035	5.4	B	claystone	6	0	2	8		
WF3-034	5.3	B	claystone	6	0	2	8		
WF3-033	5.2	B	claystone	6	0	2	8		

	BFO WF2-098	BFO WF2-097	BFO WF2-096	BFO WF2-095	BFO WF2-094	BFO WF2-093	BFO WF2-092	BFO WF2-091	BFO WF2-088	BFO WF2-087
Stratigraphic Height	110.64	110.44	110.04	109.84	109.59	109.39	109.19	108.99	108.61	108.54
SO3 >/=										
Unnormalized Major Elements (Weight %):										
SiO2	62.14	64.32	57.80	58.70	68.12	65.25	67.12	66.54	63.63	64.86
TiO2	0.713	0.700	0.757	0.748	0.762	0.771	0.820	0.804	0.751	0.761
Al2O3	19.74	18.78	23.47	23.08	17.12	19.05	17.60	17.92	18.94	18.86
FeO*	4.51	4.26	3.81	3.87	2.54	2.58	2.45	2.42	5.09	4.44
MnO	0.006	0.006	0.005	0.005	0.003	0.003	0.003	0.003	0.002	0.002
MgO	0.83	0.75	0.74	0.77	0.63	0.69	0.63	0.67	0.50	0.52
CaO	0.16	0.14	0.16	0.16	0.16	0.17	0.17	0.16	0.10	0.10
Na2O	0.66	0.54	0.84	0.81	0.59	0.65	0.61	0.62	0.57	0.56
K2O	1.68	1.70	1.45	1.54	0.77	0.96	0.64	0.71	0.30	0.32
P2O5	0.060	0.067	0.036	0.035	0.020	0.029	0.016	0.017	0.022	0.018
Sum	90.49	91.26	89.06	89.73	90.71	90.17	90.06	89.85	89.92	90.42
LOI %	8.67	8.00	10.43	10.12	8.62	9.18	9.54	9.48	9.44	9.00
Normalized Major Elements (Weight %):										
SiO2	68.67	70.47	64.90	65.42	75.10	72.37	74.53	74.06	70.76	71.72
TiO2	0.788	0.767	0.850	0.834	0.840	0.855	0.911	0.894	0.835	0.842
Al2O3	21.81	20.58	26.36	25.72	18.87	21.13	19.55	19.94	21.06	20.85
FeO*	4.98	4.67	4.27	4.31	2.80	2.86	2.72	2.69	5.66	4.91
MnO	0.007	0.007	0.006	0.006	0.003	0.004	0.003	0.003	0.003	0.002
MgO	0.92	0.82	0.83	0.86	0.69	0.77	0.70	0.74	0.56	0.57
CaO	0.18	0.16	0.18	0.18	0.17	0.19	0.18	0.18	0.12	0.11
Na2O	0.73	0.59	0.94	0.90	0.65	0.73	0.68	0.69	0.64	0.61
K2O	1.85	1.87	1.63	1.72	0.84	1.07	0.72	0.78	0.34	0.35
P2O5	0.067	0.074	0.040	0.040	0.022	0.032	0.018	0.019	0.024	0.020
Total	100.00	100.00	100.00	100.00	100.00	100.00	100.00	100.00	100.00	100.00
Unnormalized Trace Elements (ppm):										
Ni	22	26	18	15	20	29	28	23	30	29
Cr	57	56	59	56	52	55	55	55	63	64
Sc	12	12	14	14	12	13	14	13	15	14
V	115	118	125	127	112	117	123	118	140	131
Ba	314	326	232	246	177	205	165	165	117	134
Rb	105	101	102	107	61	74	55	61	17	18
Sr	77	79	79	71	53	89	86	88	52	75
Zr	171	193	146	147	310	254	316	288	203	207
Y	40	46	41	37	36	39	26	26	30	32
Nb	16.0	15.9	16.7	16.7	16.9	17.3	18.4	17.5	16.6	16.4
Ga	24	23	29	29	22	24	23	24	20	21
Cu	37	27	29	31	23	27	35	31	28	30
Zn	86	87	58	58	51	58	53	66	26	25
Pb	30	37	33	34	30	35	63	38	24	22
La	58	76	49	47	40	61	30	36	19	20
Ce	113	150	92	91	90	118	60	63	30	29
Th	16	15	18	19	17	17	19	18	17	17
Nd	49	67	40	39	36	50	23	25	13	13
U	6	7	4	5	6	6	7	7	7	6
sum tr.	1348	1462	1185	1190	1167	1289	1198	1164	870	903
in %	0.13	0.15	0.12	0.12	0.12	0.13	0.12	0.12	0.09	0.09

sum m+tr	90.63	91.41	89.18	89.85	90.83	90.30	90.18	89.97	90.01	90.51
M+Toxides	90.66	91.44	89.21	89.88	90.86	90.33	90.21	90.00	90.03	90.54
w/LOI	99.33	99.44	99.64	99.99	99.48	99.51	99.75	99.48	99.47	99.54
if Fe3+	99.83	99.91	100.07	100.42	99.76	99.80	100.03	99.74	100.04	100.04
Major elements are normalized on a volatile-free basis, with total Fe expressed as FeO.										
® denotes a duplicate bead made from the same rock powder.										
NiO	28.2	32.9	22.8	19.4	25.7	36.6	35.0	29.7	38.0	36.6
Cr2O3	83.6	81.3	85.5	82.2	76.2	80.6	80.5	80.3	92.7	93.0
Sc2O3	18.8	18.8	21.2	22.0	19.1	20.0	20.7	20.0	23.3	21.0
V2O3	169.1	173.6	184.4	187.1	164.2	171.6	180.7	174.0	205.8	192.4
BaO	350.5	363.4	258.5	274.2	197.5	229.2	184.3	184.6	131.0	149.6
Rb2O	114.7	110.3	111.5	116.5	67.1	81.2	60.1	67.0	18.9	19.6
SrO	90.6	94.0	93.5	84.1	63.0	105.3	101.9	103.8	62.0	88.7
ZrO2	231.1	260.5	197.7	199.2	419.1	343.1	426.6	389.2	274.4	280.1
Y2O3	51.2	58.3	52.4	47.1	46.2	49.5	32.9	32.9	38.6	41.0
Nb2O5	22.9	22.8	23.9	23.9	24.2	24.8	26.3	25.0	23.7	23.5
Ga2O3	32.4	31.0	38.8	38.7	30.1	32.9	31.5	32.7	27.4	28.5
CuO	46.6	33.6	36.5	38.8	28.3	34.1	43.6	38.6	34.9	37.7
ZnO	106.5	108.8	71.6	71.7	63.9	71.8	65.3	81.9	32.6	31.6
PbO	32.4	39.6	36.0	36.4	32.4	37.4	68.1	41.1	25.3	23.2
La2O3	67.7	89.3	57.5	55.5	47.4	71.4	34.6	42.3	22.6	23.5
CeO2	138.9	184.5	113.3	112.4	110.4	144.4	73.5	77.5	36.9	35.3
ThO2	18.1	16.8	19.5	20.9	19.0	19.2	21.4	20.1	18.8	19.1
Nd2O3	57.1	77.7	46.5	45.1	41.5	58.7	26.6	29.1	15.6	15.4
U2O3	6.6	7.8	4.8	5.4	6.8	6.5	7.5	7.9	7.2	6.6
sum tr.	**1667**	**1805**	**1476**	**1481**	**1482**	**1618**	**1521**	**1478**	**1130**	**1166**
in %	**0.17**	**0.18**	**0.15**	**0.15**	**0.15**	**0.16**	**0.15**	**0.15**	**0.11**	**0.12**

	BFO WF2-086	**BFO WF2-085**	**BFO WF2-084**	**BFO WF2-083**	**BFO WF2-082**	**BFO WF2-081**	**BFO WF2-080**	**BFO WF2-079**	**BFO WF2-078**	**BFO WF2-054**
Stratigraphic Height	108.43	108.36	108.26	108.15	108.06	107.96	107.86	107.76	107.66	97.41
SO3 >/=										
Unnormalized Major Elements (Weight %):										
SiO2	64.75	67.11	69.33	61.22	63.35	63.97	61.39	63.55	70.32	52.80
TiO2	0.665	0.661	0.602	0.627	0.706	0.708	0.730	0.739	0.630	0.818
Al2O3	18.21	17.48	18.21	16.69	15.77	15.51	15.94	15.50	13.39	21.76
FeO*	5.29	4.36	1.54	9.78	7.73	7.39	8.43	7.38	4.95	4.87
MnO	0.003	0.003	0.002	0.013	0.013	0.015	0.020	0.019	0.016	0.004
MgO	0.52	0.55	0.51	1.08	1.30	1.51	1.67	1.64	1.18	1.05
CaO	0.08	0.08	0.06	0.11	0.11	0.15	0.17	0.19	0.14	0.32
Na2O	0.61	0.54	0.45	0.59	0.63	0.72	0.76	0.77	0.91	1.60
K2O	0.55	0.69	0.87	1.46	1.64	1.86	1.92	1.96	2.08	0.56
P2O5	0.022	0.015	0.024	0.069	0.179	0.122	0.116	0.108	0.048	0.017
Sum	90.71	91.49	91.62	91.63	91.42	91.96	91.15	91.86	93.66	83.80
LOI %	8.70	8.00	7.84	7.98	7.50	7.46	7.96	7.34	5.58	15.54
Normalized Major Elements (Weight %):										
SiO2	71.38	73.35	75.67	66.81	69.30	69.57	67.35	69.18	75.08	63.00
TiO2	0.733	0.723	0.657	0.684	0.772	0.770	0.801	0.805	0.673	0.976
Al2O3	20.07	19.10	19.88	18.22	17.24	16.86	17.49	16.87	14.30	25.96
FeO*	5.83	4.77	1.68	10.67	8.45	8.03	9.25	8.03	5.28	5.82
MnO	0.003	0.003	0.003	0.014	0.014	0.016	0.022	0.021	0.017	0.005
MgO	0.57	0.60	0.56	1.18	1.42	1.65	1.83	1.79	1.26	1.25

CaO	0.09	0.08	0.07	0.12	0.12	0.17	0.19	0.21	0.15	0.39
Na2O	0.67	0.59	0.50	0.64	0.69	0.79	0.83	0.84	0.97	1.91
K2O	0.61	0.76	0.95	1.59	1.79	2.02	2.10	2.14	2.22	0.66
P2O5	0.025	0.017	0.026	0.075	0.195	0.133	0.127	0.117	0.051	0.020
Total	100.00	100.00	100.00	100.00	100.00	100.00	100.00	100.00	100.00	100.00
Unnormalized Trace Elements (ppm):										
Ni	30	19	17	77	76	77	78	66	38	16
Cr	59	60	52	55	64	63	65	64	53	50
Sc	14	14	12	13	14	13	15	13	10	18
V	128	131	93	137	138	143	157	144	93	149
Ba	140	211	240	304	316	341	381	351	499	279
Rb	28	35	42	74	89	99	107	107	98	29
Sr	41	66	67	131	114	78	66	64	75	176
Zr	177	180	175	155	156	165	156	181	303	158
Y	37	36	72	88	154	70	54	55	51	19
Nb	14.4	14.6	13.9	13.8	15.4	15.6	15.1	16.0	14.7	15.8
Ga	19	18	17	17	20	20	22	21	17	29
Cu	28	33	25	119	74	34	29	27	21	37
Zn	27	28	30	86	100	118	125	121	83	56
Pb	19	22	32	34	18	18	17	17	16	27
La	26	25	57	115	494	332	165	75	43	25
Ce	36	40	118	256	1334	559	208	93	64	46
Th	16	16	13	13	16	15	16	16	13	15
Nd	13	14	54	80	515	323	136	55	31	19
U	5	5	18	7	7	3	2	5	4	3
sum tr.	856	965	1149	1773	3714	2488	1815	1490	1526	1167
in %	0.09	0.10	0.11	0.18	0.37	0.25	0.18	0.15	0.15	0.12
sum m+tr	90.79	91.58	91.73	91.80	91.79	92.20	91.33	92.01	93.82	83.92
M+Toxides	90.82	91.61	91.76	91.85	91.87	92.26	91.37	92.04	93.85	83.95
w/LOI	99.51	99.61	99.60	99.82	99.38	99.72	99.33	99.39	99.43	99.49
if Fe3+	100.10	100.10	99.77	100.91	100.23	100.54	100.27	100.20	99.98	100.03
Major elements are normalized on a volatile-free basis, with total Fe expressed as FeO.										
Major elements are normalized on a volatile-free basis, with total Fe expressed as FeO.										
NiO	38.3	24.2	21.9	98.1	96.5	98.3	99.8	83.5	48.0	19.9
Cr2O3	85.9	87.1	75.7	80.7	93.6	91.8	94.6	93.2	76.7	73.1
Sc2O3	20.9	20.9	19.0	20.6	21.7	20.6	23.2	19.9	15.3	27.4
V2O3	187.6	193.2	136.5	201.2	202.7	211.0	230.2	212.3	137.3	219.9
BaO	156.2	235.1	267.7	339.2	352.5	380.2	425.6	391.7	557.4	311.5
Rb2O	30.4	37.9	46.3	80.4	97.5	107.7	117.4	116.7	107.2	31.6
SrO	49.0	78.5	79.4	155.2	135.2	92.1	78.4	76.0	88.9	208.0
ZrO2	239.0	242.8	236.9	209.9	210.9	222.7	210.3	244.2	408.8	213.3
Y2O3	46.5	45.9	91.9	111.2	196.1	88.4	68.2	70.4	65.0	24.6
Nb2O5	20.6	20.9	19.9	19.8	22.0	22.3	21.6	22.9	21.0	22.5
Ga2O3	25.0	23.8	23.3	22.9	27.0	26.7	29.6	28.4	23.1	38.6
CuO	35.2	40.7	31.0	148.7	92.7	43.1	35.7	33.9	25.8	46.1
ZnO	34.1	34.6	37.2	107.5	125.0	147.2	155.7	150.0	103.2	69.9
PbO	20.4	23.3	34.6	36.3	19.6	19.3	18.5	18.5	17.6	29.3
La2O3	30.4	29.2	66.3	134.4	579.0	389.6	193.7	88.0	50.0	29.3
CeO2	44.4	48.6	145.3	314.6	1639.8	687.4	256.2	113.8	78.1	56.5
ThO2	17.2	17.8	14.5	14.2	17.3	17.1	17.3	18.0	14.6	16.4
Nd2O3	15.5	16.5	63.2	92.8	600.5	377.0	159.1	63.9	36.6	22.6
U2O3	5.4	5.1	19.3	7.3	7.2	3.8	2.3	5.1	4.3	3.1
sum tr.	**1102**	**1226**	**1430**	**2195**	**4537**	**3046**	**2237**	**1850**	**1879**	**1464**
in %	**0.11**	**0.12**	**0.14**	**0.22**	**0.45**	**0.30**	**0.22**	**0.19**	**0.19**	**0.15**

	BFO WF2-053	BFO WF2-052	BFO WF2-051	BFO WF2-050	BFO WF2-049	BFO WF2-048	BFO WF2-047	BFO WF2-046	BFO WF2-045	BFO WF2-044
Stratigraphic Height	97.21	91.01	96.81	96.61	96.36	96.11	95.46	95.92	94.67	94.39
SO3 >/=								0.12	0.46	0.13
Unnormalized Major Elements (Weight %):										
SiO2	52.75	57.77	61.81	58.22	65.52	73.41	75.44	72.56	76.97	68.15
TiO2	0.830	0.808	0.799	0.655	0.582	0.434	0.367	0.505	0.415	0.742
Al2O3	20.68	18.52	17.09	17.29	14.29	11.95	11.09	12.20	9.04	14.42
FeO*	5.10	4.38	4.21	6.28	5.54	3.28	3.38	3.76	4.05	3.58
MnO	0.006	0.005	0.005	0.005	0.005	0.005	0.006	0.007	0.009	0.008
MgO	1.11	0.97	0.94	1.12	0.92	0.84	0.90	1.00	1.04	1.01
CaO	0.33	0.28	0.24	0.27	0.15	0.07	0.10	0.09	0.17	0.13
Na2O	1.31	1.19	1.13	1.14	0.97	1.24	1.30	1.31	1.24	1.19
K2O	1.00	1.11	1.25	1.95	2.47	2.35	2.11	2.19	1.56	2.18
P2O5	0.021	0.015	0.018	0.020	0.019	0.016	0.043	0.043	0.095	0.125
Sum	83.13	85.05	87.49	86.95	90.47	93.60	94.74	93.68	94.58	91.53
LOI %	16.28	14.37	12.08	12.35	8.92	5.68	4.31	5.51	3.81	7.84
Normalized Major Elements (Weight %):										
SiO2	63.45	67.92	70.65	66.96	72.43	78.43	79.62	77.46	81.38	74.45
TiO2	0.998	0.949	0.913	0.753	0.643	0.464	0.388	0.539	0.439	0.811
Al2O3	24.87	21.78	19.53	19.89	15.80	12.77	11.71	13.03	9.56	15.76
FeO*	6.13	5.15	4.81	7.23	6.13	3.50	3.57	4.02	4.28	3.91
MnO	0.007	0.006	0.006	0.006	0.006	0.005	0.006	0.008	0.009	0.008
MgO	1.33	1.14	1.07	1.29	1.01	0.90	0.95	1.07	1.10	1.11
CaO	0.40	0.33	0.28	0.31	0.16	0.08	0.11	0.10	0.18	0.14
Na2O	1.58	1.40	1.30	1.31	1.07	1.32	1.38	1.40	1.31	1.30
K2O	1.20	1.30	1.42	2.24	2.73	2.51	2.23	2.34	1.65	2.38
P2O5	0.025	0.017	0.021	0.023	0.021	0.017	0.045	0.046	0.100	0.137
Total	100.00	100.00	100.00	100.00	100.00	100.00	100.00	100.00	100.00	100.00
Unnormalized Trace Elements (ppm):										
Ni	13	12	13	14	14	9	11	16	11	15
Cr	41	42	43	48	46	37	29	39	29	58
Sc	18	16	15	13	10	7	6	9	6	12
V	130	115	108	121	109	84	69	88	64	128
Ba	386	474	490	293	828	524	961	490	7514	468
Rb	67	72	73	106	124	105	88	98	63	117
Sr	105	89	78	85	95	112	83	75	109	87
Zr	158	191	208	153	179	143	126	169	274	235
Y	26	23	23	24	22	32	22	40	30	27
Nb	17.8	17.9	17.8	13.4	12.0	9.7	8.7	10.8	9.2	16.4
Ga	26	24	21	21	17	15	12	14	12	18
Cu	35	33	57	60	43	25	16	28	22	32
Zn	62	56	57	72	55	51	65	68	82	63
Pb	26	21	19	20	16	15	15	21	16	27
La	48	30	31	32	28	31	47	46	33	35
Ce	106	67	71	69	63	67	84	65	56	70
Th	19	18	21	13	11	8	6	9	8	15
Nd	53	31	31	30	22	21	39	32	26	27
U	2	2	1	3	4	5	4	3	2	10
sum tr.	1339	1335	1376	1191	1698	1301	1691	1322	8366	1461
in %	0.13	0.13	0.14	0.12	0.17	0.13	0.17	0.13	0.84	0.15
sum m+tr	83.26	85.19	87.63	87.06	90.64	93.73	94.91	93.81	95.42	91.68
M+Toxides	83.29	85.22	87.66	87.09	90.67	93.76	94.94	93.84	95.53	91.71

w/LOI	99.57	99.59	99.74	99.44	99.59	99.43	99.25	99.35	99.34	99.55
if Fe3+	100.14	100.07	100.20	100.14	100.21	99.80	99.63	99.77	99.79	99.95
Major elements are normalized on a volatile-free basis, with total Fe expressed as FeO.										
® denotes a duplicate bead made from the same rock powder.										
NiO	16.1	15.3	17.1	17.2	17.8	11.2	13.5	20.5	14.3	19.6
Cr2O3	60.2	60.7	63.1	70.5	67.7	54.4	42.3	57.3	42.0	85.2
Sc2O3	27.0	24.5	22.5	19.4	15.4	10.6	8.7	13.4	8.5	17.8
V2O3	190.9	169.4	158.7	178.6	160.0	124.0	101.1	129.5	94.3	188.5
BaO	431.4	528.9	546.7	327.3	924.7	585.2	1072.8	547.5	8389.1	522.1
Rb2O	73.2	78.6	79.9	115.6	135.1	115.2	96.2	107.5	68.5	128.3
SrO	124.2	105.8	92.4	100.8	112.0	132.3	98.7	88.6	129.0	103.4
ZrO2	213.9	258.5	281.1	206.8	241.9	192.6	170.3	228.4	370.8	317.4
Y2O3	33.1	28.7	29.1	31.1	28.3	40.5	27.4	50.9	37.7	34.5
Nb2O5	25.4	25.6	25.5	19.2	17.1	13.9	12.4	15.5	13.1	23.5
Ga2O3	35.3	32.7	28.1	28.4	22.3	20.4	15.9	19.3	15.8	23.8
CuO	43.5	41.3	71.0	74.9	53.8	30.8	19.9	35.4	27.5	39.8
ZnO	77.7	69.9	70.7	90.0	68.6	63.0	80.4	84.3	102.6	77.9
PbO	28.0	22.3	20.4	21.3	17.8	16.6	16.5	22.5	17.3	29.5
La2O3	56.7	35.7	35.9	37.8	33.0	35.9	55.0	54.5	38.5	41.4
CeO2	130.3	82.5	87.5	84.3	77.0	82.0	103.0	79.9	69.2	86.0
ThO2	20.7	20.4	22.6	13.8	12.3	9.2	7.1	10.1	9.1	16.8
Nd2O3	61.4	36.0	35.6	35.3	25.8	25.0	45.5	37.4	30.8	31.7
U2O3	2.7	2.2	1.4	3.3	4.5	5.7	4.9	3.1	2.4	10.6
sum tr.	**1652**	**1639**	**1689**	**1476**	**2035**	**1568**	**1992**	**1606**	**9480**	**1798**
in %	**0.17**	**0.16**	**0.17**	**0.15**	**0.20**	**0.16**	**0.20**	**0.16**	**0.95**	**0.18**

	BFO WF2-043	**BFO WF2-042**	**BFO WF2-041**	**BFO WF2-040**	**BFO WF2-039**	**BFO WF2-038**	**BFO WF2-037**	**BFO WF2-036**	**BFO WF2-035**	**BFO WF2-034**
Stratigraphic Height	94.31	94.24	94.07	94.02	93.95	93.89	93.865	93.86	93.76	93.66
SO3 >/=										
Unnormalized Major Elements (Weight %):										
SiO2	58.97	57.31	55.30	55.69	57.71	45.00	47.83	45.26	46.81	50.65
TiO2	0.719	0.674	0.670	0.676	0.549	0.799	0.741	0.713	0.740	0.853
Al2O3	17.04	15.81	16.31	16.22	15.95	23.40	23.41	23.05	22.26	21.46
FeO*	5.58	7.61	7.68	7.44	7.94	7.92	4.43	7.44	6.87	5.22
MnO	0.009	0.020	0.016	0.017	0.012	0.006	0.004	0.007	0.005	0.005
MgO	1.43	1.95	2.00	2.14	1.46	1.28	1.25	1.32	1.24	1.14
CaO	0.08	0.88	1.16	1.23	0.56	0.28	0.44	0.28	0.29	0.22
Na2O	1.19	0.87	0.87	0.90	0.92	1.55	1.37	1.58	1.51	1.54
K2O	2.25	2.22	2.14	2.18	2.25	0.90	0.78	0.99	1.25	0.80
P2O5	0.098	0.169	0.184	0.151	0.303	0.026	0.019	0.021	0.023	0.025
Sum	87.36	87.52	86.32	86.64	87.66	81.15	80.28	80.66	81.00	81.91
LOI %	12.03	12.06	13.01	12.89	11.83	18.25	18.84	18.95	18.35	17.53
Normalized Major Elements (Weight %):										
SiO2	67.50	65.48	64.06	64.28	65.83	55.45	59.58	56.11	57.79	61.84
TiO2	0.823	0.770	0.777	0.780	0.626	0.985	0.923	0.884	0.914	1.042
Al2O3	19.51	18.06	18.89	18.72	18.19	28.83	29.16	28.58	27.49	26.20
FeO*	6.39	8.70	8.89	8.59	9.06	9.76	5.52	9.22	8.48	6.37
MnO	0.010	0.023	0.019	0.020	0.014	0.008	0.005	0.009	0.007	0.006
MgO	1.63	2.23	2.32	2.47	1.67	1.58	1.56	1.63	1.53	1.40
CaO	0.09	1.00	1.34	1.42	0.64	0.34	0.54	0.35	0.36	0.27
Na2O	1.36	1.00	1.01	1.04	1.05	1.90	1.71	1.96	1.87	1.88
K2O	2.58	2.54	2.48	2.51	2.57	1.10	0.97	1.23	1.55	0.97

P2O5	0.113	0.193	0.213	0.175	0.346	0.032	0.024	0.026	0.028	0.030
Total	100.00	100.00	100.00	100.00	100.00	100.00	100.00	100.00	100.00	100.00
Unnormalized Trace Elements (ppm):										
Ni	27	48	29	29	27	15	21	15	15	15
Cr	71	67	66	63	64	42	45	41	47	44
Sc	15	15	15	14	14	17	18	18	18	19
V	158	188	167	161	218	154	330	155	153	158
Ba	369	363	313	312	379	93	95	81	119	197
Rb	127	123	124	125	122	61	62	69	92	54
Sr	91	69	80	78	86	94	95	88	86	70
Zr	134	119	116	118	103	116	119	111	116	154
Y	31	46	44	35	67	23	21	22	23	32
Nb	14.6	13.1	13.1	13.4	10.6	15.2	14.1	13.0	14.4	17.1
Ga	22	21	21	21	22	28	31	28	28	28
Cu	50	60	49	50	44	52	111	34	56	32
Zn	74	78	73	74	62	62	63	62	62	54
Pb	30	25	22	21	27	25	136	22	23	22
La	39	39	44	40	55	44	28	31	36	56
Ce	76	69	88	76	111	75	43	50	59	113
Th	17	15	14	15	15	11	10	11	11	22
Nd	33	33	41	33	60	30	14	20	21	53
U	5	2	2	3	3	3	3	2	3	3
sum tr.	1385	1393	1320	1281	1489	961	1259	874	983	1143
in %	0.14	0.14	0.13	0.13	0.15	0.10	0.13	0.09	0.10	0.11
sum m+tr	87.50	87.66	86.45	86.77	87.81	81.25	80.40	80.74	81.10	82.02
M+Toxides	87.53	87.70	86.48	86.80	87.85	81.27	80.44	80.77	81.13	82.05
w/LOI	99.56	99.75	99.50	99.69	99.67	99.52	99.28	99.72	99.48	99.59
if Fe3+	100.18	100.60	100.35	100.51	100.56	100.40	99.77	100.54	100.24	100.17
Major elements are normalized on a volatile-free basis, with total Fe expressed as FeO.										
® denotes a duplicate bead made from the same rock powder.										
NiO	34.8	61.4	36.6	36.4	34.3	19.5	26.3	19.6	19.7	19.2
Cr2O3	103.5	97.7	95.7	92.5	93.4	61.1	65.5	59.3	68.6	64.7
Sc2O3	23.7	23.0	22.5	22.1	21.7	26.7	27.9	27.3	27.0	28.4
V2O3	233.0	276.1	245.1	237.0	320.4	226.2	485.6	228.5	225.5	232.1
BaO	412.1	405.5	349.8	348.6	423.1	104.3	106.2	90.4	133.3	220.4
Rb2O	139.0	134.9	135.4	136.8	133.4	66.3	67.4	75.4	100.7	59.6
SrO	107.8	82.0	95.0	92.2	101.3	110.9	112.0	104.5	102.0	82.4
ZrO2	181.2	160.6	157.3	159.0	139.7	157.2	160.7	150.4	156.4	207.4
Y2O3	39.1	57.9	55.5	43.8	84.5	29.7	26.3	28.1	28.8	40.5
Nb2O5	20.8	18.8	18.7	19.2	15.2	21.8	20.2	18.6	20.5	24.5
Ga2O3	29.5	28.2	28.5	28.1	30.0	37.9	42.1	38.1	37.5	37.4
CuO	63.0	75.5	61.6	63.0	55.6	65.2	139.3	42.7	69.9	39.6
ZnO	92.1	97.2	90.5	91.5	77.5	77.4	78.9	77.3	77.1	67.2
PbO	32.6	27.1	23.2	22.6	28.6	26.6	146.5	23.6	25.3	23.9
La2O3	46.2	45.5	51.5	46.9	64.2	51.9	33.3	36.8	41.8	65.4
CeO2	93.0	84.6	108.3	93.1	136.7	92.4	52.4	61.4	72.3	138.7
ThO2	18.4	16.5	15.9	16.2	16.0	11.7	10.5	11.6	12.0	24.5
Nd2O3	38.5	38.0	47.6	38.8	69.5	34.8	16.2	23.1	25.1	62.2
U2O3	5.0	2.4	2.3	3.4	3.7	2.8	3.6	2.6	3.5	3.5
sum tr.	**1713**	**1733**	**1641**	**1591**	**1849**	**1224**	**1621**	**1119**	**1247**	**1442**
in %	**0.17**	**0.17**	**0.16**	**0.16**	**0.18**	**0.12**	**0.16**	**0.11**	**0.12**	**0.14**

	BFO WF2-033	**BFO WF2-032**	**BFO WF2-031**	**BFO WF2-030**	**BFO WF2-029**	**BFO WF2-028**	**BFO WF2-027**	**BFO WF2-026**	**BFO WF2-025**	**BFO WF2-024**

Stratigraphic Height	93.56	93.46	93.36	93.26	93.16	93.06	92.96	92.86	92.76	92.66
SO3 >/=										
Unnormalized Major Elements (Weight %):										
SiO2	51.77	51.66	50.37	50.27	48.40	48.43	49.14	47.96	47.30	47.35
TiO2	0.867	0.857	0.848	0.835	0.764	0.768	0.778	0.751	0.729	0.732
Al2O3	20.90	20.79	21.52	21.63	22.27	22.68	23.28	22.95	23.22	23.72
FeO*	4.62	5.03	5.03	4.65	5.69	5.33	4.69	5.16	5.36	5.05
MnO	0.005	0.005	0.005	0.004	0.005	0.004	0.004	0.005	0.004	0.004
MgO	1.11	1.13	1.18	1.13	1.18	1.19	1.18	1.18	1.16	1.17
CaO	0.21	0.19	0.19	0.18	0.13	0.17	0.11	0.12	0.15	0.12
Na2O	1.52	1.61	1.66	1.70	1.79	1.68	1.74	1.71	1.73	1.72
K2O	0.73	0.77	0.73	0.67	0.76	0.74	0.66	0.68	0.63	0.59
P2O5	0.028	0.026	0.025	0.022	0.028	0.023	0.022	0.024	0.024	0.023
Sum	81.75	82.08	81.56	81.10	81.00	81.01	81.61	80.55	80.30	80.48
LOI %	17.51	17.35	17.96	18.41	18.44	18.57	17.70	18.78	18.91	19.01
Normalized Major Elements (Weight %):										
SiO2	63.33	62.94	61.76	61.99	59.74	59.78	60.22	59.55	58.91	58.83
TiO2	1.060	1.044	1.040	1.030	0.944	0.948	0.954	0.933	0.908	0.909
Al2O3	25.56	25.33	26.39	26.67	27.50	28.00	28.53	28.50	28.91	29.47
FeO*	5.65	6.13	6.16	5.73	7.02	6.58	5.74	6.41	6.68	6.28
MnO	0.006	0.006	0.006	0.005	0.006	0.005	0.005	0.006	0.006	0.005
MgO	1.36	1.38	1.44	1.39	1.46	1.47	1.45	1.46	1.44	1.45
CaO	0.25	0.23	0.24	0.23	0.16	0.20	0.13	0.15	0.18	0.15
Na2O	1.85	1.96	2.04	2.10	2.21	2.07	2.13	2.12	2.16	2.14
K2O	0.89	0.94	0.89	0.83	0.93	0.91	0.81	0.85	0.78	0.74
P2O5	0.034	0.031	0.031	0.028	0.034	0.028	0.027	0.030	0.029	0.028
Total	100.00	100.00	100.00	100.00	100.00	100.00	100.00	100.00	100.00	100.00
Unnormalized Trace Elements (ppm):										
Ni	14	13	13	14	15	14	14	13	14	16
Cr	44	43	45	46	50	51	56	52	53	55
Sc	19	19	19	19	17	18	18	18	17	18
V	156	143	144	151	162	154	188	166	175	163
Ba	339	777	521	419	127	91	332	308	489	480
Rb	50	53	51	49	54	56	52	52	47	44
Sr	71	74	69	67	54	55	56	55	59	63
Zr	163	159	150	148	128	121	128	120	114	112
Y	34	35	38	39	38	33	32	32	32	33
Nb	17.5	17.2	16.3	16.9	15.0	14.8	15.2	14.9	14.3	13.8
Ga	27	28	29	29	30	29	30	29	30	31
Cu	25	44	72	52	45	46	54	49	44	42
Zn	51	53	50	48	50	49	46	45	46	45
Pb	21	18	18	19	26	27	96	42	35	31
La	73	66	54	45	41	31	39	36	38	36
Ce	149	136	124	100	88	66	80	74	71	68
Th	27	26	21	23	16	16	17	15	13	12
Nd	70	60	55	45	40	34	37	36	35	32
U	3	3	2	3	2	3	2	2	2	2
sum tr.	1354	1766	1491	1332	1000	911	1292	1159	1328	1298
in %	0.14	0.18	0.15	0.13	0.10	0.09	0.13	0.12	0.13	0.13
sum m+tr	81.89	82.25	81.71	81.23	81.10	81.11	81.74	80.66	80.43	80.61
M+Toxides	81.92	82.29	81.75	81.27	81.13	81.13	81.77	80.69	80.46	80.64
w/LOI	99.43	99.65	99.71	99.68	99.58	99.70	99.47	99.47	99.37	99.64
if Fe3+	99.94	100.20	100.27	100.20	100.21	100.29	99.99	100.04	99.97	100.21

Major elements are normalized on a volatile-free basis, with total Fe expressed as FeO.
® denotes a duplicate bead made from the same rock powder.

NiO	17.5	16.8	16.5	18.1	19.1	17.3	18.4	16.8	18.1	20.4
Cr2O3	64.4	63.4	65.3	67.7	73.3	75.0	81.9	75.6	76.9	80.2
Sc2O3	28.9	29.6	29.5	28.8	26.6	27.0	28.0	27.0	26.7	28.2
V2O3	229.5	209.9	211.3	222.0	238.4	226.8	276.2	244.1	257.4	239.5
BaO	378.2	867.1	581.9	467.4	142.0	101.8	370.9	344.1	545.9	535.4
Rb2O	55.0	58.3	55.8	53.1	59.2	61.0	56.8	57.1	51.5	48.6
SrO	84.1	87.3	81.4	79.0	64.2	65.2	66.1	64.7	70.2	75.0
ZrO2	220.5	215.1	202.4	200.5	172.7	163.9	172.5	162.1	153.4	150.9
Y2O3	43.4	44.1	47.8	49.9	48.6	42.2	41.0	40.9	41.1	41.3
Nb2O5	25.1	24.6	23.3	24.2	21.5	21.1	21.7	21.4	20.5	19.8
Ga2O3	36.6	38.2	38.8	38.4	39.9	39.1	40.6	38.4	40.9	41.7
CuO	31.5	54.8	90.1	64.8	56.5	58.1	68.0	61.1	55.3	52.7
ZnO	63.0	65.8	62.4	59.9	61.7	61.4	56.7	56.4	56.6	55.9
PbO	22.2	19.8	19.5	20.7	28.0	29.5	103.4	44.9	37.5	33.8
La2O3	85.5	76.9	63.6	52.2	48.5	36.2	45.7	42.0	44.6	42.3
CeO2	183.3	166.7	152.9	122.8	108.4	81.2	97.8	91.4	86.9	84.2
ThO2	29.9	28.4	23.6	25.4	18.1	17.9	18.5	16.7	14.6	12.8
Nd2O3	82.0	70.0	64.2	52.8	46.9	40.0	43.5	42.4	40.4	37.5
U2O3	3.2	2.9	2.3	2.9	2.5	3.8	1.7	1.8	2.0	2.7
sum tr.	**1684**	**2140**	**1833**	**1651**	**1276**	**1168**	**1609**	**1449**	**1640**	**1603**
in %	**0.17**	**0.21**	**0.18**	**0.17**	**0.13**	**0.12**	**0.16**	**0.14**	**0.16**	**0.16**

	BFO WF2-023	**BFO WF2-022**	**BFO WF2-021**	**BFO WF2-020**	**BFO WF-296**	**BFO WF-295**	**BFO WF-294**	**BFO WF-293**	**BFO WF-292**	**BFO WF-291**
Stratigraphic Height	92.56	92.46	92.36	92.26	80.86	80.76	80.66	80.59	80.51	80.41
SO3 >/=										
Unnormalized Major Elements (Weight %):										
SiO2	46.61	46.83	46.03	46.04	65.67	61.71	66.05	68.16	69.50	70.65
TiO2	0.701	0.713	0.703	0.710	0.675	0.675	0.694	0.662	0.637	0.617
Al2O3	23.92	24.03	23.69	24.02	14.82	16.47	14.45	13.73	13.45	12.87
FeO*	4.91	4.76	4.58	4.66	4.07	4.84	4.79	4.84	4.62	4.68
MnO	0.004	0.004	0.003	0.004	0.006	0.007	0.005	0.005	0.007	0.010
MgO	1.19	1.22	1.24	1.27	1.08	1.20	1.06	0.94	0.99	1.01
CaO	0.09	0.10	0.10	0.08	0.28	0.33	0.28	0.24	0.19	0.17
Na2O	1.79	1.79	1.84	1.86	0.90	1.20	0.93	0.80	0.80	0.84
K2O	0.57	0.55	0.53	0.51	1.92	1.97	1.91	2.00	2.12	2.17
P2O5	0.028	0.029	0.035	0.031	0.011	0.009	0.012	0.010	0.010	0.010
Sum	79.82	80.03	78.75	79.18	89.44	88.41	90.17	91.40	92.33	93.03
LOI %	19.25	19.46	20.55	20.35	9.98	10.74	9.13	7.85	6.77	6.35
Normalized Major Elements (Weight %):										
SiO2	58.39	58.51	58.45	58.14	73.43	69.80	73.25	74.58	75.28	75.95
TiO2	0.878	0.890	0.892	0.896	0.755	0.764	0.770	0.724	0.690	0.664
Al2O3	29.97	30.02	30.09	30.33	16.57	18.63	16.03	15.03	14.57	13.84
FeO*	6.15	5.95	5.81	5.89	4.55	5.48	5.31	5.29	5.00	5.03
MnO	0.005	0.005	0.004	0.005	0.007	0.008	0.006	0.005	0.007	0.010
MgO	1.50	1.53	1.58	1.60	1.20	1.36	1.17	1.03	1.08	1.09
CaO	0.12	0.13	0.12	0.10	0.32	0.38	0.31	0.26	0.20	0.18
Na2O	2.24	2.24	2.33	2.35	1.00	1.35	1.03	0.87	0.87	0.90
K2O	0.72	0.69	0.67	0.65	2.15	2.23	2.11	2.19	2.30	2.33
P2O5	0.035	0.036	0.044	0.039	0.012	0.010	0.013	0.011	0.011	0.011
Total	100.00	100.00	100.00	100.00	100.00	100.00	100.00	100.00	100.00	100.00

Unnormalized Trace Elements (ppm):										
Ni	16	15	14	15	13	15	11	12	19	23
Cr	54	54	52	52	59	65	59	55	52	49
Sc	18	17	17	19	12	14	12	11	10	10
V	161	163	163	174	140	134	137	133	117	119
Ba	149	105	111	121	277	302	312	372	410	420
Rb	41	41	40	40	129	126	113	107	102	103
Sr	57	60	73	65	120	137	130	118	101	104
Zr	108	111	108	110	211	177	218	225	231	245
Y	34	40	45	43	22	17	18	18	17	17
Nb	13.8	14.1	13.6	13.7	14.3	13.5	14.5	13.6	14.2	14.2
Ga	31	31	32	31	19	23	18	18	15	15
Cu	45	44	42	51	18	16	13	15	18	20
Zn	44	43	40	40	74	87	67	53	50	53
Pb	35	36	34	35	19	22	25	23	22	20
La	42	47	48	53	24	17	20	24	22	25
Ce	69	83	96	104	53	27	38	45	44	51
Th	10	11	12	12	14	12	13	12	14	14
Nd	31	38	46	51	24	10	15	17	16	18
U	2	2	3	2	3	2	3	3	3	3
sum tr.	960	956	989	1032	1247	1216	1237	1276	1277	1322
in %	0.10	0.10	0.10	0.10	0.12	0.12	0.12	0.13	0.13	0.13
sum m+tr	79.92	80.13	78.85	79.28	89.56	88.53	90.30	91.52	92.45	93.16
M+Toxides	79.95	80.15	78.88	79.31	89.59	88.56	90.33	91.56	92.48	93.19
w/LOI	99.20	99.61	99.43	99.65	99.57	99.30	99.46	99.40	99.25	99.54
if Fe3+	99.74	100.14	99.94	100.17	100.02	99.84	99.99	99.94	99.77	100.06
Major elements are normalized on a volatile-free basis, with total Fe expressed as FeO.										
® denotes a duplicate bead made from the same rock powder.										
NiO	20.1	19.4	17.4	18.6	17.0	18.8	14.1	14.9	24.4	28.9
Cr2O3	79.4	78.8	76.1	75.4	86.2	94.5	86.2	80.1	76.3	71.2
Sc2O3	26.8	25.4	26.2	28.8	19.0	20.9	18.9	17.6	15.3	14.9
V2O3	236.1	239.8	239.8	255.9	205.8	197.6	202.2	195.4	171.8	175.2
BaO	166.4	116.8	123.8	135.1	309.8	337.5	348.1	415.8	458.0	468.7
Rb2O	45.3	45.2	43.4	43.9	141.6	138.0	123.4	117.2	111.3	112.4
SrO	66.8	71.1	86.4	76.9	142.3	161.5	154.3	139.4	119.3	123.1
ZrO2	146.5	149.8	145.8	148.5	284.9	239.6	293.9	304.2	311.9	331.3
Y2O3	42.5	51.3	57.7	54.4	27.6	21.5	22.7	22.4	21.5	21.8
Nb2O5	19.7	20.2	19.4	19.6	20.4	19.4	20.8	19.5	20.3	20.3
Ga2O3	41.5	42.0	42.4	42.0	26.1	30.3	24.8	23.8	20.6	19.9
CuO	56.3	54.6	52.7	64.4	22.8	20.0	16.2	19.3	22.0	25.4
ZnO	55.0	53.3	50.0	49.5	92.7	108.5	82.9	66.3	62.7	66.2
PbO	37.5	39.1	36.6	37.6	20.6	23.3	27.1	24.8	23.6	21.1
La2O3	49.3	54.7	55.7	62.1	27.7	20.4	23.7	28.5	25.9	29.2
CeO2	84.9	102.1	118.5	127.8	64.6	32.9	47.2	55.3	53.8	63.1
ThO2	11.5	12.3	12.8	13.3	15.4	13.0	14.3	13.4	14.9	14.9
Nd2O3	35.9	44.8	53.3	59.8	27.9	12.1	17.7	20.3	19.1	21.0
U2O3	2.5	2.4	3.4	2.7	3.4	2.2	3.0	3.8	3.0	3.6
sum tr.	**1224**	**1223**	**1262**	**1316**	**1556**	**1512**	**1541**	**1582**	**1576**	**1632**
in %	**0.12**	**0.12**	**0.13**	**0.13**	**0.16**	**0.15**	**0.15**	**0.16**	**0.16**	**0.16**

	BFO WF-290	**BFO WF-289**	**BFO WF-288**	**BFO WF-287**	**BFO WF-286**	**BFO WF-285**	**BFO WF-253**	**BFO WF-252**	**BFO WF-251**	**BFO WF-250**
Stratigraphic Height	80.31	80.22	80.12	80.02	79.92	79.16	70.54	70.29	70.04	69.79

SO3 >/=						0.16				
Unnormalized Major Elements (Weight %):										
SiO2	72.62	69.65	68.22	54.26	61.03	58.30	49.71	50.07	49.52	46.66
TiO2	0.594	0.648	0.605	0.505	0.557	0.353	0.855	0.864	0.868	0.768
Al2O3	12.10	12.71	11.86	9.70	10.71	6.70	22.73	22.78	22.40	23.36
FeO*	4.14	4.97	5.07	3.21	3.94	2.03	6.26	6.23	6.41	7.28
MnO	0.010	0.013	0.021	0.114	0.041	0.154	0.006	0.006	0.009	0.006
MgO	1.04	1.30	1.90	2.26	2.58	1.51	1.07	1.11	1.12	1.13
CaO	0.16	0.24	1.40	11.68	6.34	13.81	0.34	0.41	0.66	0.33
Na2O	0.94	1.25	0.96	0.76	0.89	0.75	1.56	1.54	1.46	1.60
K2O	2.18	2.28	2.16	1.71	1.90	1.41	0.51	0.59	0.62	0.59
P2O5	0.037	0.082	0.127	0.106	0.109	0.065	0.021	0.023	0.038	0.020
Sum	93.82	93.15	92.33	84.31	88.10	85.08	83.07	83.62	83.11	81.75
LOI %	5.54	6.07	7.06	14.66	11.06	13.83	16.36	15.93	16.26	17.69
Normalized Major Elements (Weight %):										
SiO2	77.40	74.77	73.89	64.36	69.27	68.52	59.84	59.88	59.58	57.08
TiO2	0.633	0.696	0.655	0.599	0.632	0.415	1.029	1.033	1.044	0.940
Al2O3	12.90	13.65	12.84	11.51	12.15	7.87	27.37	27.24	26.95	28.58
FeO*	4.42	5.34	5.49	3.80	4.47	2.39	7.53	7.45	7.72	8.91
MnO	0.010	0.014	0.023	0.136	0.046	0.181	0.007	0.007	0.010	0.008
MgO	1.11	1.39	2.06	2.68	2.93	1.78	1.29	1.33	1.35	1.39
CaO	0.17	0.26	1.52	13.85	7.20	16.23	0.41	0.49	0.80	0.40
Na2O	1.00	1.35	1.04	0.91	1.01	0.88	1.88	1.84	1.75	1.96
K2O	2.32	2.45	2.34	2.03	2.16	1.66	0.61	0.71	0.75	0.72
P2O5	0.040	0.088	0.137	0.126	0.123	0.077	0.026	0.027	0.045	0.024
Total	100.00	100.00	100.00	100.00	100.00	100.00	100.00	100.00	100.00	100.00
Unnormalized Trace Elements (ppm):										
Ni	30	39	38	29	32	10	14	14	13	15
Cr	45	51	48	39	43	27	50	45	43	45
Sc	9	10	9	9	9	4	19	18	19	18
V	103	109	104	68	87	62	176	149	131	144
Ba	441	448	454	605	450	3084	412	569	289	273
Rb	99	108	100	80	88	52	29	32	36	32
Sr	99	100	88	110	239	147	176	180	176	173
Zr	274	258	264	208	240	305	139	134	131	121
Y	23	28	30	44	27	23	17	21	23	19
Nb	12.9	14.2	13.3	11.3	11.5	8.6	15.2	17.4	16.7	14.3
Ga	13	17	15	13	13	6	30	29	28	30
Cu	24	24	26	20	25	21	18	15	15	16
Zn	52	72	68	53	61	23	63	59	54	57
Pb	17	18	17	18	16	15	28	32	31	31
La	59	78	57	61	34	24	25	28	32	33
Ce	122	164	124	123	71	39	41	53	60	61
Th	11	13	13	9	9	7	17	16	15	14
Nd	53	78	56	52	30	20	16	19	22	25
U	2	4	2	2	4	2	2	2	4	3
sum tr.	1490	1633	1526	1553	1490	3879	1287	1433	1137	1123
in %	0.15	0.16	0.15	0.16	0.15	0.39	0.13	0.14	0.11	0.11
sum m+tr	93.97	93.31	92.49	84.47	88.25	85.47	83.20	83.77	83.22	81.86
M+Toxides	94.01	93.35	92.52	84.50	88.29	85.53	83.23	83.80	83.25	81.89
w/LOI	99.55	99.42	99.58	99.16	99.35	99.36	99.60	99.73	99.51	99.58
if Fe3+	100.01	99.97	100.15	99.52	99.78	99.58	100.29	100.42	100.22	100.39

Major elements are normalized on a volatile-free basis, with total Fe expressed as FeO.

® denotes a duplicate bead made from the same rock powder.										
NiO	37.9	50.1	48.7	36.8	40.2	12.7	18.2	17.6	16.0	19.1
Cr2O3	65.8	74.4	69.5	56.6	63.5	40.2	72.6	66.4	62.3	65.5
Sc2O3	13.4	14.7	13.3	13.9	13.7	6.0	29.1	27.9	28.4	27.6
V2O3	151.7	160.8	152.6	99.8	127.3	91.7	259.3	219.8	192.9	212.1
BaO	492.7	500.1	506.8	675.6	502.0	3443.5	460.5	635.6	322.4	305.0
Rb2O	108.7	118.1	109.1	87.5	96.2	56.6	31.8	35.0	39.0	34.6
SrO	116.8	118.6	103.8	129.9	282.5	173.4	207.6	213.4	208.5	204.9
ZrO2	369.8	348.0	356.4	280.9	324.8	411.5	188.2	180.6	177.1	163.2
Y2O3	28.8	36.1	38.4	56.0	33.7	29.1	21.8	26.4	29.3	24.3
Nb2O5	18.4	20.3	19.0	16.1	16.4	12.3	21.7	24.9	23.9	20.5
Ga2O3	18.1	22.2	20.3	17.2	17.8	8.1	39.7	39.4	38.0	40.1
CuO	29.8	30.3	32.5	25.4	31.8	26.6	22.1	19.1	18.5	19.7
ZnO	64.7	90.1	84.1	65.9	75.4	28.7	78.4	73.7	67.2	71.3
PbO	18.2	19.8	18.5	19.2	17.3	16.2	29.9	34.3	32.9	33.1
La2O3	69.7	91.1	67.2	71.3	39.7	27.8	29.8	32.3	37.9	38.1
CeO2	150.3	201.6	152.8	150.7	87.2	47.4	50.4	64.8	73.6	75.4
ThO2	12.3	13.9	14.2	9.8	10.3	8.1	18.5	17.5	16.6	15.4
Nd2O3	61.8	91.1	65.4	60.4	35.5	23.1	18.4	21.8	26.1	28.9
U2O3	2.4	3.9	2.5	2.1	4.9	2.1	2.4	2.7	4.1	2.9
sum tr.	**1831**	**2005**	**1875**	**1875**	**1820**	**4465**	**1601**	**1753**	**1415**	**1402**
in %	**0.18**	**0.20**	**0.19**	**0.19**	**0.18**	**0.45**	**0.16**	**0.18**	**0.14**	**0.14**

	BFO WF-249	**BFO WF-248**	**BFO WF-247**	**BFO WF-246**	**BFO WF-245**	**BFO WF-244**	**BFO WF-237**	**BFO WF-236**	**BFO WF-235**	**BFO WF-234**
Stratigraphic Height	69.54	69.29	69.23	69.98	68.73	68.53	61.12	60.87	60.67	60.42
SO3 >/=										
Unnormalized Major Elements (Weight %):										
SiO2	57.10	57.61	59.53	64.44	71.19	75.52	52.36	48.41	50.21	50.78
TiO2	0.738	0.793	0.745	0.743	0.591	0.419	0.576	0.554	0.569	0.540
Al2O3	17.98	17.11	15.26	13.39	11.34	10.33	14.93	11.90	11.79	10.71
FeO*	6.01	6.68	7.81	7.17	5.66	2.47	5.17	4.82	3.69	3.03
MnO	0.004	0.005	0.005	0.005	0.005	0.021	0.041	0.080	0.050	0.061
MgO	1.06	1.06	0.99	1.02	0.83	0.79	3.46	3.94	3.86	4.22
CaO	0.30	0.32	0.29	0.29	0.15	1.44	5.70	11.05	10.66	11.31
Na2O	1.49	1.48	1.45	1.37	1.37	1.38	0.53	0.35	0.35	0.32
K2O	1.13	1.16	1.30	1.63	2.33	2.51	2.34	2.08	1.95	1.71
P2O5	0.013	0.015	0.014	0.018	0.020	0.068	0.157	0.206	0.186	0.128
Sum	85.83	86.22	87.38	90.08	93.49	94.94	85.26	83.38	83.32	82.81
LOI %	13.60	13.16	12.07	9.42	6.02	4.41	14.13	16.21	16.20	16.64
Normalized Major Elements (Weight %):										
SiO2	66.53	66.81	68.13	71.53	76.15	79.54	61.41	58.05	60.26	61.32
TiO2	0.860	0.920	0.852	0.825	0.632	0.441	0.675	0.664	0.683	0.653
Al2O3	20.95	19.84	17.46	14.87	12.13	10.88	17.51	14.28	14.15	12.94
FeO*	7.00	7.74	8.94	7.96	6.05	2.60	6.07	5.77	4.43	3.65
MnO	0.005	0.006	0.005	0.006	0.005	0.023	0.048	0.096	0.061	0.074
MgO	1.24	1.23	1.13	1.13	0.88	0.83	4.06	4.73	4.63	5.09
CaO	0.35	0.37	0.34	0.32	0.16	1.51	6.68	13.26	12.79	13.66
Na2O	1.74	1.71	1.66	1.52	1.47	1.45	0.62	0.41	0.42	0.39
K2O	1.32	1.34	1.49	1.81	2.49	2.65	2.74	2.49	2.35	2.07
P2O5	0.015	0.018	0.016	0.019	0.022	0.072	0.185	0.247	0.223	0.154
Total	100.00	100.00	100.00	100.00	100.00	100.00	100.00	100.00	100.00	100.00
Unnormalized Trace Elements (ppm):										

Ni	12	14	13	14	13	16	37	37	28	27
Cr	47	46	44	45	39	33	69	61	54	47
Sc	15	15	15	13	10	7	13	12	12	10
V	136	121	123	121	106	79	136	154	112	96
Ba	459	771	422	467	571	652	477	526	323	449
Rb	60	58	62	76	96	101	120	99	99	82
Sr	157	164	150	142	132	126	116	141	134	126
Zr	173	181	197	202	212	174	100	102	134	151
Y	15	16	16	18	52	28	19	26	25	23
Nb	13.5	14.2	13.0	13.0	11.7	9.1	11.8	10.7	11.7	11.3
Ga	23	22	20	19	14	11	20	16	15	12
Cu	35	25	21	19	22	29	18	26	33	58
Zn	62	64	61	54	40	35	119	126	105	89
Pb	23	26	23	21	16	12	18	15	18	14
La	22	23	19	15	49	90	30	33	33	32
Ce	37	41	31	29	103	184	57	66	57	57
Th	12	10	10	10	10	6	15	13	13	10
Nd	12	13	9	12	52	82	23	27	23	27
U	3	3	3	4	6	4	3	3	4	3
sum tr.	1315	1627	1249	1293	1554	1678	1402	1492	1231	1323
in %	0.13	0.16	0.12	0.13	0.16	0.17	0.14	0.15	0.12	0.13
sum m+tr	85.96	86.39	87.51	90.21	93.64	95.11	85.40	83.53	83.45	82.94
M+Toxides	85.99	86.42	87.54	90.24	93.68	95.14	85.43	83.56	83.48	82.97
w/LOI	99.59	99.58	99.61	99.65	99.70	99.55	99.56	99.77	99.67	99.61
if Fe3+	100.26	100.33	100.47	100.45	100.33	99.83	100.13	100.31	100.08	99.94
Major elements are normalized on a volatile-free basis, with total Fe expressed as FeO.										
® denotes a duplicate bead made from the same rock powder.										
NiO	15.3	17.4	16.5	17.3	16.4	20.7	46.6	47.0	35.5	33.8
Cr2O3	69.3	67.4	64.3	65.9	57.0	48.2	100.5	89.0	78.2	68.2
Sc2O3	23.2	23.3	22.5	19.2	15.2	11.1	20.7	17.8	17.7	14.6
V2O3	199.6	178.6	180.2	178.2	155.6	116.2	199.7	226.3	165.4	141.5
BaO	511.9	860.6	470.7	521.5	637.5	727.7	533.1	586.8	360.2	501.0
Rb2O	65.7	63.0	67.3	82.8	105.1	110.1	131.3	107.8	108.1	89.9
SrO	185.9	193.4	177.5	167.3	156.0	149.4	137.7	167.1	157.9	149.3
ZrO2	233.2	243.9	265.8	272.8	286.3	235.3	135.4	137.4	181.3	203.8
Y2O3	18.5	20.8	20.2	22.9	66.4	35.4	24.1	33.1	31.4	28.7
Nb2O5	19.3	20.3	18.6	18.6	16.7	13.1	16.8	15.3	16.8	16.1
Ga2O3	31.1	30.0	26.3	25.0	18.6	15.4	26.3	21.3	20.2	16.8
CuO	43.2	31.0	26.4	23.9	26.9	36.7	22.3	33.0	41.5	72.5
ZnO	77.3	80.0	75.4	67.2	49.5	43.2	148.5	156.9	130.1	111.0
PbO	25.2	27.6	24.5	22.5	17.1	12.7	19.2	16.6	19.9	14.8
La2O3	25.6	27.1	21.7	17.6	57.8	105.3	35.5	38.7	38.9	37.2
CeO2	45.4	50.3	38.4	36.1	126.6	225.6	69.8	80.7	69.5	70.0
ThO2	12.9	10.7	11.4	11.3	11.1	6.8	16.3	13.9	13.8	11.5
Nd2O3	14.1	15.3	10.6	14.2	61.0	95.5	26.8	31.6	26.7	31.3
U2O3	2.8	3.7	2.8	4.4	6.5	4.5	3.3	3.3	4.1	3.1
sum tr.	**1619**	**1964**	**1541**	**1589**	**1888**	**2013**	**1714**	**1824**	**1517**	**1615**
in %	**0.16**	**0.20**	**0.15**	**0.16**	**0.19**	**0.20**	**0.17**	**0.18**	**0.15**	**0.16**

	BFO WF-233	**BFO WF-232**	**BFO WF-231**	**BFO WF-219**	**BFO WF-218**	**BFO WF-217**	**BFO WF-216**	**BFO WF-215**	**BFO WF-214**	**BFO WF-213**
Stratigraphic Height	60.17	59.92	59.67	56.57	56.32	56.07	55.82	55.32	55.07	54.82
SO3 >/=										

Unnormalized Major Elements (Weight %):										
SiO2	50.48	50.91	46.18	53.85	58.27	57.11	49.15	44.29	48.51	57.53
TiO2	0.548	0.538	0.496	0.671	0.661	0.637	0.544	0.524	0.620	0.663
Al2O3	11.01	10.59	10.30	15.55	16.30	13.11	10.70	10.80	14.81	16.40
FeO*	3.53	3.15	2.84	5.70	6.31	4.51	3.48	4.15	6.88	5.87
MnO	0.047	0.056	0.049	0.074	0.036	0.048	0.226	0.410	0.127	0.037
MgO	4.24	4.32	5.12	3.05	2.25	2.84	2.87	2.72	2.81	2.38
CaO	10.80	11.22	13.24	4.98	2.01	6.15	13.35	15.44	7.91	2.59
Na2O	0.31	0.33	0.29	0.56	0.65	0.52	0.39	0.29	0.53	0.62
K2O	1.74	1.67	1.63	2.26	2.35	2.00	1.64	1.59	2.06	2.31
P2O5	0.136	0.142	0.139	0.159	0.132	0.151	0.141	0.150	0.176	0.168
Sum	82.84	82.92	80.27	86.86	88.96	87.08	82.48	80.36	84.43	88.57
LOI %	16.42	16.54	18.99	12.51	10.25	12.28	16.97	18.75	14.84	11.08
Normalized Major Elements (Weight %):										
SiO2	60.93	61.40	57.53	61.99	65.50	65.58	59.59	55.12	57.46	64.96
TiO2	0.662	0.648	0.618	0.772	0.743	0.732	0.660	0.652	0.734	0.749
Al2O3	13.29	12.77	12.83	17.91	18.33	15.06	12.97	13.44	17.54	18.52
FeO*	4.26	3.79	3.53	6.57	7.09	5.18	4.22	5.16	8.15	6.63
MnO	0.057	0.068	0.061	0.085	0.040	0.055	0.275	0.511	0.151	0.041
MgO	5.12	5.21	6.38	3.51	2.53	3.27	3.48	3.39	3.33	2.69
CaO	13.04	13.53	16.49	5.73	2.26	7.06	16.19	19.21	9.37	2.92
Na2O	0.37	0.39	0.36	0.65	0.73	0.60	0.47	0.36	0.62	0.70
K2O	2.10	2.01	2.03	2.60	2.64	2.29	1.98	1.97	2.44	2.61
P2O5	0.164	0.172	0.173	0.183	0.148	0.173	0.171	0.186	0.209	0.190
Total	100.00	100.00	100.00	100.00	100.00	100.00	100.00	100.00	100.00	100.00
Unnormalized Trace Elements (ppm):										
Ni	29	27	28	44	40	33	27	28	37	34
Cr	49	47	47	73	74	57	48	49	64	70
Sc	10	10	10	15	14	11	11	10	13	14
V	109	109	100	167	181	123	83	108	168	174
Ba	361	315	329	517	451	337	364	653	1489	878
Rb	83	79	78	124	127	102	83	86	113	131
Sr	119	117	125	105	81	94	115	125	133	121
Zr	143	148	116	118	116	152	132	111	109	128
Y	23	26	27	30	21	23	30	33	33	27
Nb	11.8	11.7	10.5	12.8	13.9	14.0	11.7	10.2	12.2	13.2
Ga	13	13	13	20	21	16	14	13	19	21
Cu	47	44	54	52	32	30	27	32	24	43
Zn	95	93	97	130	120	99	82	89	121	121
Pb	17	13	13	24	24	20	21	23	23	25
La	31	31	28	42	34	33	35	33	42	39
Ce	59	58	55	76	57	68	66	72	85	84
Th	11	10	10	15	15	13	11	12	14	15
Nd	25	25	23	33	25	31	30	34	38	36
U	3	5	13	5	6	4	4	5	4	4
sum tr.	1239	1179	1175	1604	1451	1261	1193	1525	2542	1980
in %	0.12	0.12	0.12	0.16	0.15	0.13	0.12	0.15	0.25	0.20
sum m+tr	82.96	83.04	80.38	87.02	89.10	87.21	82.60	80.51	84.68	88.77
M+Toxides	82.99	83.07	80.41	87.06	89.14	87.24	82.62	80.54	84.73	88.81
w/LOI	99.41	99.60	99.41	99.57	99.39	99.52	99.60	99.29	99.56	99.89
if Fe3+	99.80	99.95	99.72	100.20	100.09	100.02	99.98	99.75	100.33	100.54

Major elements are normalized on a volatile-free basis, with total Fe expressed as FeO.
® denotes a duplicate bead made from the same rock powder.

NiO	36.3	33.8	35.7	55.4	50.9	42.3	34.8	35.0	47.4	43.2
Cr2O3	70.9	68.0	68.6	106.9	107.7	84.0	70.7	71.0	92.8	102.4
Sc2O3	15.6	15.3	15.1	23.3	21.9	16.5	16.8	15.5	20.5	21.9
V2O3	160.7	160.4	146.7	245.7	265.8	181.3	122.7	158.7	247.3	256.2
BaO	403.3	351.5	367.7	577.4	503.7	375.8	406.1	729.3	1662.5	979.9
Rb2O	90.8	86.7	85.5	135.5	138.7	111.9	90.3	94.1	123.5	143.5
SrO	140.5	137.9	147.6	124.0	95.2	110.7	136.0	147.7	157.1	143.2
ZrO2	193.1	199.3	156.3	159.7	156.7	205.2	178.1	150.2	147.8	173.5
Y2O3	29.2	33.1	34.2	37.8	26.2	29.7	38.0	42.4	41.9	34.6
Nb2O5	16.8	16.7	15.0	18.3	19.8	20.0	16.7	14.6	17.4	18.8
Ga2O3	17.7	17.3	17.6	27.3	27.8	22.2	18.2	17.2	25.7	28.4
CuO	58.9	55.5	67.4	64.8	39.5	37.6	33.7	40.4	29.4	53.3
ZnO	118.0	115.8	120.8	161.8	149.7	123.6	102.2	110.2	151.0	150.6
PbO	18.8	14.5	14.0	25.4	25.8	21.7	22.2	25.2	24.8	26.6
La2O3	36.5	36.2	32.4	49.7	40.3	38.8	40.5	39.1	49.0	45.8
CeO2	73.0	71.3	67.2	93.9	70.3	83.6	80.8	88.6	104.5	103.2
ThO2	11.6	10.5	10.8	16.9	16.6	14.3	12.0	12.8	15.4	17.0
Nd2O3	29.4	28.6	27.2	38.9	29.2	35.9	34.6	39.5	44.7	42.6
U2O3	3.3	5.3	13.8	5.6	6.1	4.1	4.1	5.0	4.9	4.6
sum tr.	**1525**	**1458**	**1444**	**1968**	**1792**	**1559**	**1458**	**1837**	**3008**	**2389**
in %	**0.15**	**0.15**	**0.14**	**0.20**	**0.18**	**0.16**	**0.15**	**0.18**	**0.30**	**0.24**

	BFO WF-212	**BFO WF-211**	**BFO WF-210**	**BFO WF-209**	**BFO WF-208**	**BFO WF-207**	**BFO WF-169**	**BFO WF-168**	**BFO WF-167**	**BFO WF-166**
Stratigraphic Height	52.97	52.68	52.56	52.51	52.41	52.32	46.55	46.4	46.25	46.15
SO3 >/=	0.20		0.13	0.17	0.12					
Unnormalized Major Elements (Weight %):										
SiO2	60.23	60.80	61.20	59.67	60.92	67.05	60.06	58.37	57.39	57.63
TiO2	0.550	0.628	0.563	0.565	0.577	0.471	0.565	0.570	0.595	0.579
Al2O3	16.32	19.08	16.81	16.74	16.95	15.64	16.21	15.89	15.88	16.07
FeO*	6.11	3.33	5.92	6.92	6.16	3.32	7.61	9.59	11.13	10.93
MnO	0.025	0.008	0.013	0.016	0.013	0.006	0.007	0.009	0.012	0.013
MgO	2.05	1.26	1.50	1.62	1.63	1.25	1.08	1.05	1.02	1.09
CaO	1.12	0.12	0.08	0.56	0.12	0.04	0.24	0.23	0.19	0.18
Na2O	0.87	1.04	0.99	0.98	0.96	0.94	0.93	0.92	0.76	0.75
K2O	2.35	2.09	2.47	2.41	2.50	2.38	2.25	2.18	2.15	2.21
P2O5	0.230	0.055	0.073	0.326	0.091	0.036	0.043	0.071	0.089	0.102
Sum	89.86	88.41	89.63	89.80	89.92	91.13	89.00	88.89	89.21	89.55
LOI %	9.42	11.01	9.69	9.64	9.22	8.17	10.56	10.27	9.92	9.87
Normalized Major Elements (Weight %):										
SiO2	67.03	68.77	68.29	66.45	67.75	73.57	67.49	65.67	64.32	64.35
TiO2	0.612	0.710	0.628	0.629	0.641	0.517	0.635	0.641	0.667	0.647
Al2O3	18.16	21.59	18.75	18.64	18.85	17.16	18.21	17.87	17.80	17.94
FeO*	6.80	3.76	6.60	7.71	6.85	3.64	8.55	10.78	12.47	12.20
MnO	0.028	0.009	0.015	0.018	0.014	0.007	0.008	0.010	0.013	0.015
MgO	2.28	1.42	1.68	1.80	1.82	1.37	1.21	1.19	1.15	1.22
CaO	1.25	0.13	0.09	0.63	0.13	0.05	0.27	0.26	0.21	0.20
Na2O	0.96	1.18	1.11	1.09	1.07	1.03	1.05	1.04	0.85	0.83
K2O	2.62	2.36	2.76	2.68	2.78	2.61	2.53	2.46	2.41	2.47
P2O5	0.256	0.063	0.081	0.363	0.101	0.039	0.048	0.080	0.099	0.114
Total	100.00	100.00	100.00	100.00	100.00	100.00	100.00	100.00	100.00	100.00
Unnormalized Trace Elements (ppm):										
Ni	40	26	30	38	41	22	16	16	26	31
Cr	73	72	73	71	74	66	65	66	67	66

Sc	13	15	14	15	14	12	13	13	13	14
V	195	166	248	203	192	146	190	190	185	196
Ba	623	325	389	559	796	465	622	883	1163	554
Rb	121	122	136	132	137	124	130	125	123	124
Sr	97	83	101	116	100	108	177	153	144	136
Zr	101	125	105	106	111	105	110	108	109	106
Y	32	15	18	60	23	15	21	28	35	36
Nb	11.1	12.9	11.5	11.6	12.2	10.1	11.0	12.4	12.1	11.9
Ga	22	24	22	22	23	21	21	21	19	21
Cu	28	70	30	21	21	20	65	56	26	27
Zn	121	103	106	110	108	71	69	70	75	82
Pb	25	28	25	29	26	27	19	20	21	27
La	44	30	38	40	36	41	28	23	35	49
Ce	78	46	65	90	73	68	49	51	86	106
Th	15	17	15	16	16	14	14	14	16	15
Nd	36	18	23	56	31	24	17	23	35	51
U	5	6	3	6	4	4	3	5	4	4
sum tr.	1680	1301	1453	1701	1837	1365	1639	1876	2195	1658
in %	0.17	0.13	0.15	0.17	0.18	0.14	0.16	0.19	0.22	0.17
sum m+tr	90.03	88.54	89.77	89.97	90.11	91.27	89.16	89.08	89.43	89.72
M+Toxides	90.07	88.57	89.81	90.01	90.14	91.30	89.20	89.12	89.48	89.76
w/LOI	99.48	99.58	99.50	99.65	99.36	99.47	99.76	99.38	99.39	99.62
if Fe3+	100.16	99.95	100.16	100.42	100.04	99.84	100.60	100.45	100.63	100.84
Major elements are normalized on a volatile-free basis, with total Fe expressed as FeO.										
® denotes a duplicate bead made from the same rock powder.										
NiO	50.6	33.4	37.7	47.8	51.5	27.4	19.9	20.0	32.9	38.9
Cr2O3	106.9	105.2	107.1	104.3	108.6	97.0	95.1	96.7	97.2	97.0
Sc2O3	20.5	22.5	21.7	22.7	20.8	18.4	19.7	20.0	19.7	21.8
V2O3	286.5	243.5	365.0	298.7	282.5	215.4	280.2	279.7	272.5	288.3
BaO	695.7	362.4	434.7	623.8	888.4	519.6	695.0	986.4	1298.8	619.1
Rb2O	132.8	133.2	148.3	144.2	149.7	136.1	142.4	137.2	134.1	135.9
SrO	114.8	97.7	119.6	136.8	118.3	127.6	208.8	180.8	169.7	160.8
ZrO2	137.1	169.1	142.1	143.7	149.5	141.7	148.5	145.7	147.2	142.8
Y2O3	40.6	18.8	23.2	76.7	29.2	18.9	26.3	36.1	44.7	45.1
Nb2O5	15.8	18.4	16.4	16.5	17.4	14.4	15.7	17.7	17.3	17.0
Ga2O3	29.5	32.3	29.5	29.7	30.3	27.8	28.8	27.7	26.2	28.0
CuO	35.4	87.3	38.1	26.4	26.5	24.5	81.3	69.9	32.8	33.9
ZnO	150.4	128.4	131.5	137.4	134.7	88.8	85.4	86.7	93.9	102.5
PbO	27.1	29.8	26.6	31.7	28.3	28.8	20.1	21.5	22.8	29.6
La2O3	51.4	35.5	44.1	46.8	42.7	48.2	32.6	26.8	41.5	57.3
CeO2	96.5	56.5	79.7	110.3	89.6	84.1	60.1	62.1	106.0	130.5
ThO2	16.2	18.3	16.3	17.4	17.5	15.7	15.7	15.5	17.2	17.1
Nd2O3	41.5	21.0	27.1	65.2	36.2	28.0	19.3	26.3	40.9	59.1
U2O3	5.1	6.2	3.5	6.2	4.1	4.9	3.2	5.4	4.5	4.8
sum tr.	**2054**	**1619**	**1812**	**2086**	**2226**	**1667**	**1998**	**2262**	**2620**	**2030**
in %	**0.21**	**0.16**	**0.18**	**0.21**	**0.22**	**0.17**	**0.20**	**0.23**	**0.26**	**0.20**

	BFO WF-165	**BFO WF-164**	**BFO WF-163**	**BFO WF-162**	**BFO WF-161**	**BFO WF-160**	**BFO WF-159**	**BFO WF-158**	**BFO WF-157**	**BFO WF-156**
Stratigraphic Height	46.05	45.95	45.85	45.75	45.63	45.53	45.43	45.33	45.23	45.13
SO3 >/=										
Unnormalized Major Elements (Weight %):										
SiO2	56.80	62.99	61.23	52.36	60.62	60.88	59.31	63.81	60.00	54.76

TiO2	0.502	0.506	0.564	0.521	0.642	0.671	0.662	0.520	0.641	0.631
Al2O3	15.44	16.34	16.93	14.71	16.83	16.77	17.03	16.54	15.95	14.27
FeO*	13.17	6.58	7.36	19.82	6.70	7.23	7.42	5.92	6.78	6.50
MnO	0.017	0.008	0.010	0.026	0.013	0.015	0.023	0.013	0.027	0.057
MgO	1.08	1.13	1.23	1.10	1.37	1.39	1.69	1.30	2.11	2.56
CaO	0.16	0.15	0.27	0.33	0.26	0.32	0.78	0.30	1.51	5.48
Na2O	0.64	0.70	0.68	0.58	0.77	0.71	0.65	0.61	0.60	0.50
K2O	2.13	2.39	2.39	2.08	2.51	2.43	2.39	2.40	2.38	2.03
P2O5	0.143	0.044	0.149	0.190	0.090	0.141	0.169	0.116	0.192	0.167
Sum	90.09	90.84	90.81	91.71	89.81	90.55	90.14	91.54	90.18	86.94
LOI %	9.18	8.42	8.60	7.23	9.47	8.91	9.28	8.04	9.33	12.33
Normalized Major Elements (Weight %):										
SiO2	63.04	69.34	67.43	57.09	67.50	67.23	65.81	69.71	66.53	62.98
TiO2	0.557	0.557	0.621	0.568	0.715	0.741	0.734	0.568	0.710	0.726
Al2O3	17.14	17.99	18.64	16.04	18.74	18.51	18.89	18.06	17.68	16.41
FeO*	14.62	7.24	8.10	21.61	7.46	7.99	8.23	6.47	7.51	7.48
MnO	0.019	0.008	0.012	0.029	0.014	0.016	0.026	0.014	0.030	0.065
MgO	1.20	1.25	1.35	1.20	1.53	1.53	1.88	1.42	2.34	2.94
CaO	0.18	0.17	0.30	0.36	0.29	0.35	0.87	0.33	1.67	6.30
Na2O	0.71	0.77	0.75	0.63	0.85	0.79	0.73	0.67	0.66	0.57
K2O	2.37	2.63	2.64	2.27	2.79	2.68	2.65	2.62	2.64	2.33
P2O5	0.158	0.049	0.165	0.208	0.100	0.156	0.187	0.126	0.213	0.192
Total	100.00	100.00	100.00	100.00	100.00	100.00	100.00	100.00	100.00	100.00
Unnormalized Trace Elements (ppm):										
Ni	41	29	39	47	40	43	44	36	42	35
Cr	65	68	69	65	68	69	73	72	70	64
Sc	13	13	13	13	15	14	15	13	14	12
V	200	159	156	230	166	175	178	171	169	146
Ba	619	449	437	409	454	433	472	677	573	725
Rb	120	129	136	116	152	145	137	129	137	116
Sr	109	125	130	97	173	119	116	113	107	132
Zr	94	94	100	95	122	127	119	98	121	127
Y	51	31	55	60	28	38	46	43	32	37
Nb	10.4	10.5	11.6	11.7	12.9	13.8	13.8	10.4	13.9	13.3
Ga	20	20	20	18	22	22	22	21	21	18
Cu	63	14	29	42	45	30	22	18	22	24
Zn	104	74	92	103	118	114	113	92	117	104
Pb	23	24	22	41	22	24	23	21	22	24
La	96	54	112	82	103	61	51	47	33	37
Ce	249	111	269	207	130	105	86	84	61	73
Th	13	14	16	13	16	16	17	13	15	14
Nd	147	54	142	111	42	51	39	35	26	31
U	7	4	5	10	3	4	2	3	3	4
sum tr.	2043	1477	1853	1772	1734	1603	1588	1696	1600	1735
in %	0.20	0.15	0.19	0.18	0.17	0.16	0.16	0.17	0.16	0.17
sum m+tr	90.29	90.99	91.00	91.89	89.98	90.71	90.29	91.71	90.34	87.12
M+Toxides	90.34	91.02	91.04	91.93	90.02	90.75	90.33	91.74	90.38	87.15
w/LOI	99.52	99.44	99.64	99.16	99.49	99.66	99.61	99.78	99.71	99.48
if Fe3+	100.99	100.17	100.45	101.36	100.24	100.46	100.43	100.44	100.46	100.20
Major elements are normalized on a volatile-free basis, with total Fe expressed as FeO.										
® denotes a duplicate bead made from the same rock powder.										
NiO	52.3	37.1	50.0	60.4	50.5	55.0	56.3	45.7	52.9	45.0
Cr2O3	94.3	99.1	101.2	95.7	100.0	101.1	107.1	104.6	101.6	93.0
Sc2O3	20.6	19.3	20.3	19.8	23.3	21.5	22.4	20.3	22.0	18.7

V2O3	294.9	233.3	230.1	338.8	244.2	257.3	261.2	252.1	248.4	215.0
BaO	691.1	501.3	487.9	456.6	507.3	483.0	526.9	755.9	639.7	809.2
Rb2O	131.3	141.5	148.4	126.5	166.0	158.4	149.4	141.1	149.7	126.6
SrO	128.9	148.1	153.3	114.2	204.3	140.8	136.9	134.1	126.6	155.6
ZrO2	126.5	127.2	135.2	128.1	164.9	170.9	160.6	131.8	163.5	171.6
Y2O3	64.6	39.9	70.1	76.4	36.1	48.2	58.5	54.9	41.1	46.5
Nb2O5	14.9	15.0	16.5	16.8	18.4	19.8	19.7	14.8	19.8	19.0
Ga2O3	27.0	27.2	26.5	24.7	29.3	29.9	29.5	27.8	28.8	24.5
CuO	78.8	17.9	36.9	52.7	56.6	37.2	27.4	23.0	27.9	29.6
ZnO	128.9	91.8	114.8	128.6	147.1	142.3	141.2	115.1	145.5	129.7
PbO	24.8	26.3	23.7	44.2	23.8	26.2	24.9	22.1	23.9	25.3
La2O3	112.5	63.3	130.8	95.8	121.3	71.2	60.3	54.6	38.4	43.3
CeO2	306.0	136.4	330.1	255.0	159.5	129.0	105.9	102.8	75.0	89.8
ThO2	14.5	15.4	17.3	14.5	17.6	17.2	18.3	14.7	17.1	16.0
Nd2O3	171.1	62.7	165.3	129.7	49.5	59.3	45.2	40.6	30.2	36.5
U2O3	7.2	4.1	5.5	11.1	3.7	4.1	2.5	3.3	3.3	4.1
sum tr.	**2490**	**1807**	**2264**	**2190**	**2123**	**1972**	**1954**	**2059**	**1956**	**2099**
in %	**0.25**	**0.18**	**0.23**	**0.22**	**0.21**	**0.20**	**0.20**	**0.21**	**0.20**	**0.21**

	BFO WF-155	**BFO WF-154**	**BFO WF-153**	**BFO WF-152**	**BFO WF-151**	**BFO WF-150**	**BFO WF-149**	**BFO WF-148**	**BFO WF-147**	**BFO WF-146**
Stratigraphic Height	45.03	44.93	44.83	44.73	44.63	44.53	44.43	44.33	44.23	44.13
SO3 >/=										
Unnormalized Major Elements (Weight %):										
SiO2	53.73	54.15	51.96	53.12	54.44	53.19	55.48	52.53	53.43	53.61
TiO2	0.615	0.602	0.597	0.626	0.618	0.590	0.622	0.618	0.607	0.608
Al2O3	14.16	14.34	13.35	14.15	13.95	13.46	14.56	13.71	13.49	13.20
FeO*	6.30	6.33	6.55	6.63	5.83	6.43	5.96	6.45	6.41	5.85
MnO	0.081	0.082	0.094	0.078	0.068	0.087	0.053	0.079	0.073	0.060
MgO	2.63	2.61	2.56	2.61	2.60	2.60	2.50	2.63	2.68	2.84
CaO	6.47	5.97	7.99	6.32	6.19	7.00	5.22	7.06	6.59	6.91
Na2O	0.49	0.49	0.45	0.51	0.51	0.47	0.50	0.51	0.50	0.48
K2O	2.05	2.08	1.88	1.96	1.95	1.93	2.09	1.91	1.93	1.88
P2O5	0.167	0.169	0.163	0.154	0.146	0.167	0.145	0.176	0.165	0.133
Sum	86.68	86.82	85.58	86.16	86.30	85.92	87.14	85.68	85.88	85.57
LOI %	12.89	12.50	13.81	13.10	12.85	13.37	12.13	13.73	13.33	13.66
Normalized Major Elements (Weight %):										
SiO2	61.98	62.37	60.71	61.65	63.08	61.91	63.67	61.31	62.22	62.65
TiO2	0.710	0.693	0.698	0.726	0.716	0.687	0.714	0.722	0.707	0.710
Al2O3	16.33	16.52	15.60	16.43	16.16	15.67	16.71	16.00	15.71	15.42
FeO*	7.27	7.29	7.65	7.70	6.75	7.48	6.84	7.52	7.46	6.83
MnO	0.094	0.094	0.110	0.090	0.078	0.101	0.061	0.093	0.085	0.070
MgO	3.03	3.00	2.99	3.03	3.01	3.02	2.87	3.08	3.12	3.32
CaO	7.47	6.88	9.34	7.33	7.17	8.15	5.99	8.24	7.68	8.08
Na2O	0.56	0.56	0.52	0.60	0.60	0.55	0.57	0.60	0.58	0.57
K2O	2.36	2.40	2.20	2.28	2.26	2.25	2.40	2.23	2.25	2.20
P2O5	0.192	0.195	0.191	0.179	0.169	0.194	0.166	0.205	0.192	0.155
Total	100.00	100.00	100.00	100.00	100.00	100.00	100.00	100.00	100.00	100.00
Unnormalized Trace Elements (ppm):										
Ni	36	37	34	34	31	32	32	28	29	29
Cr	64	63	59	65	60	60	62	62	61	56
Sc	12	13	13	13	13	13	13	13	12	11
V	135	134	138	139	123	137	130	132	139	128
Ba	481	404	784	466	433	669	577	560	531	422

Rb	116	118	107	112	111	108	118	112	112	106
Sr	127	127	138	132	132	139	130	143	133	131
Zr	119	111	117	118	124	114	119	122	119	135
Y	37	37	38	33	31	35	27	39	33	26
Nb	12.2	12.6	12.2	12.5	12.7	12.3	13.1	13.2	12.6	13.3
Ga	19	18	17	19	18	16	18	17	17	17
Cu	19	19	24	24	22	21	19	22	20	33
Zn	104	103	101	100	92	98	97	93	97	98
Pb	22	22	20	23	21	20	22	20	20	19
La	37	34	40	34	32	41	33	42	36	33
Ce	70	68	75	65	63	77	56	74	68	56
Th	15	15	14	15	14	14	15	15	15	14
Nd	32	29	32	30	27	34	23	32	30	23
U	5	6	4	3	4	5	4	5	5	3
sum tr.	1461	1372	1767	1436	1364	1647	1510	1542	1489	1351
in %	0.15	0.14	0.18	0.14	0.14	0.16	0.15	0.15	0.15	0.14
sum m+tr	86.82	86.96	85.76	86.30	86.44	86.09	87.29	85.83	86.03	85.70
M+Toxides	86.85	86.99	85.80	86.33	86.47	86.12	87.32	85.87	86.06	85.74
w/LOI	99.74	99.49	99.61	99.43	99.32	99.49	99.46	99.59	99.39	99.39
if Fe3+	100.44	100.19	100.34	100.17	99.97	100.20	100.12	100.31	100.10	100.04
Major elements are normalized on a volatile-free basis, with total Fe expressed as FeO.										
® denotes a duplicate bead made from the same rock powder.										
NiO	46.2	46.8	43.4	43.9	39.4	40.7	40.3	36.2	37.3	36.6
Cr2O3	93.3	92.5	85.9	94.4	87.8	88.3	91.2	90.5	89.3	81.2
Sc2O3	18.8	19.2	20.0	19.4	19.3	20.3	19.7	19.4	18.4	16.7
V2O3	199.2	197.1	203.7	204.3	181.5	201.6	190.9	194.3	204.2	188.0
BaO	537.3	451.5	874.9	519.7	483.4	746.9	644.6	624.8	592.6	471.1
Rb2O	126.5	129.2	117.5	122.8	121.8	118.3	129.2	122.0	122.2	115.6
SrO	150.3	150.0	163.3	156.6	156.1	164.8	153.6	168.9	157.2	154.9
ZrO2	160.1	150.3	157.7	159.9	167.5	153.3	160.6	164.5	160.8	182.4
Y2O3	46.8	47.0	48.0	41.5	39.2	44.0	34.1	50.2	41.9	33.3
Nb2O5	17.4	18.0	17.4	17.8	18.2	17.6	18.7	18.9	18.1	19.1
Ga2O3	25.0	24.5	23.1	25.3	23.8	22.0	24.9	23.1	23.5	22.5
CuO	24.2	24.2	29.6	29.6	27.9	26.6	24.4	27.2	25.2	40.8
ZnO	129.4	128.5	125.6	124.0	115.0	122.6	121.3	115.2	120.2	121.9
PbO	23.7	23.9	21.5	24.9	22.6	21.8	24.0	22.0	21.2	20.0
La2O3	43.0	40.3	47.0	39.7	37.9	48.3	39.0	48.8	42.5	38.4
CeO2	85.7	83.6	91.7	80.1	77.1	94.9	68.9	90.6	83.1	69.4
ThO2	16.4	16.4	15.4	16.3	15.3	15.5	16.9	16.0	16.5	15.0
Nd2O3	36.9	33.4	37.7	34.6	30.9	39.5	26.7	37.8	35.5	26.4
U2O3	5.5	6.9	4.2	3.2	4.1	5.7	4.2	5.0	5.3	3.4
sum tr.	**1786**	**1683**	**2128**	**1758**	**1669**	**1993**	**1833**	**1875**	**1815**	**1657**
in %	**0.18**	**0.17**	**0.21**	**0.18**	**0.17**	**0.20**	**0.18**	**0.19**	**0.18**	**0.17**

	BFO WF-145	**BFO WF-144**	**BFO WF-143**	**BFO WF-133**	**BFO WF-132**	**BFO WF-131**	**BFO WF-130**	**BFO WF-129**	**BFO WF-128**	**BFO WF-127**
Stratigraphic Height	44.03	43.93	43.68	41.36	41.11	40.86	40.61	40.36	40.11	39.86
SO3 >/=										
Unnormalized Major Elements (Weight %):										
SiO2	54.77	54.87	57.90	50.07	50.48	50.75	49.91	52.10	51.59	48.91
TiO2	0.629	0.593	0.651	0.825	0.800	0.793	0.790	0.693	0.748	0.785
Al2O3	14.20	13.52	18.26	21.99	21.82	21.57	21.85	22.02	21.82	22.44
FeO*	6.31	6.38	5.48	5.69	5.92	5.79	6.02	3.57	4.53	6.22

MnO	0.053	0.077	0.009	0.007	0.007	0.007	0.007	0.003	0.004	0.006
MgO	2.70	2.88	1.26	1.08	1.09	1.10	1.16	0.98	0.99	1.00
CaO	5.57	5.53	0.36	0.42	0.43	0.41	0.41	0.46	0.43	0.54
Na2O	0.52	0.53	1.12	1.61	1.58	1.54	1.50	1.46	1.49	1.52
K2O	2.04	2.03	2.01	0.57	0.78	0.92	1.13	0.82	0.83	0.65
P2O5	0.143	0.181	0.078	0.016	0.018	0.022	0.031	0.019	0.034	0.058
Sum	86.94	86.59	87.13	82.27	82.91	82.90	82.82	82.12	82.47	82.13
LOI %	12.67	12.96	12.29	17.05	16.58	16.20	16.62	16.98	16.89	17.17
Normalized Major Elements (Weight %):										
SiO2	63.00	63.37	66.46	60.86	60.88	61.22	60.26	63.44	62.56	59.55
TiO2	0.724	0.685	0.747	1.003	0.965	0.957	0.954	0.844	0.907	0.956
Al2O3	16.33	15.61	20.96	26.72	26.31	26.01	26.38	26.81	26.46	27.33
FeO*	7.26	7.37	6.29	6.91	7.14	6.99	7.27	4.35	5.49	7.57
MnO	0.061	0.089	0.010	0.009	0.008	0.008	0.009	0.004	0.005	0.007
MgO	3.10	3.32	1.45	1.31	1.32	1.33	1.40	1.19	1.20	1.22
CaO	6.41	6.39	0.41	0.51	0.51	0.50	0.49	0.56	0.52	0.66
Na2O	0.60	0.61	1.29	1.96	1.90	1.86	1.82	1.77	1.81	1.86
K2O	2.35	2.35	2.30	0.69	0.94	1.11	1.37	1.00	1.01	0.79
P2O5	0.164	0.209	0.089	0.020	0.022	0.027	0.038	0.023	0.041	0.070
Total	100.00	100.00	100.00	100.00	100.00	100.00	100.00	100.00	100.00	100.00
Unnormalized Trace Elements (ppm):										
Ni	27	27	21	16	16	17	18	22	21	18
Cr	58	62	54	38	39	39	42	44	46	44
Sc	12	13	16	20	19	19	18	19	15	19
V	127	146	141	165	165	157	160	156	157	177
Ba	456	437	284	73	97	113	119	149	164	146
Rb	119	118	126	35	49	60	83	75	71	40
Sr	126	125	120	170	162	152	116	125	154	249
Zr	124	113	119	135	135	133	126	138	124	146
Y	27	39	29	19	19	22	32	16	30	35
Nb	13.7	12.3	13.3	17.0	16.7	16.3	16.8	15.1	16.1	16.1
Ga	18	19	23	28	28	28	28	29	29	30
Cu	23	31	65	33	30	28	26	52	63	46
Zn	94	96	86	72	72	71	70	89	87	72
Pb	19	19	20	24	29	32	30	24	28	38
La	29	35	48	22	22	29	64	26	51	72
Ce	60	65	92	35	42	48	143	35	92	104
Th	15	14	15	14	14	15	12	10	11	13
Nd	26	30	42	14	16	18	64	13	39	41
U	4	5	6	3	3	3	3	3	3	2
sum tr.	1379	1405	1320	932	974	999	1170	1040	1201	1308
in %	0.14	0.14	0.13	0.09	0.10	0.10	0.12	0.10	0.12	0.13
sum m+tr	87.07	86.73	87.26	82.37	83.01	83.00	82.94	82.22	82.59	82.26
M+Toxides	87.10	86.76	87.29	82.39	83.04	83.03	82.97	82.25	82.62	82.30
w/LOI	99.78	99.73	99.58	99.44	99.62	99.23	99.59	99.23	99.51	99.47
if Fe3+	100.48	100.44	100.19	100.07	100.27	99.87	100.26	99.62	100.01	100.16
Major elements are normalized on a volatile-free basis, with total Fe expressed as FeO.										
® denotes a duplicate bead made from the same rock powder.										
NiO	34.1	34.3	26.5	20.3	20.3	21.3	22.4	27.4	26.9	22.5
Cr2O3	85.3	90.3	79.1	55.7	57.0	56.7	61.1	64.2	67.2	64.7
Sc2O3	17.8	20.0	24.2	30.1	29.0	28.8	27.7	28.8	23.4	28.5
V2O3	186.9	214.7	207.0	242.1	242.0	230.9	236.0	229.9	231.0	260.5
BaO	508.9	488.4	316.6	81.0	107.9	126.3	132.4	166.7	182.6	162.7
Rb2O	130.5	128.7	138.3	38.2	54.1	66.2	90.7	81.6	77.8	44.2

SrO	149.5	147.8	141.8	201.0	192.1	179.3	137.5	147.6	181.8	294.8
ZrO2	167.4	153.0	161.3	182.4	182.4	180.0	169.5	186.6	167.8	196.6
Y2O3	34.9	49.3	36.3	23.9	23.6	27.6	41.1	20.9	38.6	44.1
Nb2O5	19.6	17.6	19.1	24.3	23.8	23.3	24.0	21.6	23.0	23.0
Ga2O3	24.3	25.1	31.2	37.5	38.2	37.7	37.6	38.6	39.1	40.2
CuO	28.2	38.6	80.9	41.2	37.2	34.6	32.8	65.2	79.1	57.3
ZnO	117.5	119.1	106.6	90.0	89.5	88.4	86.9	110.2	108.4	90.1
PbO	20.9	20.2	22.0	26.2	31.3	34.1	32.3	26.2	30.2	41.5
La2O3	34.0	41.5	56.4	25.8	26.2	34.4	74.7	30.5	59.7	84.6
CeO2	73.7	80.0	112.6	42.6	52.1	58.5	175.6	42.5	112.9	127.5
ThO2	16.9	15.3	16.5	15.7	15.9	16.3	13.0	10.9	11.9	14.0
Nd2O3	29.9	34.5	49.1	16.0	18.3	21.0	74.9	15.2	45.6	47.7
U2O3	4.9	6.0	7.1	3.8	2.9	3.6	3.7	3.8	3.2	2.6
sum tr.	**1685**	**1724**	**1633**	**1198**	**1244**	**1269**	**1474**	**1318**	**1510**	**1647**
in %	**0.17**	**0.17**	**0.16**	**0.12**	**0.12**	**0.13**	**0.15**	**0.13**	**0.15**	**0.16**

	BFO WF-126	**BFO WF-125**	**BFO WF-124**	**BFO WF-123**	**BFO WF-068**	**BFO WF-067**	**BFO WF-066**	**BFO WF-065**	**BFO WF-064**	**BFO WF-063**
Stratigraphic Height	39.61	39.36	39.26	39	20.71	20.46	20.21	19.96	17.87	17.62
SO3 >/=										
Unnormalized Major Elements (Weight %):										
SiO2	47.68	49.38	63.44	65.08	57.01	59.16	58.48	59.26	67.88	66.86
TiO2	0.716	0.718	0.662	0.585	0.949	0.995	0.954	0.969	0.887	0.873
Al2O3	22.28	22.44	14.94	13.85	21.99	19.93	18.84	19.09	14.24	15.37
FeO*	7.38	6.87	8.06	8.17	3.82	4.77	6.36	5.59	6.34	5.21
MnO	0.006	0.008	0.008	0.015	0.005	0.007	0.008	0.007	0.011	0.009
MgO	1.01	0.98	0.85	0.84	0.50	0.51	0.56	0.55	0.55	0.47
CaO	0.56	0.53	0.18	0.08	0.26	0.27	0.26	0.28	0.21	0.20
Na2O	1.55	1.40	0.72	1.10	1.12	1.03	1.06	1.07	1.04	0.95
K2O	0.71	0.90	2.05	1.84	0.13	0.13	0.20	0.20	0.65	0.56
P2O5	0.034	0.028	0.031	0.024	0.010	0.019	0.022	0.018	0.015	0.022
Sum	81.92	83.27	90.93	91.58	85.81	86.82	86.76	87.04	91.82	90.53
LOI %	16.96	16.17	8.44	7.59	13.59	12.49	12.11	12.08	7.64	8.80
Normalized Major Elements (Weight %):										
SiO2	58.20	59.31	69.76	71.06	66.44	68.14	67.41	68.08	73.92	73.86
TiO2	0.875	0.863	0.728	0.638	1.106	1.146	1.100	1.114	0.967	0.965
Al2O3	27.20	26.95	16.43	15.12	25.63	22.96	21.72	21.94	15.51	16.98
FeO*	9.00	8.26	8.86	8.92	4.45	5.49	7.33	6.42	6.90	5.75
MnO	0.007	0.009	0.009	0.016	0.005	0.008	0.010	0.009	0.012	0.009
MgO	1.23	1.18	0.94	0.92	0.59	0.59	0.65	0.64	0.60	0.52
CaO	0.69	0.64	0.19	0.08	0.31	0.31	0.30	0.32	0.22	0.22
Na2O	1.89	1.68	0.79	1.20	1.31	1.19	1.22	1.23	1.13	1.05
K2O	0.87	1.08	2.25	2.01	0.15	0.15	0.23	0.23	0.71	0.62
P2O5	0.042	0.033	0.035	0.026	0.012	0.022	0.025	0.021	0.016	0.024
Total	100.00	100.00	100.00	100.00	100.00	100.00	100.00	100.00	100.00	100.00
Unnormalized Trace Elements (ppm):										
Ni	18	18	18	57	9	8	7	6	5	3
Cr	41	43	53	48	38	34	32	32	20	22
Sc	18	18	13	11	18	17	17	17	11	13
V	156	148	138	123	134	135	158	133	97	98
Ba	85	108	324	284	469	914	3138	1995	693	870
Rb	43	53	111	96	8	8	11	11	27	24
Sr	139	131	75	56	126	121	151	133	91	104
Zr	130	133	165	181	195	210	232	249	412	351

Y	34	34	28	28	17	21	18	17	17	18
Nb	14.3	14.8	14.3	12.6	20.4	21.8	21.3	21.5	20.4	19.6
Ga	29	28	19	18	29	26	24	24	18	17
Cu	39	48	25	30	23	19	18	25	18	20
Zn	70	65	70	85	42	39	45	41	41	30
Pb	27	33	18	28	21	23	22	21	20	20
La	24	44	28	21	16	20	21	19	19	19
Ce	47	102	52	40	30	38	39	30	37	38
Th	15	14	14	12	23	15	16	17	14	13
Nd	19	49	20	16	16	14	15	12	16	17
U	2	3	2	2	4	4	3	3	3	4
sum tr.	952	1085	1188	1150	1237	1690	3988	2806	1578	1699
in %	0.10	0.11	0.12	0.11	0.12	0.17	0.40	0.28	0.16	0.17
sum m+tr	82.02	83.37	91.05	91.69	85.93	86.99	87.15	87.32	91.98	90.70
M+Toxides	82.04	83.40	91.08	91.72	85.96	87.03	87.22	87.37	92.01	90.73
w/LOI	99.01	99.57	99.52	99.32	99.54	99.52	99.32	99.45	99.65	99.54
if Fe3+	99.82	100.33	100.41	100.22	99.97	100.05	100.03	100.07	100.35	100.12
Major elements are normalized on a volatile-free basis, with total Fe expressed as FeO.										
® denotes a duplicate bead made from the same rock powder.										
NiO	23.4	22.4	22.6	72.3	11.9	9.7	9.1	7.5	6.9	3.6
Cr2O3	59.8	63.5	77.7	70.5	56.3	50.4	47.2	46.7	29.7	31.9
Sc2O3	28.2	27.3	20.3	16.8	28.2	25.7	26.8	26.7	17.3	19.6
V2O3	229.3	218.1	203.3	180.8	196.5	198.3	232.3	195.3	142.3	143.9
BaO	95.2	120.3	361.3	316.8	523.2	1020.8	3503.0	2227.7	773.6	971.1
Rb2O	46.6	57.8	120.9	105.5	8.6	8.9	11.6	12.6	29.3	26.4
SrO	164.6	155.4	89.0	66.7	148.6	143.0	178.9	157.2	108.0	122.8
ZrO2	176.0	179.1	223.5	243.9	263.0	284.3	313.1	336.7	555.9	473.7
Y2O3	43.1	42.7	35.6	35.7	21.6	26.0	23.2	21.8	21.8	23.4
Nb2O5	20.5	21.2	20.4	18.0	29.2	31.2	30.5	30.8	29.2	28.0
Ga2O3	39.5	37.6	25.8	24.2	38.4	34.9	31.9	31.7	23.5	23.3
CuO	48.7	60.2	31.6	37.9	28.4	24.4	22.8	30.8	22.4	24.4
ZnO	87.4	80.6	87.4	105.6	52.4	49.0	55.8	51.0	50.5	37.8
PbO	29.6	35.8	19.2	30.5	22.2	25.2	24.1	22.4	21.3	21.1
La2O3	28.7	51.1	32.4	25.1	18.5	23.5	24.5	21.9	21.9	22.5
CeO2	57.5	125.0	64.0	49.2	37.2	46.6	48.3	36.3	45.9	47.0
ThO2	16.0	15.2	15.7	13.2	25.2	16.7	17.2	18.4	15.0	13.8
Nd2O3	22.5	57.0	23.3	18.9	18.6	16.5	17.7	14.4	18.1	19.6
U2O3	1.8	3.6	2.4	2.5	4.4	4.9	3.0	3.1	3.6	4.4
sum tr.	**1218**	**1374**	**1477**	**1434**	**1532**	**2040**	**4621**	**3293**	**1936**	**2058**
in %	**0.12**	**0.14**	**0.15**	**0.14**	**0.15**	**0.20**	**0.46**	**0.33**	**0.19**	**0.21**

	BFO WF-062	**BFO WF-061**	**BFO WF-044**	**BFO WF-043**	**BFO WF-042**	**BFO WF-041**	**BFO WF-040**	**BFO WF-039**	**BFO WF-038**	**BFO WF-037**
Stratigraphic Height	17.37	17.12	13.14	12.89	12.64	12.39	12.14	11.89	11.64	11.39
SO3 >/=			0.68							0.17
Unnormalized Major Elements (Weight %):										
SiO2	68.03	71.56	52.98	55.39	56.63	57.22	61.40	62.40	61.59	61.53
TiO2	0.888	0.816	0.848	0.890	0.900	0.914	0.890	0.914	0.896	0.872
Al2O3	14.49	12.74	19.02	19.55	18.29	19.11	17.66	17.43	17.35	16.73
FeO*	5.65	4.88	7.45	7.07	8.29	6.32	5.46	4.88	5.46	5.89
MnO	0.009	0.009	0.008	0.009	0.010	0.010	0.008	0.007	0.008	0.009
MgO	0.51	0.47	0.64	0.70	0.64	0.65	0.57	0.58	0.59	0.63
CaO	0.18	0.15	0.34	0.34	0.31	0.29	0.26	0.24	0.25	0.29

Na2O	1.00	0.91	1.30	1.33	1.19	1.24	1.17	1.15	1.23	1.23
K2O	0.62	0.63	0.48	0.58	0.63	0.64	0.62	0.62	0.72	0.75
P2O5	0.014	0.017	0.018	0.014	0.036	0.014	0.024	0.019	0.014	0.023
Sum	91.39	92.17	83.09	85.86	86.93	86.41	88.05	88.24	88.12	87.94
LOI %	7.72	6.73	13.56	13.42	12.58	12.90	11.48	11.15	11.23	10.77
Normalized Major Elements (Weight %):										
SiO2	74.44	77.64	63.77	64.51	65.15	66.22	69.73	70.71	69.89	69.97
TiO2	0.971	0.886	1.021	1.037	1.036	1.058	1.011	1.035	1.016	0.992
Al2O3	15.86	13.82	22.89	22.77	21.04	22.11	20.05	19.75	19.70	19.02
FeO*	6.18	5.29	8.96	8.23	9.54	7.32	6.20	5.53	6.20	6.69
MnO	0.010	0.010	0.009	0.011	0.011	0.011	0.010	0.008	0.009	0.010
MgO	0.56	0.51	0.78	0.81	0.73	0.75	0.64	0.65	0.67	0.72
CaO	0.19	0.16	0.41	0.39	0.36	0.34	0.29	0.28	0.28	0.33
Na2O	1.10	0.98	1.56	1.55	1.37	1.44	1.33	1.30	1.40	1.39
K2O	0.68	0.68	0.58	0.67	0.72	0.74	0.71	0.71	0.81	0.85
P2O5	0.015	0.018	0.022	0.016	0.041	0.016	0.027	0.021	0.016	0.026
Total	100.00	100.00	100.00	100.00	100.00	100.00	100.00	100.00	100.00	100.00
Unnormalized Trace Elements (ppm):										
Ni	4	3	9	9	7	8	8	8	8	8
Cr	21	18	24	28	26	28	31	31	30	31
Sc	12	10	15	17	15	16	15	15	15	14
V	102	91	137	127	145	126	124	116	124	137
Ba	765	2229	19360	979	980	308	310	660	268	4930
Rb	27	26	26	31	36	36	34	34	38	40
Sr	92	94	264	148	130	131	124	123	123	141
Zr	373	453	175	187	204	207	255	258	247	231
Y	19	21	11	11	12	13	23	20	15	15
Nb	19.6	18.2	18.9	20.0	20.1	20.4	20.5	21.1	20.5	19.6
Ga	17	15	23	24	23	24	22	22	21	21
Cu	18	21	19	16	11	16	15	16	15	19
Zn	35	34	48	53	52	55	50	50	50	52
Pb	19	17	25	20	19	21	22	22	22	20
La	23	25	12	15	19	21	47	39	23	21
Ce	53	61	19	29	38	40	130	104	44	33
Th	12	10	15	14	17	16	15	17	15	15
Nd	22	27	7	11	13	14	58	45	16	12
U	4	4	3	3	5	5	5	5	4	4
sum tr.	1637	3176	20213	1740	1772	1105	1307	1605	1098	5762
in %	0.16	0.32	2.02	0.17	0.18	0.11	0.13	0.16	0.11	0.58
sum m+tr	91.56	92.49	85.11	86.04	87.10	86.52	88.18	88.40	88.23	88.51
M+Toxides	91.59	92.54	85.36	86.07	87.14	86.55	88.21	88.44	88.25	88.60
w/LOI	99.31	99.27	98.92	99.49	99.72	99.45	99.70	99.59	99.48	99.37
if Fe3+	99.94	99.81	99.75	100.28	100.64	100.15	100.30	100.13	100.09	100.03

Major elements are normalized on a volatile-free basis, with total Fe expressed as FeO.
® denotes a duplicate bead made from the same rock powder.

NiO	4.6	3.6	11.7	11.1	8.9	10.2	10.6	10.4	10.2	9.8
Cr2O3	30.1	26.6	34.4	40.6	37.9	41.5	45.4	44.8	44.4	44.8
Sc2O3	19.0	16.0	23.5	25.8	23.6	25.2	23.4	23.3	22.5	22.2
V2O3	149.5	134.5	201.5	187.3	213.0	185.8	182.9	171.2	181.8	201.2
BaO	854.0	2488.2	21615.4	1093.3	1094.3	343.7	345.8	736.8	299.2	5504.1
Rb2O	29.1	27.9	28.7	33.8	38.9	39.0	36.9	37.0	41.3	43.8
SrO	108.4	110.8	312.6	175.1	153.7	154.7	146.3	145.0	145.5	167.0
ZrO2	504.5	611.4	236.9	252.9	275.2	279.7	344.3	348.9	333.6	311.7
Y2O3	24.3	26.3	13.7	13.5	15.6	16.9	28.6	25.7	18.9	19.4

Nb2O5	28.0	26.0	27.0	28.6	28.8	29.2	29.3	30.2	29.3	28.0
Ga2O3	22.6	19.8	31.5	32.0	31.1	31.7	29.3	29.5	28.2	27.7
CuO	22.9	26.8	23.4	19.4	13.8	20.5	19.2	20.0	18.3	23.4
ZnO	43.3	42.7	60.0	65.3	64.9	67.8	61.9	61.9	62.5	64.3
PbO	20.1	18.1	27.4	21.0	20.8	22.9	23.6	23.3	23.3	21.9
La2O3	27.0	28.7	14.6	17.2	21.8	24.3	54.7	45.8	27.2	25.1
CeO2	65.3	75.0	23.0	35.2	47.2	48.9	159.5	127.7	54.2	40.0
ThO2	13.7	11.4	16.8	15.9	18.2	17.5	16.5	18.6	16.9	16.7
Nd2O3	25.7	31.0	8.5	12.6	15.4	16.6	67.2	52.2	18.7	13.5
U2O3	4.5	4.8	3.8	3.7	5.7	5.4	5.8	5.1	4.3	4.3
sum tr.	**1997**	**3730**	**22714**	**2084**	**2129**	**1382**	**1631**	**1957**	**1380**	**6589**
in %	**0.20**	**0.37**	**2.27**	**0.21**	**0.21**	**0.14**	**0.16**	**0.20**	**0.14**	**0.66**

	BFO WF3-066	**BFO WF3-065**	**BFO WF3-064**	**BFO WF3-063**	**BFO WF3-062**	**BFO WF3-061**	**BFO WF3-060**	**BFO WF3-059**	**BFO WF3-058**	**BFO WF3-057**
Stratigraphic Height	9.46	9.4	9.15	8.9	8.77	8.67	8.57	8.43	8.33	8.23
SO3 >/=										
Unnormalized Major Elements (Weight %):										
SiO2	67.73	68.98	64.77	69.52	71.05	73.31	71.46	66.91	66.10	66.18
TiO2	0.744	0.691	0.728	0.677	0.934	0.937	0.915	0.879	0.882	0.843
Al2O3	14.49	14.09	16.12	14.51	13.03	11.60	13.14	15.16	15.90	15.56
FeO*	5.33	4.66	5.96	4.48	4.72	4.71	4.47	5.37	5.18	5.65
MnO	0.009	0.008	0.006	0.008	0.008	0.007	0.007	0.007	0.007	0.008
MgO	0.53	0.52	0.66	0.54	0.50	0.45	0.47	0.57	0.55	0.56
CaO	0.30	0.30	0.23	0.29	0.22	0.21	0.24	0.24	0.26	0.26
Na2O	1.35	1.34	1.28	1.39	1.13	1.07	1.14	1.18	1.23	1.22
K2O	1.13	1.19	1.26	1.23	0.64	0.56	0.58	0.70	0.53	0.51
P2O5	0.026	0.033	0.028	0.036	0.031	0.028	0.030	0.027	0.024	0.033
Sum	91.65	91.80	91.05	92.67	92.26	92.88	92.46	91.06	90.66	90.81
LOI %	7.89	7.64	8.58	6.84	6.97	6.29	7.07	8.06	8.61	8.48
Normalized Major Elements (Weight %):										
SiO2	73.91	75.14	71.14	75.02	77.01	78.93	77.29	73.48	72.91	72.88
TiO2	0.812	0.753	0.800	0.730	1.012	1.009	0.989	0.965	0.972	0.929
Al2O3	15.81	15.34	17.71	15.66	14.13	12.49	14.21	16.65	17.53	17.13
FeO*	5.82	5.08	6.55	4.83	5.12	5.07	4.84	5.90	5.72	6.22
MnO	0.010	0.009	0.007	0.008	0.009	0.008	0.008	0.007	0.008	0.008
MgO	0.58	0.56	0.73	0.58	0.54	0.49	0.51	0.63	0.61	0.61
CaO	0.33	0.33	0.26	0.32	0.24	0.22	0.26	0.27	0.29	0.28
Na2O	1.47	1.46	1.40	1.50	1.23	1.15	1.23	1.29	1.35	1.34
K2O	1.23	1.29	1.38	1.33	0.69	0.60	0.62	0.77	0.58	0.56
P2O5	0.029	0.036	0.031	0.039	0.033	0.030	0.032	0.030	0.027	0.036
Total	100.00	100.00	100.00	100.00	100.00	100.00	100.00	100.00	100.00	100.00
Unnormalized Trace Elements (ppm):										
Ni	10	9	12	10	12	10	11	12	13	12
Cr	27	28	35	29	29	27	29	35	32	32
Sc	10	11	14	11	11	11	12	14	14	13
V	85	86	111	88	96	91	91	106	103	103
Ba	312	334	262	330	191	192	184	165	142	141
Rb	46	49	58	52	31	27	27	36	26	26
Sr	130	128	136	133	124	107	108	120	124	119
Zr	341	294	242	275	418	449	438	335	313	293
Y	20	22	22	27	33	37	41	36	34	37
Nb	16.7	15.2	16.3	14.8	22.0	22.2	21.2	20.2	20.3	19.5
Ga	17	17	19	17	17	15	16	19	19	20

Cu	13	17	10	15	12	15	14	12	11	11
Zn	38	37	45	36	43	40	40	44	46	47
Pb	22	21	23	20	25	22	21	23	23	22
La	58	66	57	72	74	71	71	70	60	87
Ce	109	132	110	155	147	149	152	132	117	178
Th	11	11	13	12	17	18	18	17	16	15
Nd	52	71	51	84	71	79	86	69	61	102
U	3	3	3	5	4	3	4	4	2	4
sum tr.	1322	1350	1238	1386	1378	1385	1381	1268	1176	1280
in %	0.13	0.13	0.12	0.14	0.14	0.14	0.14	0.13	0.12	0.13
sum m+tr	91.78	91.94	91.18	92.81	92.39	93.01	92.60	91.19	90.78	90.94
M+Toxides	91.81	91.97	91.21	92.84	92.43	93.05	92.63	91.22	90.81	90.97
w/LOI	99.70	99.61	99.78	99.69	99.40	99.34	99.71	99.29	99.42	99.46
if Fe3+	100.29	100.13	100.45	100.18	99.92	99.86	100.20	99.88	99.99	100.08
Major elements are normalized on a volatile-free basis, with total Fe expressed as FeO.										
® denotes a duplicate bead made from the same rock powder.										
NiO	12.7	11.5	15.4	13.2	15.2	12.8	14.5	14.6	16.2	15.1
Cr2O3	39.8	40.7	50.9	42.9	42.6	38.8	41.7	51.3	46.3	47.2
Sc2O3	15.9	16.2	20.7	17.1	17.3	16.6	17.7	21.0	21.3	20.3
V2O3	125.7	126.7	163.6	129.8	140.8	134.4	133.2	156.1	152.1	151.4
BaO	348.0	372.6	292.9	368.4	213.2	214.0	205.5	183.7	158.9	157.0
Rb2O	50.7	54.0	63.4	56.7	34.1	29.1	29.2	39.3	29.0	28.5
SrO	153.3	150.9	161.3	157.2	146.8	126.9	127.5	141.7	146.2	141.2
ZrO2	460.2	397.1	327.2	371.4	564.2	606.4	591.2	453.1	422.9	395.9
Y2O3	24.9	28.2	27.3	33.9	41.7	47.2	51.9	46.0	42.7	47.0
Nb2O5	23.9	21.7	23.3	21.1	31.5	31.8	30.3	28.9	29.0	27.9
Ga2O3	23.2	22.7	25.5	23.4	22.4	20.3	21.1	26.1	26.1	26.9
CuO	15.9	21.8	12.9	18.2	15.5	18.6	17.2	15.5	13.5	13.5
ZnO	47.9	45.9	55.4	44.5	53.8	50.0	49.9	54.4	57.3	58.3
PbO	23.9	22.2	24.5	21.5	27.0	23.7	23.1	25.0	24.5	23.4
La2O3	67.7	77.3	66.4	84.4	87.3	83.4	83.2	81.5	70.8	101.6
CeO2	134.3	161.8	134.8	190.1	181.1	183.5	187.2	161.8	143.8	218.5
ThO2	12.2	11.8	14.2	12.8	19.0	19.4	19.4	18.4	17.2	16.3
Nd2O3	60.7	82.8	59.6	98.5	82.3	92.3	100.1	80.0	70.8	119.1
U2O3	3.7	3.2	2.9	5.5	4.3	3.5	3.9	4.4	2.1	4.0
sum tr.	**1644**	**1669**	**1542**	**1711**	**1740**	**1753**	**1748**	**1603**	**1491**	**1613**
in %	**0.16**	**0.17**	**0.15**	**0.17**	**0.17**	**0.18**	**0.17**	**0.16**	**0.15**	**0.16**

	BFO WF3-056	**BFO WF3-055**	**BFO WF3-054**	**BFO WF3-053**	**BFO WF3-052**	**BFO WF3-051**	**BFO WF3-050**	**BFO WF3-037**	**BFO WF3-036**	**BFO WF3-035**
Stratigraphic Height	8.13	8.03	7.93	7.83	7.73	7.59	7.53	6.61	5.53	5.4
SO3 >/=										
Unnormalized Major Elements (Weight %):										
SiO2	68.78	70.47	63.34	71.25	65.30	68.31	71.11	63.39	66.00	72.68
TiO2	0.754	0.760	0.939	0.803	0.832	0.898	0.871	0.789	0.708	0.601
Al2O3	14.38	14.15	16.63	13.31	16.01	14.53	13.52	16.77	15.48	12.99
FeO*	5.13	4.27	6.36	4.66	5.89	5.08	4.00	6.12	5.51	3.22
MnO	0.008	0.008	0.007	0.007	0.007	0.009	0.008	0.014	0.015	0.017
MgO	0.53	0.50	0.61	0.48	0.59	0.54	0.50	0.69	0.70	0.55
CaO	0.25	0.26	0.27	0.23	0.26	0.24	0.21	0.41	0.41	0.63
Na2O	1.28	1.31	1.31	1.16	1.30	1.23	1.18	1.43	1.48	1.52
K2O	0.82	0.94	0.54	0.60	0.67	0.52	0.47	1.40	1.60	1.47
P2O5	0.028	0.048	0.024	0.017	0.024	0.013	0.014	0.074	0.100	0.114

Sum	91.96	92.71	90.04	92.53	90.88	91.37	91.88	91.08	92.01	93.79
LOI %	7.22	6.82	9.53	7.05	8.67	7.99	7.37	8.36	7.39	5.42
Normalized Major Elements (Weight %):										
SiO2	74.79	76.02	70.35	77.00	71.85	74.77	77.39	69.60	71.73	77.50
TiO2	0.820	0.820	1.043	0.868	0.915	0.983	0.948	0.867	0.769	0.641
Al2O3	15.64	15.26	18.48	14.39	17.61	15.91	14.71	18.42	16.83	13.85
FeO*	5.58	4.60	7.07	5.04	6.48	5.56	4.35	6.71	5.99	3.43
MnO	0.008	0.008	0.008	0.007	0.008	0.009	0.009	0.016	0.017	0.018
MgO	0.58	0.54	0.68	0.52	0.65	0.59	0.54	0.75	0.76	0.59
CaO	0.27	0.28	0.30	0.25	0.28	0.26	0.23	0.45	0.45	0.67
Na2O	1.39	1.41	1.45	1.26	1.43	1.34	1.28	1.57	1.61	1.62
K2O	0.89	1.01	0.60	0.65	0.74	0.57	0.51	1.54	1.74	1.56
P2O5	0.030	0.052	0.027	0.018	0.026	0.014	0.016	0.081	0.109	0.121
Total	100.00	100.00	100.00	100.00	100.00	100.00	100.00	100.00	100.00	100.00
Unnormalized Trace Elements (ppm):										
Ni	9	12	16	13	13	14	11	15	15	11
Cr	28	26	32	28	33	29	26	35	38	36
Sc	12	11	15	11	13	13	12	12	11	9
V	89	87	111	87	116	100	94	105	108	76
Ba	272	316	127	158	142	137	143	342	315	557
Rb	36	39	30	29	34	29	26	68	77	65
Sr	111	121	125	114	125	114	105	128	109	103
Zr	299	317	306	347	261	299	360	256	247	250
Y	29	44	36	27	29	27	30	40	48	44
Nb	17.0	17.7	21.3	18.2	19.3	20.3	20.2	17.9	15.5	13.2
Ga	18	16	21	17	20	19	16	20	19	16
Cu	15	14	8	9	14	11	12	50	27	35
Zn	46	39	57	43	51	49	47	52	48	35
Pb	20	20	24	20	21	22	20	24	18	15
La	57	124	66	43	46	32	48	57	48	40
Ce	121	250	124	61	60	45	69	110	101	70
Th	13	14	17	15	14	16	17	11	12	9
Nd	63	144	70	35	39	23	47	47	45	35
U	3	4	3	2	3	3	4	3	3	2
sum tr.	1258	1616	1211	1076	1054	1003	1108	1392	1304	1420
in %	0.13	0.16	0.12	0.11	0.11	0.10	0.11	0.14	0.13	0.14
sum m+tr	92.09	92.87	90.16	92.64	90.99	91.47	91.99	91.22	92.14	93.93
M+Toxides	92.12	92.91	90.19	92.67	91.02	91.50	92.02	91.26	92.17	93.96
w/LOI	99.34	99.73	99.72	99.72	99.68	99.49	99.39	99.61	99.56	99.38
if Fe3+	99.91	100.20	100.43	100.24	100.34	100.06	99.84	100.29	100.18	99.74
Major elements are normalized on a volatile-free basis, with total Fe expressed as FeO.										
® denotes a duplicate bead made from the same rock powder.										
NiO	11.5	14.8	20.1	16.3	17.1	17.9	14.1	19.5	18.7	13.9
Cr2O3	40.9	38.0	46.3	40.5	48.6	41.7	38.1	51.4	55.8	52.2
Sc2O3	18.6	16.8	23.6	17.3	20.0	19.6	18.1	19.0	17.6	14.0
V2O3	130.5	127.4	163.5	127.8	171.4	147.6	138.9	154.9	159.1	112.1
BaO	304.0	353.1	142.3	176.1	158.6	152.6	160.0	381.3	351.7	621.7
Rb2O	39.3	42.5	33.2	31.6	37.6	31.6	28.0	74.4	83.8	71.1
SrO	131.7	143.3	148.2	134.9	147.3	134.9	124.6	151.5	129.3	121.7
ZrO2	404.3	428.8	413.6	468.5	352.9	403.3	486.5	345.4	333.3	337.6
Y2O3	37.3	55.4	45.4	34.7	36.4	34.3	38.6	50.4	60.9	56.3
Nb2O5	24.3	25.3	30.5	26.0	27.6	29.0	28.9	25.6	22.1	18.9
Ga2O3	23.7	22.0	28.4	22.9	26.3	26.1	21.8	27.0	25.9	20.8
CuO	18.7	17.9	10.3	10.9	17.2	14.0	15.4	62.2	33.7	43.6

ZnO	57.8	49.0	71.2	53.6	63.2	61.0	58.5	64.4	59.9	43.3
PbO	21.4	21.2	25.8	21.7	23.0	24.1	21.2	26.0	19.8	15.9
La2O3	66.8	145.4	77.6	50.8	54.3	37.4	56.8	66.4	56.2	46.3
CeO2	148.1	307.4	152.7	74.4	74.2	55.7	84.3	134.6	124.4	85.8
ThO2	14.0	15.0	19.1	16.0	15.1	17.9	18.2	12.5	12.9	10.0
Nd2O3	73.0	167.6	81.5	40.7	46.0	27.1	54.5	54.8	52.0	41.1
U2O3	3.3	4.6	3.3	2.5	2.9	3.0	4.3	3.3	2.8	2.5
sum tr.	**1569**	**1996**	**1536**	**1367**	**1340**	**1279**	**1411**	**1725**	**1620**	**1729**
in %	**0.16**	**0.20**	**0.15**	**0.14**	**0.13**	**0.13**	**0.14**	**0.17**	**0.16**	**0.17**

	BFO WF3-034	**BFO WF3-033**	**BFO WF3-032**	**BFO WF3-031**	**BFO WF2-097**	**BFO WF2-097®**	**BFO WF2-026**	**BFO WF2-026®**	**BFO WF-249**
Stratigraphic Height	5.3	5.2	5.05	4.9	110.44		92.86		69.54
SO3 >/=									
Unnormalized Major Elements (Weight %):									
SiO2	58.05	59.31	67.65	72.56	64.32	64.73	47.96	48.08	57.10
TiO2	0.782	0.756	0.721	0.634	0.700	0.701	0.751	0.754	0.738
Al2O3	18.07	17.92	16.17	13.82	18.78	18.90	22.95	23.03	17.98
FeO*	8.36	7.39	3.03	2.24	4.26	4.19	5.16	5.20	6.01
MnO	0.014	0.012	0.009	0.011	0.006	0.006	0.005	0.005	0.004
MgO	0.91	0.90	0.76	0.54	0.75	0.74	1.18	1.16	1.06
CaO	0.34	0.33	0.40	0.56	0.14	0.14	0.12	0.12	0.30
Na2O	1.32	1.26	1.41	1.48	0.54	0.48	1.71	1.76	1.49
K2O	1.64	1.72	1.67	1.50	1.70	1.71	0.68	0.68	1.13
P2O5	0.112	0.096	0.112	0.163	0.067	0.065	0.024	0.021	0.013
Sum	89.59	89.71	91.92	93.51	91.26	91.66	80.55	80.82	85.83
LOI %	9.85	9.61	7.43	5.57	8.00	8.00	18.78	18.78	13.60
Normalized Major Elements (Weight %):									
SiO2	64.79	66.12	73.59	77.60	70.47	70.62	59.55	59.50	66.53
TiO2	0.872	0.843	0.785	0.678	0.767	0.765	0.933	0.933	0.860
Al2O3	20.17	19.98	17.59	14.78	20.58	20.62	28.50	28.50	20.95
FeO*	9.33	8.24	3.30	2.40	4.67	4.57	6.41	6.43	7.00
MnO	0.016	0.013	0.009	0.012	0.007	0.007	0.006	0.006	0.005
MgO	1.01	1.01	0.82	0.58	0.82	0.80	1.46	1.43	1.24
CaO	0.38	0.36	0.43	0.60	0.16	0.15	0.15	0.15	0.35
Na2O	1.47	1.41	1.53	1.58	0.59	0.52	2.12	2.18	1.74
K2O	1.84	1.92	1.82	1.60	1.87	1.86	0.85	0.84	1.32
P2O5	0.126	0.107	0.122	0.175	0.074	0.071	0.030	0.026	0.015
Total	100.00	100.00	100.00	100.00	100.00	100.00	100.00	100.00	100.00
Unnormalized Trace Elements (ppm):									
Ni	19	17	20	5	26	26	13	13	12
Cr	47	52	48	38	56	54	52	54	47
Sc	16	15	13	9	12	13	18	18	15
V	134	133	102	86	118	120	166	168	136
Ba	219	236	310	463	326	330	308	308	459
Rb	89	90	82	64	101	103	52	53	60
Sr	121	124	118	108	79	80	55	55	157
Zr	188	178	231	238	193	195	120	119	173
Y	51	40	38	46	46	46	32	32	15
Nb	17.1	16.8	15.9	13.8	15.9	15.8	14.9	14.5	13.5
Ga	23	22	21	16	23	24	29	30	23
Cu	20	36	51	144	27	27	49	49	35
Zn	68	63	61	33	87	89	45	45	62
Pb	19	19	23	16	37	38	42	42	23

La	52	53	35	37	76	74	36	36	22
Ce	94	91	67	81	150	147	74	75	37
Th	14	14	13	10	15	16	15	15	12
Nd	41	40	28	36	67	64	36	35	12
U	3	4	5	6	7	7	2	2	3
sum tr.	1235	1244	1281	1452	1462	1466	1159	1164	1315
in %	0.12	0.12	0.13	0.15	0.15	0.15	0.12	0.12	0.13
sum m+tr	89.72	89.83	92.05	93.65	91.41	91.81	80.66	80.93	85.96
M+Toxides	89.75	89.86	92.08	93.69	91.44	91.84	80.69	80.96	85.99
w/LOI	99.60	99.47	99.51	99.26	99.44	99.84	99.47	99.74	99.59
if Fe3+	100.53	100.29	99.85	99.50	99.91	100.30	100.04	100.32	100.26
Major elements are normalized on a volatile-free basis, with total Fe expressed as FeO.									
®denotes a duplicate bead made from the same rock powder.									
NiO	24.4	22.0	25.7	6.0	32.9	32.8	16.8	16.5	15.3
Cr2O3	69.0	76.5	69.9	55.4	81.3	79.5	75.6	79.3	69.3
Sc2O3	24.5	23.0	20.3	14.4	18.8	19.2	27.0	27.3	23.2
V2O3	196.6	195.5	149.8	127.2	173.6	176.7	244.1	247.8	199.6
BaO	244.3	264.0	346.6	516.8	363.4	368.0	344.1	343.8	511.9
Rb2O	97.2	98.1	89.2	70.3	110.3	112.4	57.1	57.9	65.7
SrO	142.6	146.4	139.2	128.2	94.0	94.1	64.7	64.5	185.9
ZrO2	253.5	240.5	312.0	322.1	260.5	263.0	162.1	161.4	233.2
Y2O3	64.7	50.3	48.1	58.4	58.3	58.0	40.9	40.8	18.5
Nb2O5	24.4	24.0	22.7	19.8	22.8	22.6	21.4	20.8	19.3
Ga2O3	31.5	29.7	28.6	21.3	31.0	31.9	38.4	40.6	31.1
CuO	25.4	45.4	64.0	180.3	33.6	34.3	61.1	61.4	43.2
ZnO	84.6	77.8	76.1	41.1	108.8	110.7	56.4	55.8	77.3
PbO	20.6	21.0	24.5	17.4	39.6	40.5	44.9	45.3	25.2
La2O3	61.2	61.8	41.5	43.9	89.3	86.9	42.0	41.8	25.6
CeO2	115.3	111.9	82.0	100.1	184.5	180.1	91.4	92.2	45.4
ThO2	15.1	15.9	14.2	10.6	16.8	17.1	16.7	16.6	12.9
Nd2O3	48.1	46.5	32.4	41.8	77.7	74.5	42.4	41.2	14.1
U2O3	3.2	4.1	5.0	6.7	7.8	7.7	1.8	2.1	2.8
sum tr.	**1546**	**1554**	**1592**	**1782**	**1805**	**1810**	**1449**	**1457**	**1619**
in %	**0.15**	**0.16**	**0.16**	**0.18**	**0.18**	**0.18**	**0.14**	**0.15**	**0.16**

	BFO WF-249®	**BFO WF-209**	**BFO WF-209®**	**BFO WF-149**	**BFO1 WF-149®**	**BFO WF-063**	**BFO1 WF-063®**	**BFO WF3-054**	**BFO WF3-054®**
Stratigraphic Height		52.51		44.43		17.62		7.93	
SO3 >/=		0.17	0.17						
Unnormalized Major Elements (Weight %):									
SiO2	57.09	59.67	59.35	55.48	55.59	66.86	67.10	63.34	62.89
TiO2	0.737	0.565	0.563	0.622	0.618	0.873	0.871	0.939	0.936
Al2O3	17.98	16.74	16.62	14.56	14.50	15.37	15.28	16.63	16.55
FeO*	6.05	6.92	6.86	5.96	5.93	5.21	5.13	6.36	6.51
MnO	0.004	0.016	0.016	0.053	0.053	0.009	0.009	0.007	0.008
MgO	1.04	1.62	1.60	2.50	2.51	0.47	0.46	0.61	0.60
CaO	0.29	0.56	0.57	5.22	5.18	0.20	0.20	0.27	0.28
Na2O	1.57	0.98	0.94	0.50	0.49	0.95	0.95	1.31	1.29
K2O	1.14	2.41	2.39	2.09	2.08	0.56	0.56	0.54	0.54
P2O5	0.013	0.326	0.325	0.145	0.143	0.022	0.023	0.024	0.024
Sum	85.92	89.80	89.23	87.14	87.09	90.53	90.59	90.04	89.63
LOI %	13.60	9.64	9.64	12.13	12.13	8.80	8.80	9.53	9.53

Normalized Major Elements (Weight %):									
SiO2	66.44	66.45	66.52	63.67	63.83	73.86	74.07	70.35	70.17
TiO2	0.857	0.629	0.631	0.714	0.709	0.965	0.962	1.043	1.045
Al2O3	20.92	18.64	18.62	16.71	16.65	16.98	16.87	18.48	18.47
FeO*	7.04	7.71	7.69	6.84	6.81	5.75	5.67	7.07	7.26
MnO	0.005	0.018	0.018	0.061	0.061	0.009	0.010	0.008	0.009
MgO	1.22	1.80	1.79	2.87	2.88	0.52	0.51	0.68	0.67
CaO	0.34	0.63	0.64	5.99	5.94	0.22	0.23	0.30	0.31
Na2O	1.83	1.09	1.06	0.57	0.57	1.05	1.05	1.45	1.44
K2O	1.33	2.68	2.67	2.40	2.39	0.62	0.62	0.60	0.60
P2O5	0.015	0.363	0.365	0.166	0.165	0.024	0.026	0.027	0.027
Total	100.00	100.00	100.00	100.00	100.00	100.00	100.00	100.00	100.00
Unnormalized Trace Elements (ppm):									
Ni	12	38	40	32	35	3	3	16	15
Cr	49	71	70	62	64	22	23	32	31
Sc	14	15	14	13	12	13	11	15	14
V	134	203	201	130	133	98	95	111	110
Ba	458	559	552	577	574	870	864	127	125
Rb	61	132	130	118	117	24	24	30	30
Sr	156	116	116	130	131	104	103	125	125
Zr	173	106	106	119	120	351	349	306	309
Y	14	60	60	27	27	18	19	36	35
Nb	12.9	11.6	11.4	13.1	13.0	19.6	20.0	21.3	21.3
Ga	23	22	21	18	17	17	18	21	21
Cu	34	21	21	19	19	20	19	8	8
Zn	60	110	109	97	98	30	29	57	58
Pb	23	29	29	22	22	20	20	24	24
La	22	40	41	33	35	19	17	66	65
Ce	41	90	89	56	56	38	42	124	131
Th	11	16	14	15	15	13	12	17	18
Nd	14	56	56	23	26	17	16	70	75
U	3	6	5	4	4	4	3	3	3
sum tr.	1315	1701	1684	1510	1515	1699	1686	1211	1219
in %	0.13	0.17	0.17	0.15	0.15	0.17	0.17	0.12	0.12
sum m+tr	86.05	89.97	89.40	87.29	87.24	90.70	90.76	90.16	89.75
M+Toxides	86.08	90.01	89.44	87.32	87.28	90.73	90.79	90.19	89.79
w/LOI	99.68	99.65	99.08	99.46	99.41	99.54	99.60	99.72	99.32
if Fe3+	100.35	100.42	99.84	100.12	100.07	100.12	100.17	100.43	100.04
Major elements are normalized on a volatile-free basis, with total Fe expressed as FeO.									
® denotes a duplicate bead made from the same rock powder.									
NiO	15.7	47.8	50.3	40.3	44.5	3.6	3.3	20.1	19.0
Cr2O3	71.1	104.3	102.6	91.2	93.0	31.9	33.0	46.3	45.9
Sc2O3	21.5	22.7	21.5	19.7	18.1	19.6	17.6	23.6	21.6
V2O3	197.5	298.7	295.7	190.9	196.0	143.9	139.6	163.5	161.8
BaO	511.8	623.8	615.7	644.6	640.3	971.1	964.6	142.3	140.0
Rb2O	67.0	144.2	142.5	129.2	127.9	26.4	25.9	33.2	33.1
SrO	185.0	136.8	137.1	153.6	154.3	122.8	122.0	148.2	147.4
ZrO2	233.1	143.7	143.3	160.6	161.6	473.7	471.0	413.6	417.0
Y2O3	17.9	76.7	75.8	34.1	34.2	23.4	23.5	45.4	44.6
Nb2O5	18.5	16.5	16.3	18.7	18.6	28.0	28.6	30.5	30.5
Ga2O3	30.5	29.7	28.8	24.9	22.4	23.3	23.9	28.4	28.6
CuO	43.0	26.4	26.4	24.4	24.0	24.4	24.3	10.3	9.4
ZnO	74.4	137.4	135.2	121.3	121.5	37.8	36.5	71.2	72.2
PbO	25.3	31.7	31.0	24.0	23.5	21.1	21.1	25.8	25.3

La2O3	26.0	46.8	47.6	39.0	40.9	22.5	19.7	77.6	76.5
CeO2	50.1	110.3	109.9	68.9	69.2	47.0	51.5	152.7	161.5
ThO2	12.1	17.4	15.9	16.9	16.2	13.8	13.5	19.1	19.5
Nd2O3	15.9	65.2	64.7	26.7	30.0	19.6	19.1	81.5	87.6
U2O3	3.0	6.2	5.0	4.2	4.1	4.4	3.2	3.3	3.6
sum tr.	**1619**	**2086**	**2065**	**1833**	**1840**	**2058**	**2042**	**1536**	**1545**
in %	**0.16**	**0.21**	**0.21**	**0.18**	**0.18**	**0.21**	**0.20**	**0.15**	**0.15**

Sample ID	Stratigraphic Height (m)	δ13C (VPDB)	%C	lithology
WF-001	6.39			clayey siltstone
WF-002	6.6			clayey siltstone
WF-003	6.7			clayey siltstone
WF-004	6.8			clayey siltstone
WF-005	6.9			clayey siltstone
WF-006	7			clayey siltstone
WF-007	7.1			clayey siltstone
WF-008	7.2			clayey siltstone
WF-009	7.3			clayey siltstone
WF-010	7.4			sandstone
WF-011	7.5			sandstone
WF-012	7.79			siltstone
WF-013	7.89			siltstone
WF-014	7.99			siltstone
WF-015	8.09			siltstone
WF-016	8.19			siltstone
WF-017	8.29			siltstone
WF-018	8.39			siltstone
WF-019	8.49			siltstone
WF-020	8.59			siltstone
WF-021	8.69			siltstone
WF-022	8.84			siltstone
WF-023	8.94			siltstone
WF-024	9.04			siltstone
WF-025	9.14			siltstone
WF-026	9.24			clayey siltstone
WF-027	9.34			siltstone
WF-028	9.44			siltstone
WF-029	9.54	-22.89	0.08	siltstone
WF-030	9.64			siltstone
WF-031	9.89			siltstone
WF-032	10.14			siltstone
WF-033	10.39			siltstone
WF-034	10.64			siltstone
WF-035	10.89			siltstone
WF-036	11.14	-21.96	0.14	siltstone
WF-037	11.39			siltstone
WF-038	11.64			siltstone
WF-039	11.89			siltstone
WF-040	12.14			clayey siltstone
WF-041	12.39			clayey siltstone
WF-042	12.64			silty claystone
WF-043	12.89	-21.83	0.13	silty claystone
WF-044	13.14	-21.80	0.05	silty claystone
WF-045	13.39	-21.85	0.17	silty claystone
WF-046	13.64	-22.09	0.16	silty claystone
WF-047	13.89	-22.10	0.17	silty claystone

WF-048	14.14	-22.03	0.21	silty claystone
WF-049	14.39	-22.23	0.24	silty claystone
WF-049z	14.39	-21.67	0.26	silty claystone
WF-050	14.4	-22.23	0.24	silty claystone
WF-050z	14.4	-21.49	0.25	silty claystone
WF-051	14.65	-22.33	0.23	silty claystone
WF-052	14.9			silty claystone
WF-053	15.12	-22.90	0.24	silty claystone
WF-053z	15.12	*-22.39*	*0.70*	silty claystone
WF-054	15.37	-22.50	0.11	clayey siltstone
WF-055	15.62	-22.67	0.11	clayey siltstone
WF-056	15.87			clayey siltstone
WF-057	16.12			clayey siltstone
WF-058	16.37			clayey siltstone
WF-059	16.62			clayey siltstone
WF-060	16.87	-22.00	0.18	clayey siltstone
WF-061	17.12			sandstone
WF-062	17.37			sandstone
WF-063	17.62	-23.23	0.11	sandstone
WF-063z	17.62	-20.22	0.32	sandstone
WF-064	17.87	-22.22	0.16	sandstone
WF-065	19.96	-22.42	0.20	clayey siltstone
WF-066	20.21			clayey siltstone
WF-067	20.46			clayey siltstone
WF-068	20.71			clayey siltstone
WF-069	20.96			clayey siltstone
WF-070	21.21	-22.51	0.37	clayey siltstone
WF-070z	21.21	*-21.28*	*0.35*	clayey siltstone
WF-071	21.46	-22.63	0.46	clayey siltstone
WF-072	21.71	-23.39	0.32	clayey siltstone
WF-072z	21.71	*-22.51*	*0.40*	clayey siltstone
WF-073	21.96	-23.18	0.28	clayey siltstone
WF-073z	21.96	*-22.51*	*0.42*	clayey siltstone
WF-074	22.21	-23.49	0.39	clayey siltstone
WF-074z	22.21	*-23.17*	*0.57*	clayey siltstone
WF-075	22.46	-23.19	0.33	clayey siltstone
WF-075z	22.46	*-22.95*	*0.46*	clayey siltstone
WF-076	22.61			claystone
WF-077	22.86			claystone
WF-078	23.11			claystone
WF-079	23.36	-22.83	0.26	claystone
WF-079z	23.36	-22.35	0.28	claystone
WF-080	23.61	-22.58	0.25	claystone
WF-080z	23.61	-22.04	0.28	claystone
WF-081	23.86	-22.59	0.27	claystone
WF-081z	23.86	-21.99	0.35	claystone
WF-082	24.11	-22.66	0.27	claystone
WF-082z	24.11	*-22.28*	*0.41*	claystone
WF-083	24.36	-22.56	0.27	silty claystone
WF-083z	24.36	*-22.48*	*0.39*	silty claystone
WF-084	24.61	-22.86	0.22	silty claystone
WF-084z	24.61	-22.49	0.32	silty claystone
WF-085	24.89			clayey siltstone
WF-086	25.14			clayey siltstone
WF-087	25.39			clayey siltstone
WF-088	25.72			claystone
WF-089	25.97	-20.75	0.15	claystone
WF-090	26.22	-22.28	0.16	claystone

WF-090z	26.22	-21.84	0.17	claystone
WF-091	26.47			claystone
WF-092	26.72	-22.16	0.25	claystone
WF-093	26.97			claystone
WF-094	27.22	-22.65	0.18	claystone
WF-094z	27.22	-22.03	0.25	claystone
WF-094z	27.22	*-25.30*	*0.41*	claystone
WF-095	27.47			claystone
WF-096	27.72			claystone
WF-097	27.97			claystone
WF-098	28.25			claystone
WF-099	28.5	-22.80	0.49	claystone
WF-099z	28.5	*-20.86*	*0.46*	claystone
WF-100	28.75			claystone
WF-101	29	-22.74	0.27	claystone
WF-101z	29	-22.15	0.35	claystone
WF-102	29.25	-22.85	0.26	claystone
WF-102z	29.25	*-22.18*	*0.38*	claystone
WF-103	29.75	-23.76	0.67	claystone
WF-103z	29.75	*-23.68*	*0.68*	claystone
WF-104	30	-23.39	0.35	claystone
WF-104z	30	*-23.24*	*0.44*	claystone
WF-105	30.25			claystone
WF-106	32.2			claystone
WF-107	32.42			claystone
WF-108	32.54			claystone
WF-109	32.7	-22.65	0.92	claystone
WF-110	32.85			silty claystone
WF-111	33.1			silty claystone
WF-112	34.4	-24.12	0.41	claystone
WF-112z	34.4	*-23.45*	*0.52*	claystone
WF-113	34.65	-23.53	0.51	claystone
WF-113z	34.65	-23.51	0.59	claystone
WF-114	34.9	-23.21	0.23	claystone
WF-114z	34.9	-22.92	0.30	claystone
WF-115	35.15			claystone
WF-116	35.4			claystone
WF-117	35.65			claystone
WF-118	35.9			claystone
WF-119	36.15			sandstone
WF-120	36.4			sandstone
WF-121	26.65			sandstone
WF-122	36.9	-21.97	0.21	sandstone
WF-123	39	-23.47	0.13	sandstone
WF-124	39.26	-23.27	0.13	sandstone
WF-125	39.36			claystone
WF-126	39.61			claystone
WF-127	39.86			claystone
WF-128	40.11			claystone
WF-129	40.36	-23.11	0.42	claystone
WF-130	40.61			claystone
WF-131	40.86	*-22.95*	*0.64*	claystone
WF-132	41.11	-22.85	0.31	claystone
WF-133	41.36	-28.94	7.21	claystone
WF-133z	41.36	-22.69	0.30	claystone
WF-134	41.56	-22.48	0.20	sandstone
WF-135	41.81			sandstone
WF-136	41.96			claystone

WF-137	42.21			claystone
WF-138	42.41			claystone
WF-139	42.7	-23.38	0.50	claystone
WF-140	42.95			claystone
WF-141	43.2	-22.28	2.56	claystone
WF-142	43.45	-24.96	0.37	claystone
WF-142z	43.45	*-22.31*	*0.50*	claystone
WF-143	43.68	-23.35	0.31	claystone
WF-143z	43.68	*-23.36*	*0.40*	claystone
WF-144	43.93	-22.05	0.16	silty claystone
WF-145	44.03	-21.42	0.11	silty claystone
WF-146	44.13			silty claystone
WF-147	44.23	-21.51	0.18	silty claystone
WF-148	44.33			silty claystone
WF-149	44.43			silty claystone
WF-150	44.53	-21.36	0.09	silty claystone
WF-151	44.63	-21.86	0.09	silty claystone
WF-152	44.73	-21.62	0.10	silty claystone
WF-153	44.83			silty claystone
WF-154	44.93	-21.49	0.09	silty claystone
WF-155	45.03			silty claystone
WF-156	45.13	-22.01	0.11	silty claystone
WF-157	45.23			silty claystone
WF-158	45.33	-22.17	0.09	claystone
WF-159	45.43	-22.77	0.11	claystone
WF-160	45.53			claystone
WF-161	45.63			claystone
WF-162	45.75			silty claystone
WF-163	45.85	-22.14	0.08	silty claystone
WF-164	45.95			silty claystone
WF-165	46.05	-22.49	0.08	silty claystone
WF-166	46.15			silty claystone
WF-167	46.25	-22.18	0.11	silty claystone
WF-168	46.4	-23.26	0.18	silty claystone
WF-169	46.55	-23.20	0.17	silty claystone
WF-170	46.8	-23.13	0.45	silty claystone
WF-171	47.05	-25.76	0.25	silty claystone
WF-172	47.4			silty claystone
WF-173	47.65	-21.93	0.36	silty claystone
WF-174	48			silty claystone
WF-175	48.15	-22.69	0.34	silty claystone
WF-176	48.4	-22.65	0.33	silty claystone
WF-177	48.75	-24.26	0.76	silty claystone
WF-178	48.9	-22.78	0.32	silty claystone
WF-179	49.15	-22.93	0.43	silty claystone
WF-180	49.45	-21.69	0.10	silty claystone
WF-181	49.55	-21.40	0.08	silty claystone
WF-182	49.65	-21.03	0.07	silty claystone
WF-183	49.75	-21.29	0.11	silty claystone
WF-184	49.85	-21.43	0.07	silty claystone
WF-185	49.95	-21.77	0.08	silty claystone
WF-186	50.05	-21.24	0.10	silty claystone
WF-187	50.15	-21.08	0.10	silty claystone
WF-188	50.25			silty claystone
WF-189	50.45	-21.17	0.08	silty claystone
WF-190	50.55			silty claystone
WF-191	50.65	-21.81	0.06	silty claystone
WF-192	50.75	-21.52	0.08	silty claystone

WF-193	50.85	-21.02	0.08	silty claystone
WF-194	50.95	-21.32	0.07	silty claystone
WF-195	51.05	-21.01	0.06	silty claystone
WF-196	51.15			silty claystone
WF-197	51.25	-29.26	7.46	silty claystone
WF-198	51.35	-21.66	0.07	silty claystone
WF-199	51.45	-21.66	0.30	silty claystone
WF-199z	51.45	-21.42	0.06	silty claystone
WF-200	51.55			silty claystone
WF-201	51.65	-20.75	0.03	silty claystone
WF-202	51.75	-21.98	0.02	sandstone
WF-203	51.85	-21.06	0.02	sandstone
WF-204	51.95	-22.18	0.04	sandstone
WF-205	52.15	-21.93	0.06	clayey siltstone
WF-205z	52.15	-21.72	0.23	clayey siltstone
WF-206	52.23	-22.29	0.23	clayey siltstone
WF-206z	52.23	*-22.09*	*0.34*	clayey siltstone
WF-207	52.32	*-22.03*	*0.09*	silty claystone
WF-208	52.41			claystone
WF-209	52.51			claystone
WF-210	52.56	-22.37	0.34	claystone
WF-211	52.68			silty claystone
WF-212	52.97	-21.35	0.09	silty claystone
WF-213	54.82	-20.59	0.07	silty claystone
WF-214	55.07	-20.90	0.06	silty claystone
WF-215	55.32			silty claystone
WF-216	55.82			silty claystone
WF-217	56.07	-21.29	0.07	silty claystone
WF-218	56.32	-20.47	0.07	silty claystone
WF-219	56.57	-20.01	0.10	silty claystone
WF-220	56.82	-23.29	0.53	silty claystone
WF-221	57.12	-20.57	0.07	silty claystone
WF-222	57.42	-21.00	0.04	siltstone
WF-223	57.72	-20.75	0.04	siltstone
WF-224	58.02	-22.17	0.04	sandstone
WF-225	58.22	-22.25	0.14	siltstone
WF-226	58.47			siltstone
WF-227	58.72	*-24.13*	*1.05*	claystone
WF-228	58.97	-23.46	0.42	claystone
WF-228z	58.97	-21.79	0.28	claystone
WF-229	59.17	-22.70	0.06	claystone
WF-230	59.42	-29.19	7.35	claystone
WF-230z	59.42	-21.93	0.33	claystone
WF-231	59.67			sandstone
WF-232	59.92	-21.83	0.23	sandstone
WF-233	60.17			sandstone
WF-234	60.42			sandstone
WF-235	60.67	-21.88	0.16	sandstone
WF-236	60.87			silty claystone
WF-237	61.12	-21.48	0.13	silty claystone
WF-238	61.37			siltstone
WF-239	61.62			siltstone
WF-240	61.72			claystone
WF-241	61.97			claystone
WF-242	62.22			claystone
WF-243	62.68			sandstone
WF-244	68.53	-24.21	0.02	sandstone
WF-245	68.73	-23.88	0.02	siltstone

WF-246	68.98	-21.98	0.17	siltstone
WF-246z	68.98	-22.80	0.28	siltstone
WF-247	69.23			siltstone
WF-248	69.29			silty claystone
WF-249	69.54			silty claystone
WF-250	69.79			silty claystone
WF-251	70.04			silty claystone
WF-252	70.29			silty claystone
WF-253	70.54	-23.09	0.19	silty claystone
WF-254	70.79			silty claystone
WF-255	71.04			silty claystone
WF-256	71.29	-23.73	0.15	silty claystone
WF-257	71.54	-23.42	0.18	silty claystone
WF-258	71.79	-23.17	0.29	silty claystone
WF-259	72.04	-22.64	0.56	silty claystone
WF-260	72.29	-22.97	0.44	silty claystone
WF-261	72.54	-24.67	0.41	silty claystone
WF-262	72.79	-23.78	0.19	silty claystone
WF-263	73.03	-29.16	7.42	silty claystone
WF-264	73.28			claystone
WF-265	73.53			claystone
WF-266	73.78			claystone
WF-267	74.13			silty claystone
WF-268	74.38	-21.23	0.06	silty claystone
WF-269	74.63	-20.45	0.10	silty claystone
WF-270	74.88	-21.08	0.06	silty claystone
WF-271	75.13			silty claystone
WF-272	75.38	-20.92	0.07	silty claystone
WF-273	75.63			silty claystone
WF-274	75.88	-22.32	0.02	silty claystone
WF-275	76.13			silty claystone
WF-276	76.78	-21.20	0.04	silty claystone
WF-277	77.03	-17.62	0.08	silty claystone
WF-278	77.28			silty claystone
WF-279	77.53			silty claystone
WF-280	77.78			silty claystone
WF-281	78.03	-21.80	0.02	silty claystone
WF-282	78.28			silty claystone
WF-283	78.53	-23.21	0.23	silty claystone
WF-284	78.78	-22.24	0.01	silty claystone
WF-285	79.16			sandstone
WF-286	79.92	-22.89	0.04	sandstone
WF-287	80.02	-21.62	0.02	sandstone
WF-288	80.12	-23.01	0.02	sandstone
WF-289	80.22			sandstone
WF-290	80.31	-22.32	0.01	sandstone
WF-291	80.41	-20.95	0.03	sandy siltstone
WF-292	80.51			sandy siltstone
WF-293	80.59	-22.06	0.02	sandy siltstone
WF-294	80.66	-20.26	0.03	clayey siltstone
WF-295	80.76	-22.35	0.06	clayey siltstone
WF-296	80.86	-22.24	0.07	clayey siltstone
WF-297	80.96	-22.35	0.07	clayey siltstone
WF-298	81.06			clayey siltstone
WF-299	81.16			clayey siltstone
WF-300	81.28			clayey siltstone
WF-301	81.38			clayey siltstone
WF2-001	83.99			siltstone

WF2-002	84.19			siltstone
WF2-003	84.34			siltstone
WF2-004	84.64			silty claystone
WF2-005	84.83			silty claystone
WF2-006	85.04			clayey siltstone
WF2-007	86.32			silty claystone
WF2-008	86.61			claystone
WF2-009	89.32			claystone
WF2-010	89.56	-20.41	0.75	claystone
WF2-011	89.77			claystone
WF2-012	89.91	-24.12	1.18	claystone
WF2-013	89.94	-25.11	0.69	claystone
WF2-014	90.16	-24.27	0.85	claystone
WF2-015	90.38	-24.91	6.56	claystone
WF2-016	90.58	-23.45	0.44	claystone
WF2-017	90.78	-19.86	0.34	claystone
WF2-018	90.98	-23.55	0.34	claystone
WF2-019	91.07	-23.39	0.42	claystone
WF2-020	92.26	-22.13	0.54	siltstone
WF2-021	92.36	-23.29	0.29	clayey siltstone
WF2-021z	92.36	*-23.27*	*0.48*	clayey siltstone
WF2-022	92.46	-23.15	0.43	clayey siltstone
WF2-023	92.56	-23.38	0.28	clayey siltstone
WF2-024	92.66	-23.26	0.31	clayey siltstone
WF2-025	92.76	-25.05	0.35	clayey siltstone
WF2-026	92.86			clayey siltstone
WF2-027	92.96			claystone
WF2-028	93.06	-23.04	0.31	claystone
WF2-029	93.16	-23.23	0.26	claystone
WF2-030	93.26	-23.22	0.32	claystone
WF2-030z	93.26	-25.23	0.32	claystone
WF2-031	93.36	-22.96	0.39	claystone
WF2-032	93.46	-22.99	0.35	silty claystone
WF2-033	93.56	-22.83	0.32	silty claystone
WF2-034	93.66	-22.93	0.32	silty claystone
WF2-035	93.76			silty claystone
WF2-036	93.86	-23.35	0.23	silty claystone
WF2-037	93.865	-23.64	0.23	claystone
WF2-038	93.89			claystone
WF2-039	93.95			claystone
WF2-040	94.02			claystone
WF2-041	94.07			claystone
WF2-042	94.24			claystone
WF2-043	94.31			clayey siltstone
WF2-044	94.39			clayey siltstone
WF2-045	94.67			sandstone
WF2-046	94.92			sandstone
WF2-047	95.46			sandstone
WF2-048	96.11			silty sandstone
WF2-049	96.36			silty sandstone
WF2-050	96.61			silty sandstone
WF2-051	96.81	-22.31	0.15	clayey siltstone
WF2-052	97.01	-22.43	0.24	clayey siltstone
WF2-053	97.21	-22.13	0.23	clayey siltstone
WF2-054	97.41	-22.57	0.21	clayey siltstone
WF2-055	97.61	-22.45	0.18	clayey siltstone
WF2-056	97.81	-22.94	0.17	clayey siltstone
WF2-057	98.01			clayey siltstone

WF2-058	98.21			clayey siltstone
WF2-059	98.41			claystone
WF2-060	98.61			claystone
WF2-061	98.81			claystone
WF2-062	99.01			claystone
WF2-063	99.08			claystone
WF2-064	99.405			claystone
WF2-065	99.69			claystone
WF2-066	101.29	-23.69	0.19	clayey siltstone
WF2-066z	101.29	-22.95	0.05	clayey siltstone
WF2-067	101.43			clayey siltstone
WF2-068	101.99	-23.31	0.04	siltstone
WF2-069	102.19			siltstone
WF2-070	102.39			silty claystone
WF2-071	103.19	-22.88	0.02	silty claystone
WF2-072	103.59			silty claystone
WF2-073	103.89			silty claystone
WF2-074	104.04			silty claystone
WF2-075	104.19			siltstone
WF2-076	104.34			siltstone
WF2-077	104.54			siltstone
WF2-078	107.66			silty claystone
WF2-079	107.76			silty claystone
WF2-080	107.86			silty claystone
WF2-081	107.96			silty claystone
WF2-082	108.06			silty claystone
WF2-083	108.15			silty claystone
WF2-084	108.26			sandstone
WF2-085	108.36			sandstone
WF2-086	108.43			siltstone
WF2-087	108.54			siltstone
WF2-088	108.61			siltstone
WF2-089	108.68	*-23.03*	*0.51*	siltstone
WF2-090	108.76			siltstone
WF2-091	108.99	-25.48	0.26	siltstone
WF2-092	109.19	-25.37	0.22	siltstone
WF2-093	109.39	-25.53	0.22	siltstone
WF2-094	109.59			siltstone
WF2-095	109.84			clayey siltstone
WF2-096	110.04			clayey siltstone
WF2-097	110.44	-24.77	0.12	clayey siltstone
WF2-098	110.64	-24.70	0.14	clayey siltstone
WF2-099	112.28			silty claystone
WF2-100	112.38			silty claystone
WF2-101	112.53			claystone
WF2-102	112.73			claystone
WF2-103	112.93			claystone
WF2-104	113.13			claystone
WF2-105	113.23			claystone
WF2-106	113.31			claystone
WF2-107	114.34			claystone
WF2-108	114.59			siltstone
WF2-109	114.83			clayey siltstone
WF2-110	115.03			clayey siltstone
WF2-111	112.53			clayey siltstone
WF2-112	115.7			clayey siltstone
WF2-113	115.87			siltstone
WF2-114	117.03			clayey siltstone

WF2-115	117.18			clayey siltstone
WF2-116	117.29			clayey siltstone
WF2-117	117.51			claystone
WF2-118	117.71			claystone
WF2-119	117.91			claystone
WF2-120	118.11			claystone
WF2-121	118.31			claystone
WF2-122	118.57			claystone
WF2-123	118.68			claystone
WF2-124	108.97			claystone
WF2-125	120.29			claystone
WF2-126	120.36	-28.22	0.17	claystone
WF3-001	0.1			silty claystone
WF3-002	0.2	-22.37	0.04	silty claystone
WF3-003	0.4			silty claystone
WF3-004	0.5			silty claystone
WF3-005	0.7			silty claystone
WF3-006	0.8			silty claystone
WF3-007	0.9			silty claystone
WF3-008	1.06			siltstone
WF3-009	1.16			siltstone
WF3-010	1.3			claysey siltstone
WF3-011	1.4			claysey siltstone
WF3-012	1.95			claysey siltstone
WF3-013	2.15			claysey siltstone
WF3-014	2.35			claysey siltstone
WF3-015	2.55			claysey siltstone
WF3-016	2.75			claysey siltstone
WF3-017	3.03			claysey siltstone
WF3-018	3.23			claysey siltstone
WF3-019	3.43			claysey siltstone
WF3-020	3.54			claystone
WF3-021	3.64			claystone
WF3-022	3.74			claystone
WF3-023	3.84			claystone
WF3-024	3.94			claystone
WF3-025	4.04			claystone
WF3-026	4.14	-22.71	0.13	claystone
WF3-027	4.23			claystone
WF3-028	4.34			claystone
WF3-029	4.44	-21.68	0.04	claystone
WF3-030	4.65	-23.28	0.02	sandstone
WF3-031	4.9	-22.30	0.02	siltstone
WF3-032	5.05	-21.09	0.03	siltstone
WF3-033	5.2	-22.35	0.03	claystone
WF3-034	5.3	-21.78	0.04	claystone
WF3-035	5.4	-20.96	0.03	claystone
WF3-036	5.53	-20.99	0.04	claystone
WF3-037	6.61	-21.49	0.05	claystone
WF3-038	6.29	-21.77	0.03	siltstone
WF3-039	6.44			siltstone
WF3-040	6.54	-21.02	0.06	siltstone
WF3-041	6.64	-21.44	0.07	siltstone
WF3-042	6.78	-21.83	0.03	siltstone
WF3-043	6.88			siltstone
WF3-044	6.98			siltstone
WF3-045	7.08	-21.55	0.06	siltstone
WF3-046	7.18	-20.16	0.04	siltstone

WF3-047	7.28	-20.29	0.04	siltstone
WF3-048	7.38	-21.60	0.05	siltstone
WF3-049	7.47			siltstone
WF3-050	7.53	-23.43	0.06	siltstone
WF3-051	7.59			siltstone
WF3-052	7.73	-21.40	0.06	claystone
WF3-053	7.83	-21.62	0.05	claystone
WF3-054	7.93	-21.55	0.06	claystone
WF3-055	8.03	-21.71	0.03	claystone
WF3-056	8.13	*-21.89*	*0.06*	claystone
WF3-057	8.23	-21.91	0.05	claystone
WF3-058	8.33	-21.73	0.05	claystone
WF3-059	8.43			claystone
WF3-060	8.57	-21.18	0.06	siltstone
WF3-061	8.67			siltstone
WF3-062	8.77			siltstone
WF3-063	8.9			claystone
WF3-064	9.15			claystone
WF3-065	9.4			claystone
WF3-066	9.46			claystone